DNA BASE PAIRS

~20 Å

3.4 Å

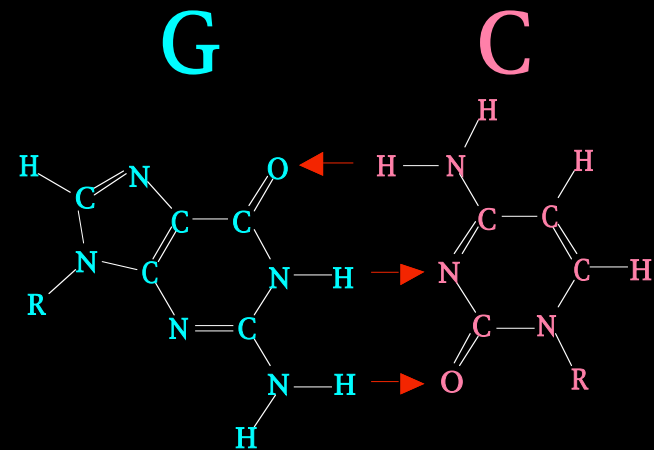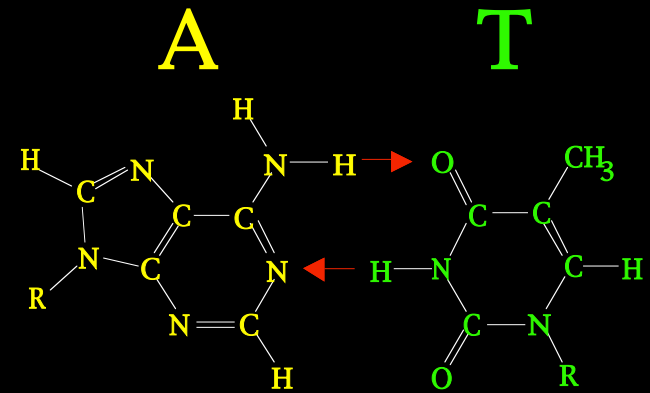10-10.5 Pairs/Turn

A   T

G   C

N. Seeman

OBJECTIVES

[1] **Architectural Control**

DESIGN MOLECULES TO ASSEMBLE INTO ORDERED ARRAYS.

[A] SCAFFOLD MACROMOLECULAR CRYSTALLIZATION (PERIODIC).
[B] SCAFFOLD NANOELECTRONICS ASSEMBLY (PERIODIC).
[C] GENERATE ALGORITHMIC PATTERNS (APERIODIC).

[2] **Nanomechanical Devices**

[A] NANOROBOTICS.
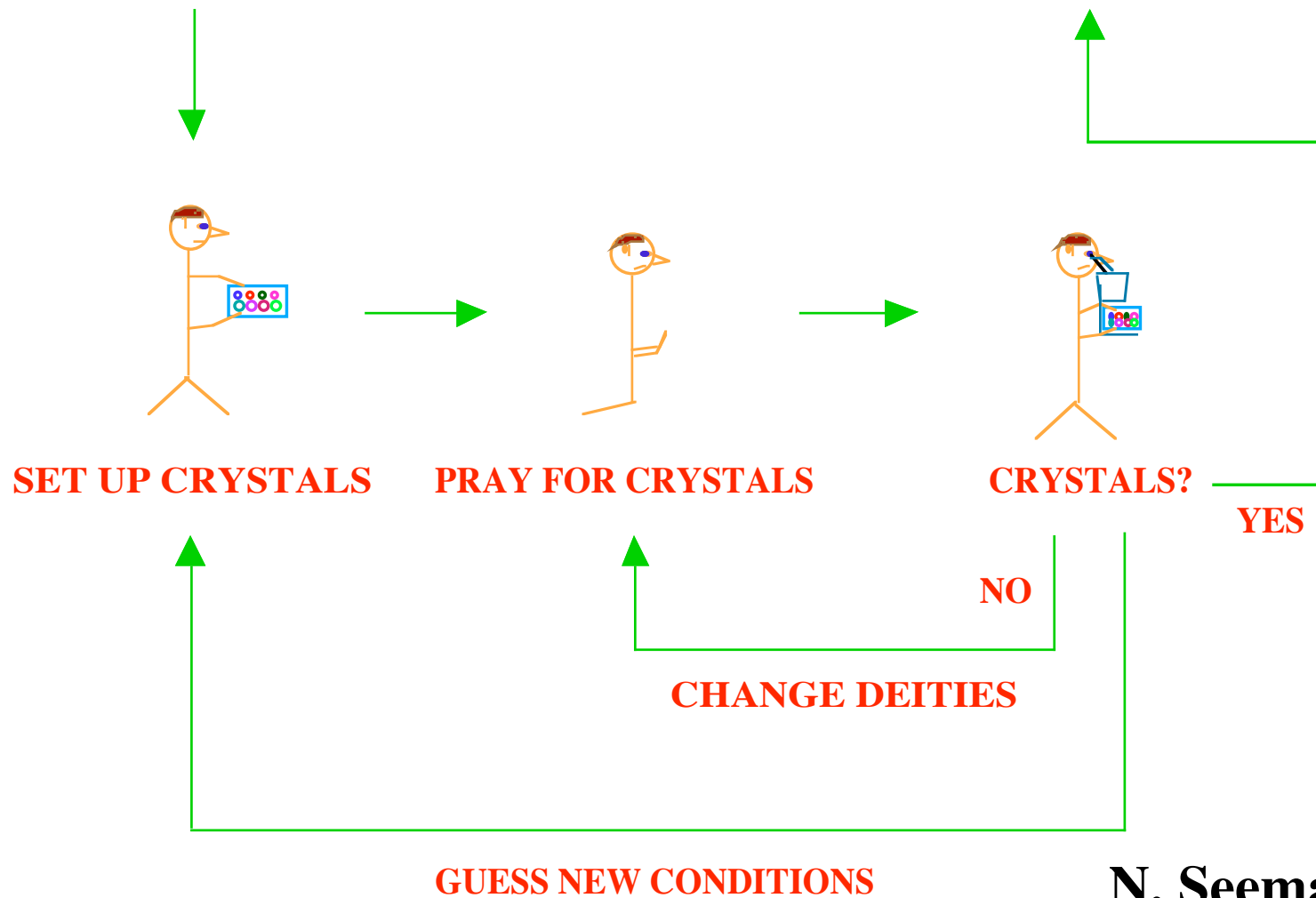[B] NANOFABRICATION.
[C] MOLECULAR PEGBOARDS.

[3] **Self-Replicating Systems**   **N. Seeman**

CURRENT CRYSTALLIZATION PROTOCOL

GUESS CONDITIONS

DO CRYSTALLOGRAPHY

SET UP CRYSTALS

PRAY FOR CRYSTALS

CRYSTALS?

YES

NO

CHANGE DEITIES
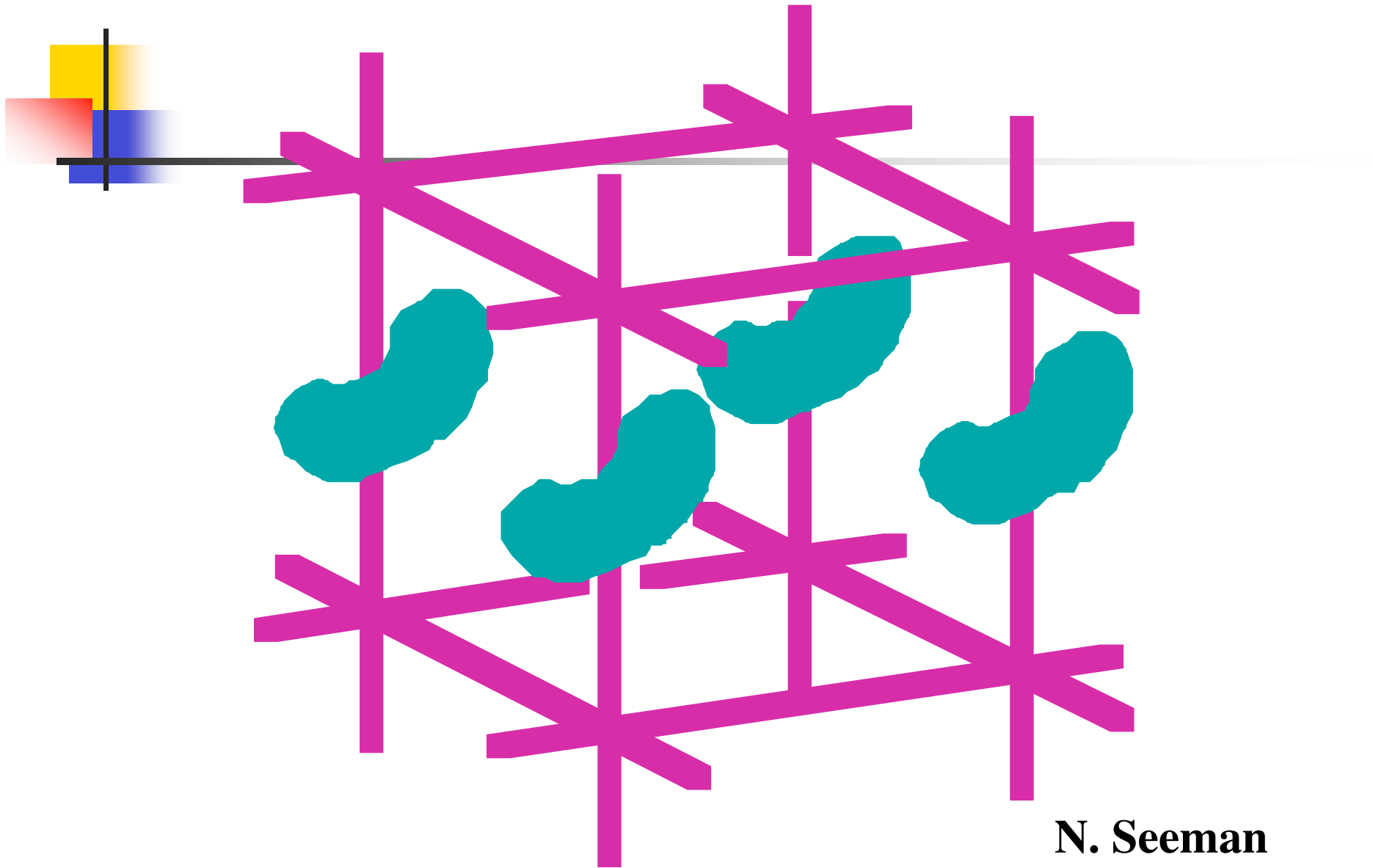
GUESS NEW CONDITIONS

N. Seeman

The Biological Problem

- The rate-limiting step in establishing the 3D structures of large biological macromolecules is their crystallization.

- Seeman group aims to solve this problem by using 3D DNA arrays to scaffold their organization into crystalline arrays.

A New Suggestion for Producing Macromolecular Crystals

N. Seeman

LaBean COMPSCI 296.5   Seeman, N.C. (1982), *J. Theor. Biol.* **99**, 237-247.

OBJECTIVES

- Organizing DNA in 3D Crystalline Lattices.

- Organizing DNA in 3D to Scaffold Biological Macromolecules, Nanodevices and Nanoelectronic Components in Crystalline Lattices.

OBJECTIVES

[1] **Architectural Control**

DESIGN MOLECULES TO ASSEMBLE INTO ORDERED ARRAYS.

[A] SCAFFOLD MACROMOLECULAR CRYSTALLIZATION (PERIODIC).
[B] SCAFFOLD NANOELECTRONICS ASSEMBLY (PERIODIC).
[C] GENERATE ALGORITHMIC PATTERNS (APERIODIC).

[2] **Nanomechanical Devices**

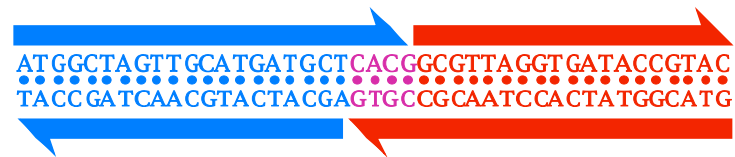[A] NANOROBOTICS.
[B] NANOFABRICATION.
[C] MOLECULAR PEGBOARDS.

[3] **Self-Replicating Systems**

N. Seeman

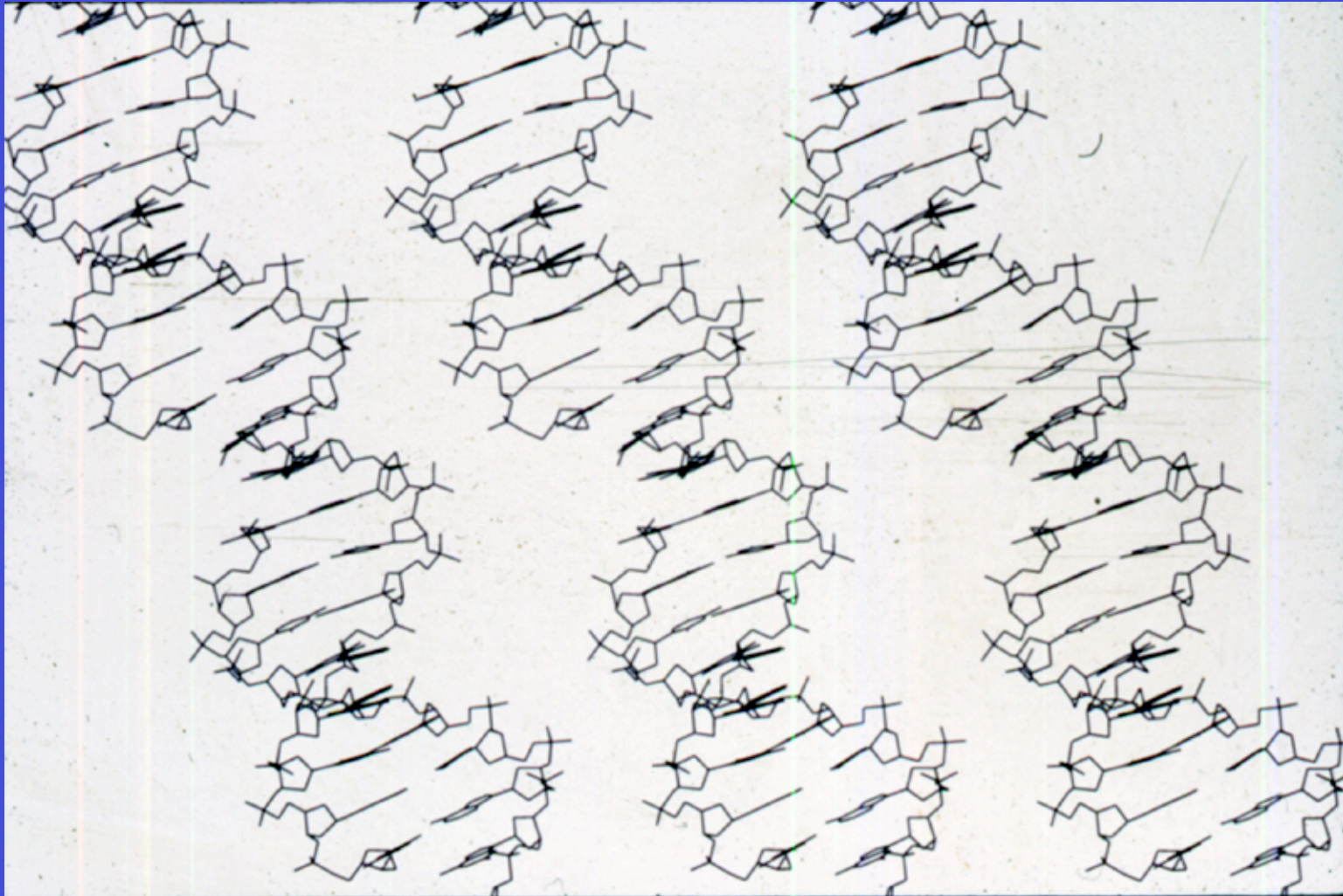# Sticky-Ended Cohesion: Affinity

N. Seeman

Sticky-Ended Cohesion: Structure
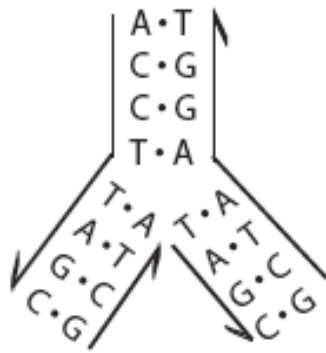

Qiu, H., Dewan, J.C. & Seeman, N.C. (1997) *J. Mol. Biol.* **267**, 881-898.

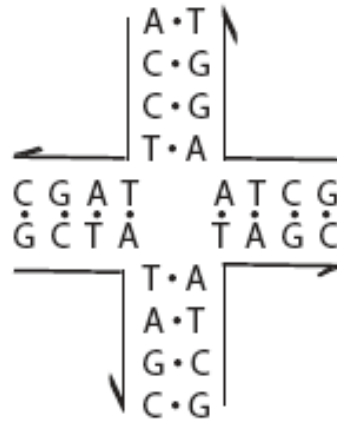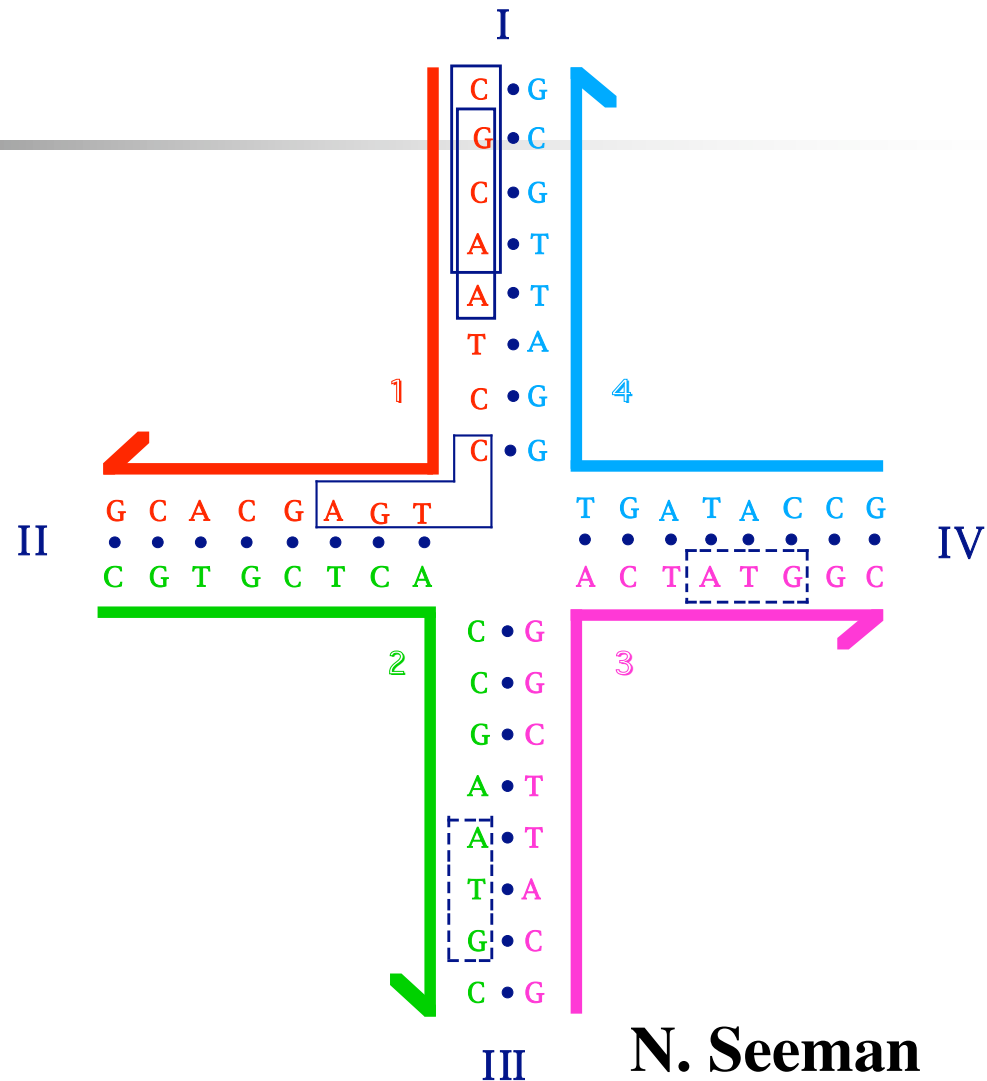**N. Seeman**

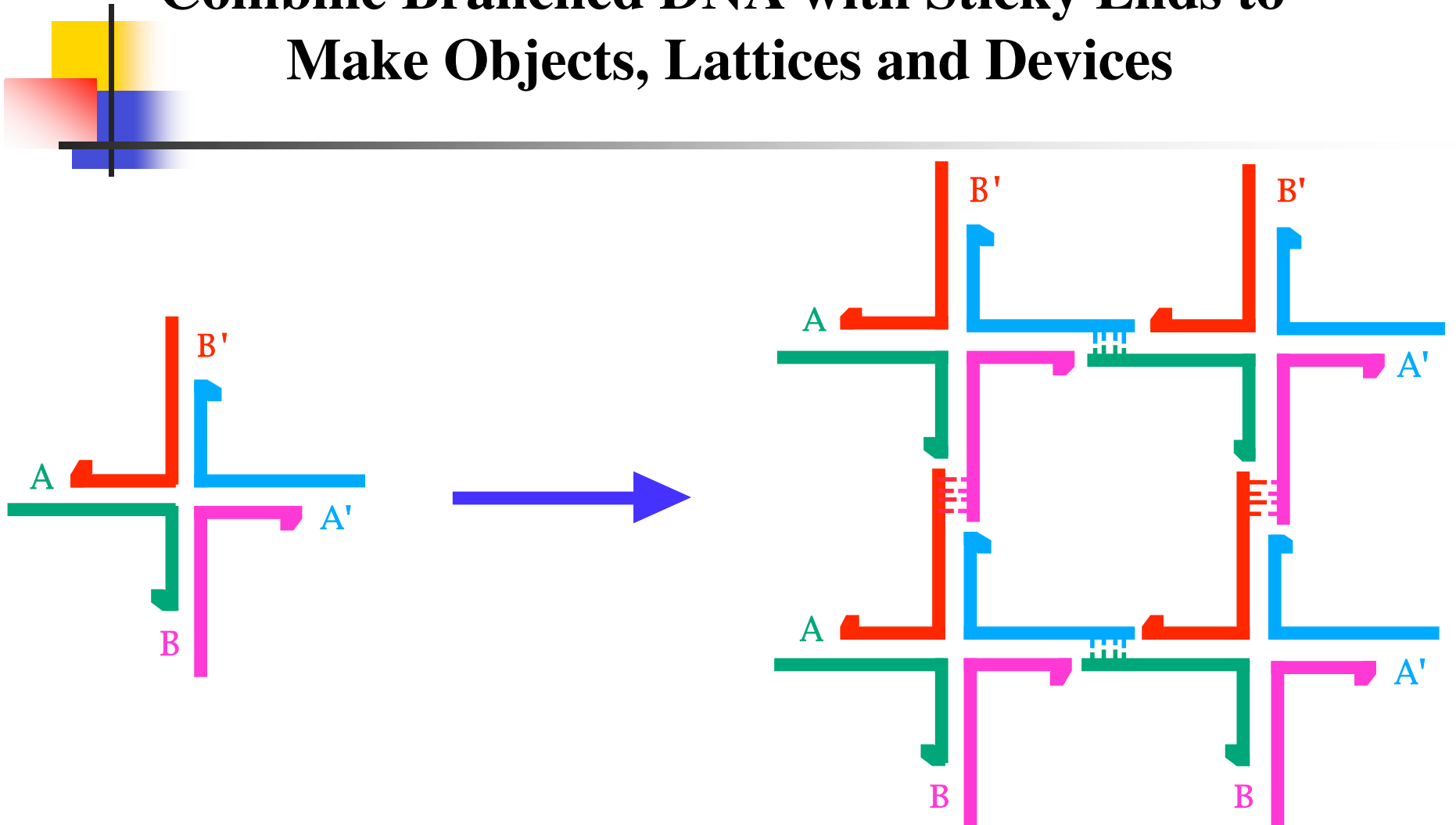# Linear vs branched junctions

dsDNS   3-arm Junction   4-arm Junction

Design of Immobile Branched Junctions: Minimize Sequence Symmetry
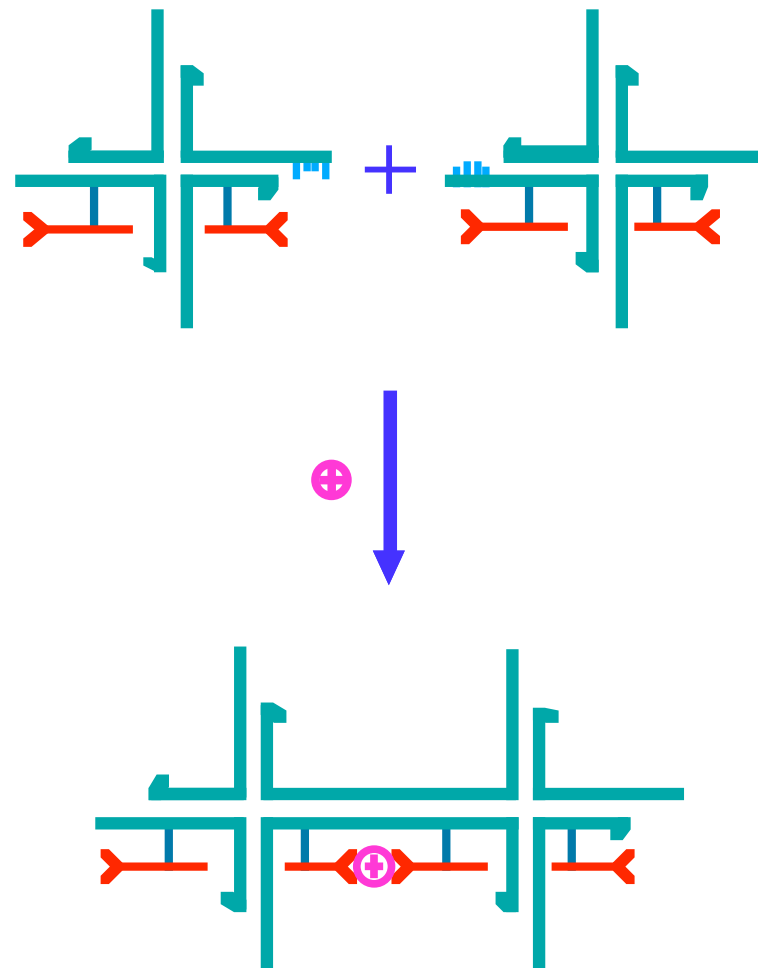

N. Seeman

The Central Concept:
Combine Branched DNA with Sticky Ends to
Make Objects, Lattices and Devices
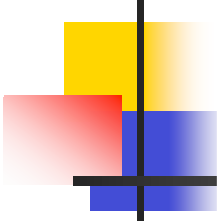

N. Seeman

LaBean COMPSCI 296.5

Seeman, N.C. (1982), *J. Theor.Biol.* **99**, 237-247.

A Method for Organizing Nano-Electronic Components

N. Seeman

Robinson, B.H. & Seeman, N.C. (1987), *Protein Eng*. **1**, 295-300.**.**

WHY DNA?

PREDICTABLE INTERMOLECULAR INTERACTIONS

CONVENIENT AUT OMATED CHEMISTRY

CONVENIENT MODIFYING ENZYMES

LOCALLY STIFF POLYMER

EXTERNALLY READABLE CODE

HIGH FUNCTIONAL GROUP DENSITY

PROTOTYPE FOR MANY DERIVATIVES

N. Seeman

REQUIREMENTS FOR LATTICE DESIGN COMPONENTS
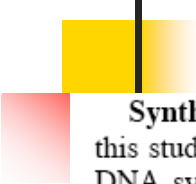
PREDICTABLE INTERACTIONS

PREDICTABLE LOCAL PRODUCT STRUCTURES

STRU CTURAL INTEGRITY

N. Seeman

Some Methods

Synthesis and Purification of DNA. All DNA molecules used in this study are synthesized on an Applied Biosystems 380B automatic DNA synthesizer, removed from the support, and deprotected using routine phosphoramidite procedures.[31] All strands are purified by polyacrylamide gel electrophoresis.

Formation of Hydrogen-Bonded Complexes. Complexes are formed by mixing a stoichiometric quantity of each strand, as estimated by OD_{260}. This mixture is then heated to 90 °C for 5 min and cooled to the desired temperature by the following protocol: 20 min at 65 °C, 20 min at 45 °C, 30 min at 37 °C, 30 min at room temperature, and (if desired) 30 min at 4 °C. Exact stoichiometry is determined, if necessary, by titrating pairs of strands designed to hydrogen bond together and visualizing them by native gel electrophoresis; absence of monomer is taken to indicate the endpoint.

Hydroxyl Radical Analysis. Individual strands of the DAE complexes are radioactively labeled and are additionally gel purified from a 10−20% denaturing polyacrylamide gel. Each of the labeled strands [approximately 1 pmol in 50 mM Tris·HCl (pH 7.5) containing 10 mM $MgCl_2$] is annealed to a tenfold excess of the unlabeled complementary strands, or it is annealed to a tenfold excess of a mixture of the other strands forming the complex, or it is left untreated as a control, or it is treated with sequencing reagents[32] for a sizing ladder. The samples are annealed by heating to 90 °C for 3 min and then cooled slowly to 4 °C. Hydroxyl radical cleavage of the double-strand and double-crossover-complex samples for all strands takes place at 4 °C for 2 min and 40 s,[33] with modifications noted by Churchill et al.[30] The reaction is stopped by addition of thiourea. The sample is dried,

dissolved in a formamide/dye mixture, and loaded directly onto a 10−20% polyacrylamide/8.3 M urea sequencing gel. Autoradiograms are analyzed on a BioRad GS-250 Molecular Imager.

Polyacrylamide Gel Electrophoresis. Denaturing Gels. These gels contain 8.3 M urea and are run at 55 °C. Gels contain 10% acrylamide (19:1, acrylamide:bisacrylamide). The running buffer consists of 89 mM Tris·HCl, pH 8.0, 89 mM boric acid, 2 mM EDTA (TBE). The sample buffer consists of 10 mM NaOH, 1 mM EDTA, containing 0.1% xylene cyanol FF tracking dye. Gels are run on an IBI Model STS 45 electrophoresis unit at 70 W (50 V/cm, constant power), or on a Hoefer SE 600 electrophoresis unit at 60 °C (31 V/cm, constant voltage). They are then dried onto Whatman 3MM paper and exposed to X-ray film for up to 15 h.

Nondenaturing Gels. Gels contain 8% acrylamide (19:1, acrylamide:bisacrylamide). DNA is suspended in 10−25 μL of a solution containing 40 mM Tris·HCl, pH 8.0, 20 mM acetic acid, 2 mM EDTA, and 12.5 mM magnesium acetate (TAEMg); the quantities loaded vary as noted below. The solution is boiled and allowed to cool slowly to 16 °C. Samples are then brought to a final volume of 10 μL with a solution containing TAEMg, 50% glycerol, and 0.02% each of bromophenol blue and xylene cyanol FF tracking dyes. Gels are run on a Hoefer SE-600 gel electrophoresis unit at 11 V/cm at 16 °C, and exposed to X-ray film for up to 15 h or stained with Stainsall dye.

Enzymatic Reactions. A. Kinase Labeling. An individual strand of DNA (10 pmols) is dissolved in 20 μL of a solution containing 66 mM Tris·HCl, pH 7.6, 6.6 mM $MgCl_2$, and 10 mM dithiothreitol (DTT) and mixed with 2 μL of 2.2 μM γ-^{32}P-ATP (10 mCi/mL) and 6 units of polynucleotide kinase (U.S. Biochemical) for 2 h at 37 °C. Radioactive labeling is followed by addition of 1 μL unlabeled of 10 mM ATP, and incubation proceeds for another 10 min. The reaction is stopped by heat inactivation, followed by gel purification.

B. Ligations. T4 polynucleotide ligase (10 units) (U.S. Biochemical) in 30 μL of a buffer supplied by the manufacturer are added to 10 pmol of each strand, and the reaction is allowed to proceed at 16 °C for 10−16 h. Thus, the concentration of DNA in each ligation reaction is about 333 nM. The reaction is stopped by phenol/chloroform extraction. Samples are then ethanol precipitated.

C. Restriction Endonuclease Digestions. Restriction enzymes are purchased from New England Biolabs and used in buffers suggested by the supplier. Digestion is performed at 37 °C for 2 h with 20 units of Hha I or 10 units of Rsa I. The reaction is stopped by two or three phenol extractions, followed by ethanol precipitation.

D. Exonuclease III Treatment. Exonuclease III (exo III) (100 units), purchased from U.S. Biochemical, is added directly to the ligation mixture, and the reaction is allowed to proceed for 0.5−2 h at 37 °C. The reaction is stopped by heat inactivation.

E. Exonuclease I Treatment. Exonuclease I (exo I) (10 units), purchased from U.S. Biochemical, is added directly to the ligation mixture, and the reaction is allowed to proceed for 0.5−2 h at 37 °C. The reaction is stopped by heat inactivation.

A Specific Quadrilateral Synthesized from DNA Branched Junctions

Jung-Huei Chen, Neville R. Kallenbach, and Nadrian C. Seeman*

Contribution from the Department of Chemistry, New York University,
New York, New York 10003. Received June 13, 1988

Abstract: Four different three-arm branched DNA junctions have been synthesized and covalently linked together in a prescribed arrangement to form a macrocycle of previously specified sequence. One end of each individual junction is closed by a hairpin loop. Each open arm of the four junctions terminates in a unique single-stranded cohesive ("sticky") end; there are four pairs of complementary sticky ends among the eight arms, two pairs with 3′ overhangs, and two pairs with 5′ overhangs. The associations between junctions are directed by the sequences of these cohesive ends. The junctions that associate in this fashion are enzymatically joined together by the use of bacteriophage T4 DNA ligase. The final product is a "quadrilateral" the sides of which are each 16 nucleotide pairs long, approximately 1.5 turns of DNA. The quadrilateral is designed to be composed of two hextuply linked circles of DNA.
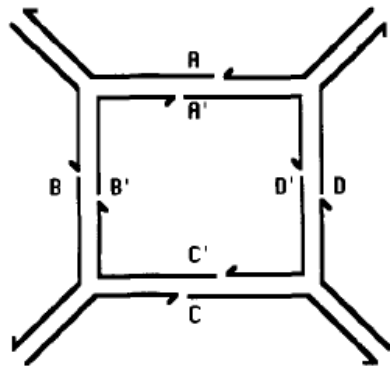
Figure 1. Tetramer designed from four components. Each of the individual components of this tetramer is a three-arm junction. The parallel lines represent regions of double-helical DNA. The half-arrowheads are at the 3′ ends of the individual strands. The letters indicate the individual 5′ overhangs which direct the cohesion of the different junction synthons: The sequence represented by A is complementary to the sequence represented by A′; similar relationships exist for B and B′, C and C′, and D and D′. Individual junctions thus have sticky ends A and B′, B and C′, C and D′, and D and A′.

COMPSCI 296.5
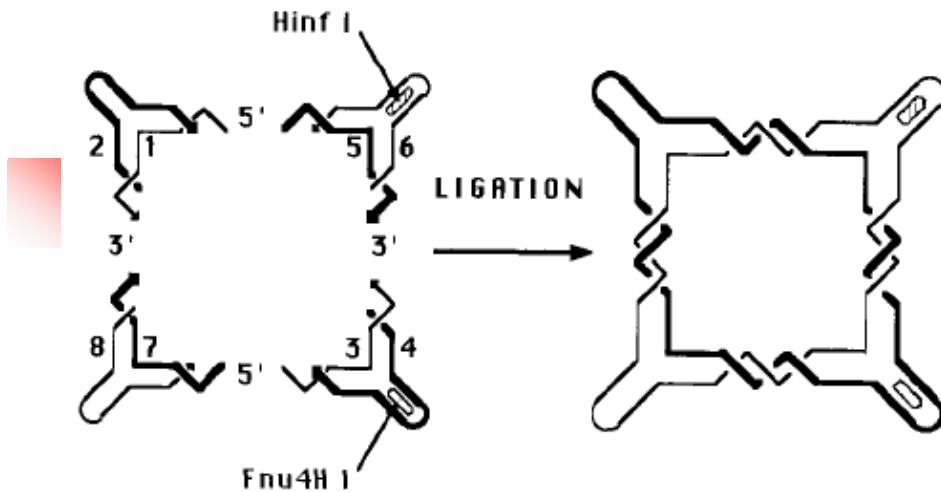
Figure 2. Scheme of the synthesis of the DNA quadrilateral. The individual reactant junctions are shown on the left of the figure, and the target product is shown on the right. For clarity, the double helicity of the DNA has been represented merely as parallel lines in the vicinity of the branch sites and is confined to regions distal to the branch sites; nevertheless, all the twisting expected on the main cycle is shown on both sides of the figure. On the left, thick strands and the thin strands are associated in pairs to form three-arm junctions, in which one "exocyclic" arm is closed in a hairpin loop. Arrowheads represent the 3′ ends of individual strands. Strand numbering is indicated on the left by the numbers from 1 to 8. The 5′ and 3′ symbols indicate the sense of the single-stranded overhangs. The overhangs are all on the short strands. The filled region in the exocyclic stem formed by strand 6 represents a *Hin*fI restriction site, while the filled region in the stem of strand 4 corresponds to a *Fnu*4HI site, as indicated. When the ligation is complete, the four junctions form two intersecting DNA circles which are linked six times.
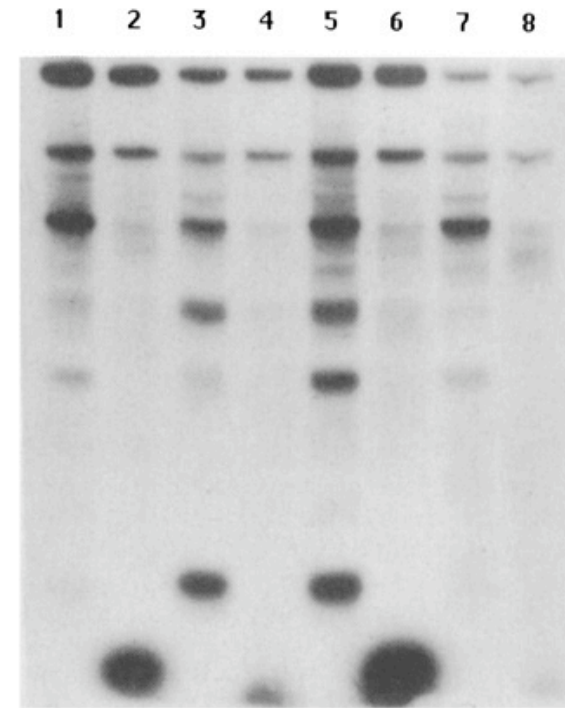
Figure 5. Digestion of product with exonuclease III. This figure shows a denaturing gel of the products of the ligation with four different radioactive-labeling schemes. The lanes are grouped in pairs. The first lane of each pair is crude reaction product, and the second lane has been digested with exonuclease III. Starting from the left, the labeling for each pair has been respectively in strands 3, 2, 4, and 1. Note that only two products withstand digestion by exonuclease III.
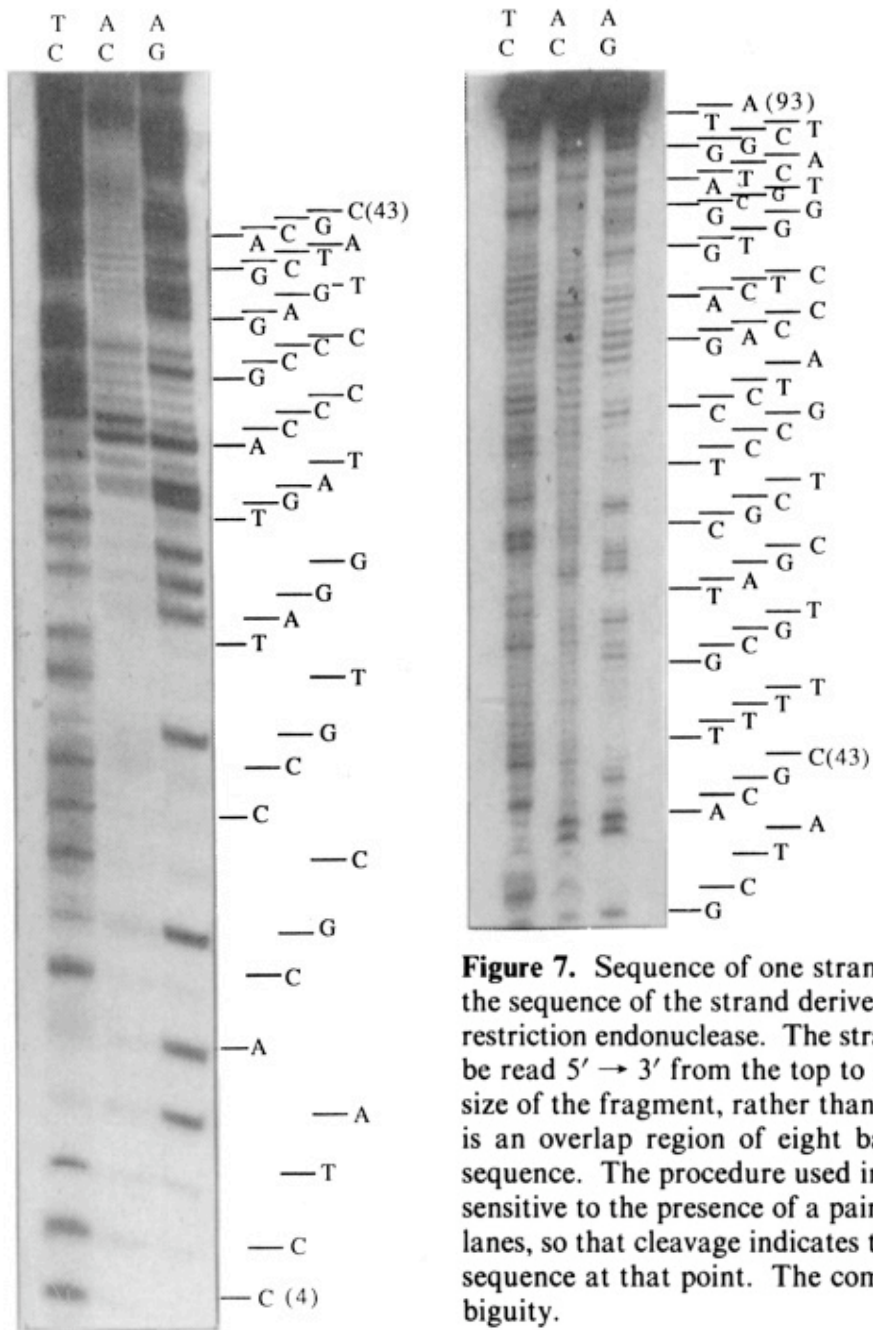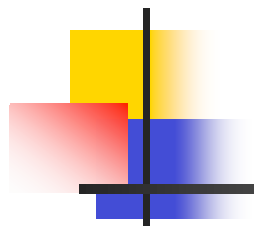
Figure 7. Sequence of one strand of the quadrilateral. This gel shows the sequence of the strand derived when the product is cleaved by *Hin*fI restriction endonuclease. The strand is 3′ labeled, so the sequence should be read 5′ → 3′ from the top to the bottom. The numbers indicate the size of the fragment, rather than linear position in the sequence. There is an overlap region of eight bands between the two portions of the sequence. The procedure used involves reactions that are differentially sensitive to the presence of a pair of nucleotides, listed at the tops of the lanes, so that cleavage indicates the presence of one of those bases in the sequence at that point. The combination of two lanes resolves the ambiguity.

3/2(

DNA Cube

Chen & Seeman (1991) *Nature* **350**, 631-633.
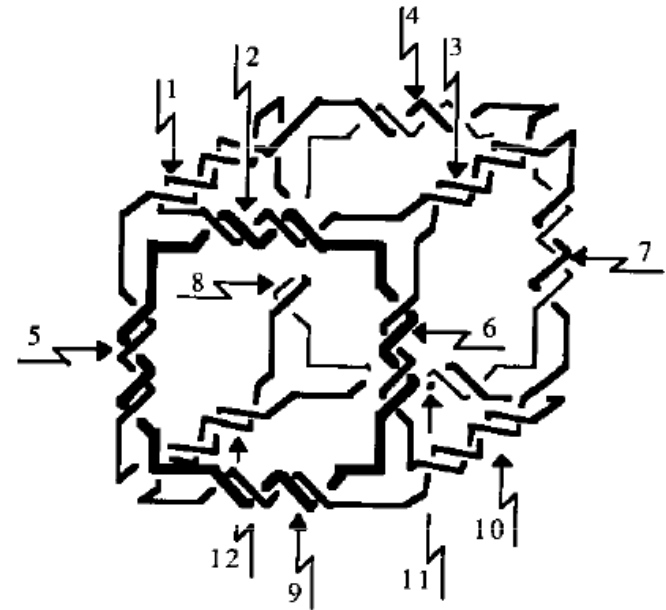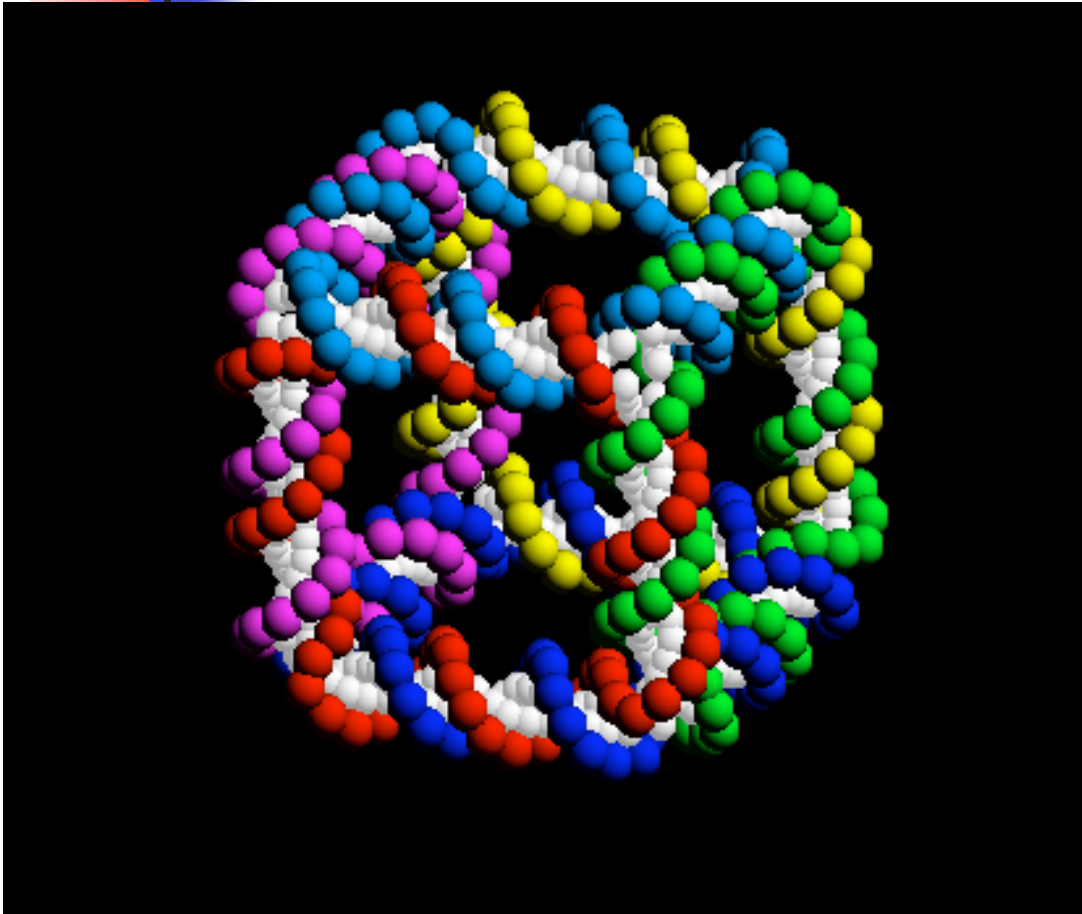
Figure 6. *A DNA molecule whose helix axes have the connectivity of a cube.* For simplicity, the object is shown as a cube, although there has been no characterization of the angles between the edges. The object contains twelve edges formed from double helical DNA. Each edge is numbered, and the numbers are indicated as being associated with thunderbolt-shaped arrows. These arrows indicate not only the edge numbering, but also the twelve unique restriction sites in the molecule. Edges 1-4 are on the top of the object, edges 5-8 form the vertical sides of the object, and edges 9-12 form the bottom. The restriction sites are: 1-Dde I; 2-BstE II; 3-Sau96 I; 4-BstN I; 5-Rsa I; 6-BstU I; 7-Hha I; 8-Alu I; 9-Hinf I; 10-Taq I; 11-Sty I; 12-Hae III. For clarity, the double helicity of the

The use of branched DNA for nanoscale fabrication

Nadrian C Seeman

Department of Chemistry, New York University, New York, NY 10003, USA
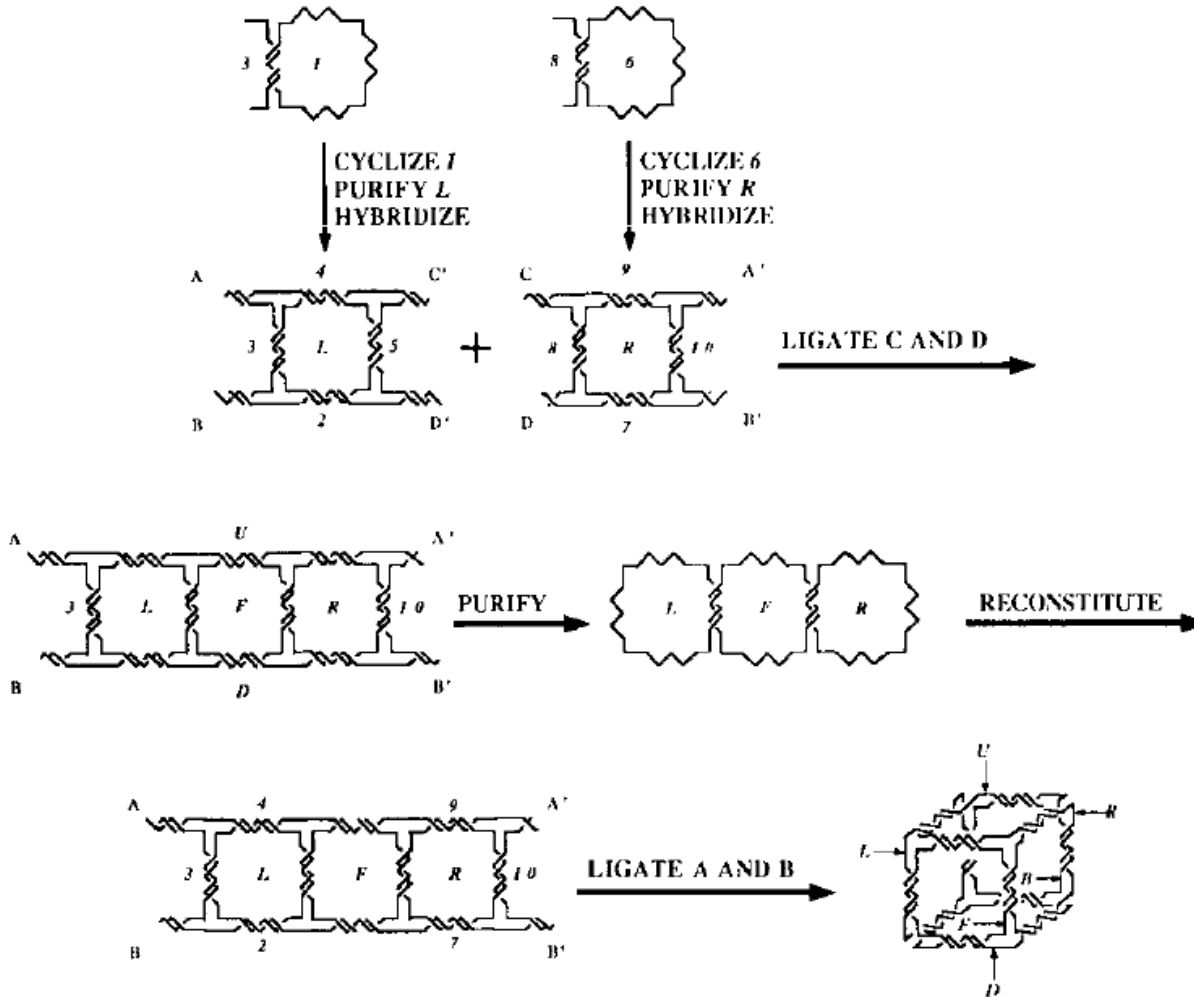
~5 femtomoles produced

The use of branched DNA for nanoscale fabrication

Nadrian C Seeman

Department of Chemistry, New York University, New York, NY 10003, USA
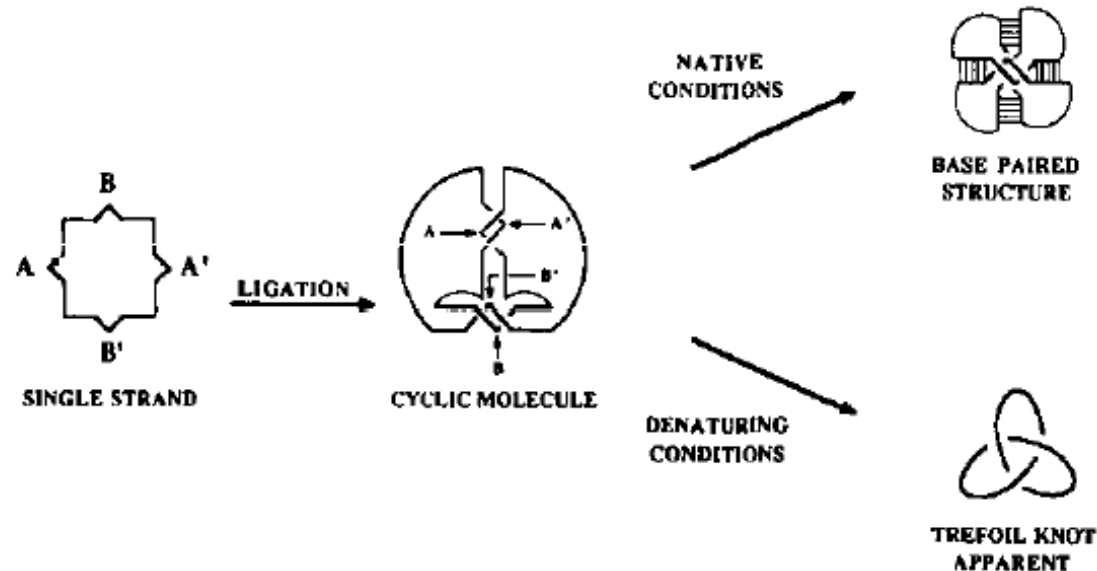
Figure 8. *Synthetic scheme for the single-stranded DNA knot.* The starting material is illustrated on the far left—A (ACTGGACCTCT), B (CGTAGCCGCAT), A' and B' refer to the regions that are expected to pair by Watson–Crick hydrogen bonding. Each side of the square figure shown corresponds to a quarter of the molecule. The projections represent the regions that will pair according to the letter codes; they are flanked by the oligo-T linkers. The arrowhead within the A projection represents the 3' end of the strand. The central portion of the figure represents a version of the molecule distorted from its expected structure, in order to illustrate the interlinking of the strands. The regions from the left part of the

Assembly and Characterization of Five-Arm and Six-Arm DNA Branched Junctions[†]

Yinli Wang,[‡] John E. Mueller,[‡,§] Börries Kemper,[‖] and Nadrian C. Seeman[*,‡]

Department of Chemistry, New York University, New York, New York 10003, and Institute of Genetics, University of Köln, 5000 Köln 41, Germany

ABSTRACT: DNA branched junctions have been constructed that contain either five arms or six arms surrounding a branch point. These junctions are not as stable as junctions containing three or four arms; unlike the smaller junctions, they cannot be shown to migrate as a single band on native gels when each of their arms contains eight nucleotide pairs. However, they can be stabilized if their arms contain 16 nucleotide pairs. Ferguson analysis of these junctions in combination with three-arm and four-arm junctions indicates a linear increase in friction constant as the number of arms increases, with the four-arm junction migrating anomalously. The five-arm junction does not appear to have any unusual stacking structure, and all strands show similar responses to hydroxyl radical autofootprinting analysis. By contrast, one strand of the six-arm junction shows virtually no protection from hydroxyl radicals, suggesting that it is the helical strand of a preferred stacking domain. Both junctions are susceptible to digestion by T4 endonuclease VII, which resolves Holliday junctions. However, the putative helical strand of the six-arm junction shows markedly reduced cleavage, supporting the notion that its structure is largely found in a helical conformation. Branched DNA molecules can be assembled into structures whose helix axes form multiply connected objects and networks. The ability to construct five-arm and six-arm junctions vastly increases the number of structures and networks that can be built from branched DNA components. Icosahedral deltahedra and 11 networks with 432 symmetry, constructed from Platonic and Archimedean solids, are among the structures whose construction is feasible, now that these junctions can be made.

3/20/06   LaBean COMPSCI 296.5
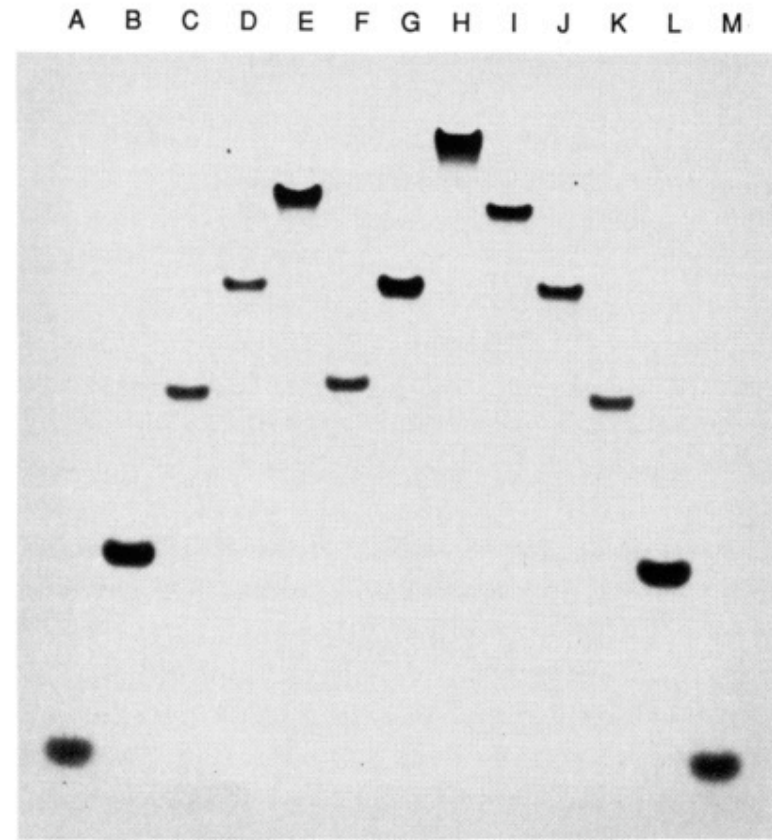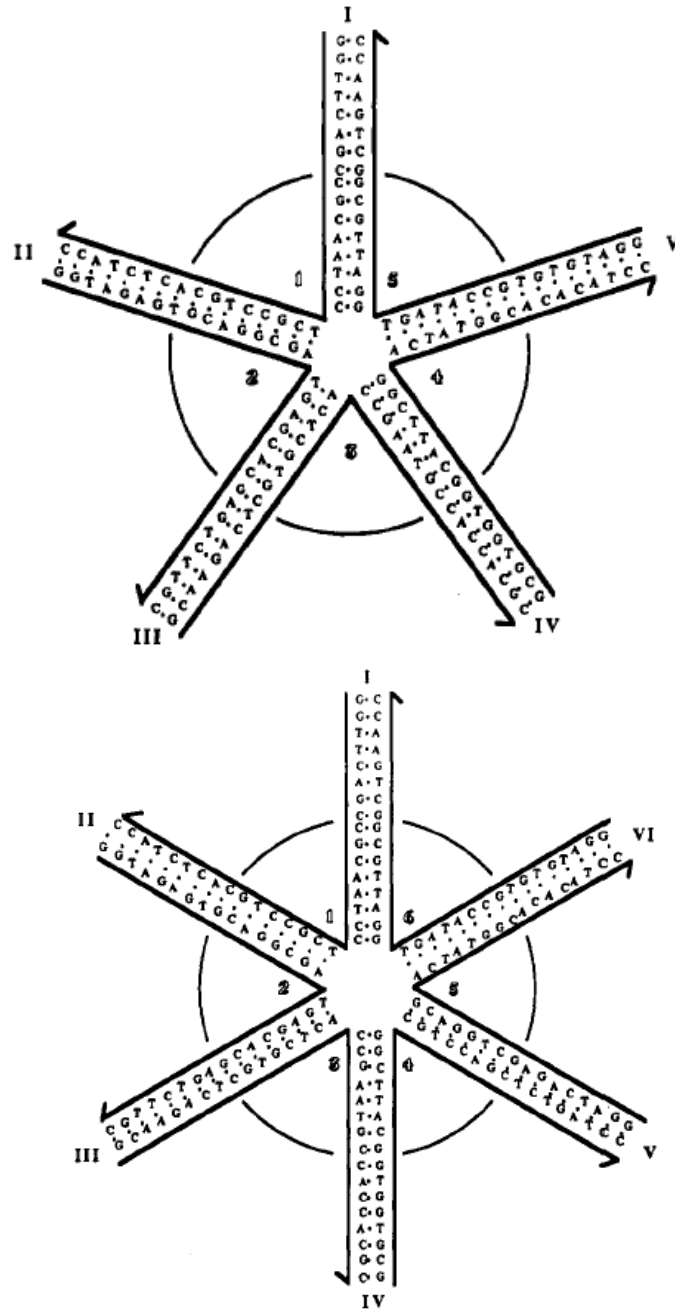
FIGURE 3: Electrophoresis of equimolar ratios of J5YLG and J6YLG. The gel shown here is a 10% native gel stained with Stainsall dye. Lane F contains a three-arm junction, JYG, with 16 nucleotide pairs per arm, and lane G contains a four-arm junction, JXG, with 16 nucleotide pairs per arm. Lanes A and M contain 4 μg of strand J5YLG.3, lane B contains 2 μg of J5YLG.4 + J5YLG.5, and lane L contains 2 μg of each of J6YLG.4 + J6YLG.5. Lanes C–K (except F and G) contain 1 μg each of the following components: (C) J5YLG.1 + J5YLG.2 + J5YLG.3; (D) J5YLG.1 + J5YLG.2 + J5YLG.3 + J5YLG.4; (E) all strands of J5YLG; (H) all strands of J6YLG; (I) J6YLG.1 + J6YLG.2 + J6YLG.3 + J6YLG.4 + J6YLG.5; (J) J6YLG.1 + J6YLG.2 + J6YLG.3 + J6YLG.4; (K) J6YLG.1 + J6YLG.2 + J6YLG.3. Note that in contrast to the analogous Figure 2, all species migrate as single bands.

FIGURE 7: Five-connected and six-connected networks. The left side of this drawing illustrates a five-connected network. The polyhedra that compose it are regular octahedra whose centers are placed at the corners of a cube. To accommodate the octahedra, the cube has been transformed into a truncated cube. The size of the octahedra determines the symmetry of the faces of the truncated cube; when the edges of the octahedron are the same length as the space between them, the face of the truncated cube is a regular octagon. The centers of the cubes and octahedra are loci of 432 symmetry, although DNA structures would be of lower symmetry because their base sequences would not be symmetric. Note that every vertex of this network has five edges meeting there. The simplest conceptual network, the six-connected cubic lattice, is shown on the right side of this drawing. If the object depicted were ligated into a lattice, only one "box" out of eight would correspond to this object, and the others would be formed by connections between the boxes. The object shown has, ideally, 432 symmetry, but a lower symmetry box and lattice could be formed by making the edges and/or the connections between edges of unequal lengths.

FIGURE 5: Hydroxyl radical cleavage of five-arm and six-arm junctions. (a) The cleavage pattern of J5YLG is shown as a densitometer trace of the denaturing gel on which the products of the reaction are run. The labeled strand is indicated above each of the five panels, and the numbers indicate the residue number. These positions have been calibrated by the Maxam–Gilbert (1977) G-reaction (Maxam & Gilbert, 1977). The upper portion of each panel (ds) corresponds to each strand in a double-helical environment, while the lower portion (J) indicates the same results when the strand is incorporated into the junction. The two nucleotides that flank the junction (16 and 17) are indicated by a "J" to facilitate interpretation. Note that, in every case, the junction is protected to some extent, relative to the double strand. (b) This figure illustrates the same experiment conducted on J6YLG. The same conventions apply as in (a). Note that strand 5 does not appear to be protected relative to the double strand, in contrast to the rest of the strands of J6YLG.

3/20/06   LaBean COMPSCI 296.5

A Solid-Support Methodology for the Construction of Geometrical Objects from DNA

Yuwen Zhang and Nadrian C. Seeman*

Contribution from the Department of Chemistry, New York University, New York, New York 10003. Received August 21, 1991
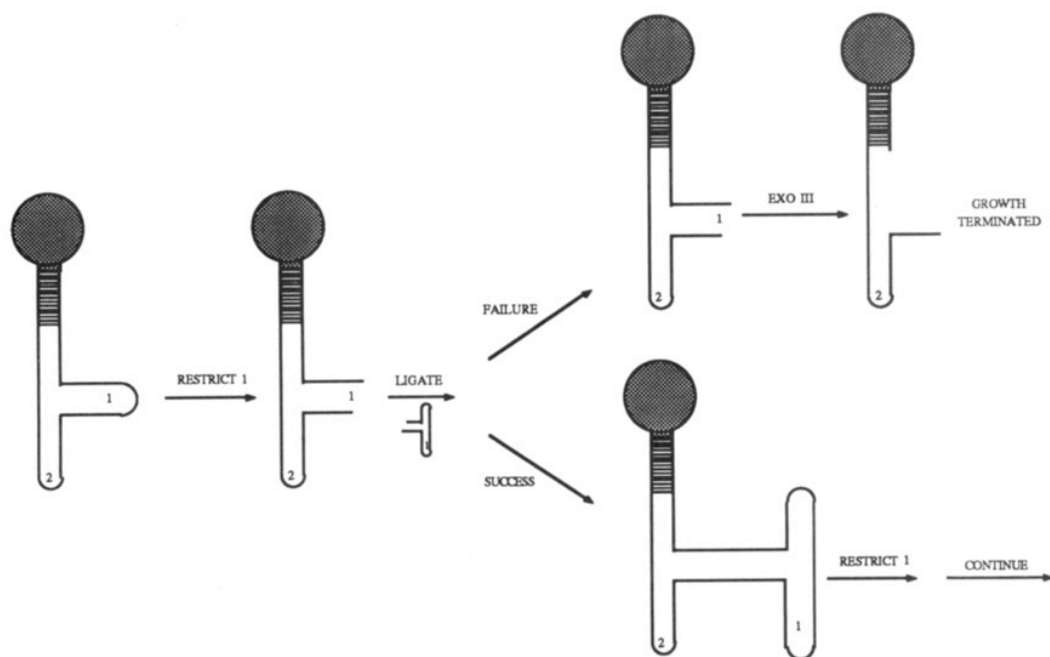
Figure 2. Solid-state synthesis with exonuclease III destruction of unligated material. The solid support is represented as the gray ball, and the cross-link is illustrated as crossbars. The portion below the cross-linked site has a restriction site for removal from the support. This diagram illustrates the use of solid-state synthesis in the first step of a synthesis. We emphasize the case of imperfect yield on a ligation step. Because the successful ligation results in a closed object, exonuclease III treatment only destroys the failure object, not the successful ligation, which can then continue. Thus, synthesis using this strategy destroys failure products, thereby effecting a purification on the support. In a complicated synthesis, the product may not be degraded all the way, but it should still be separable from the successful product.
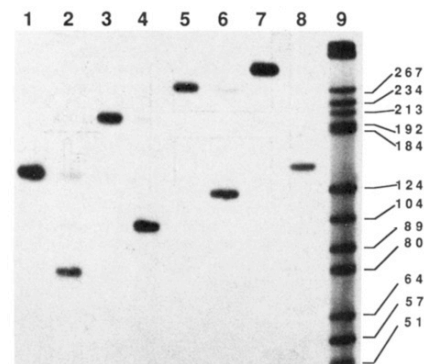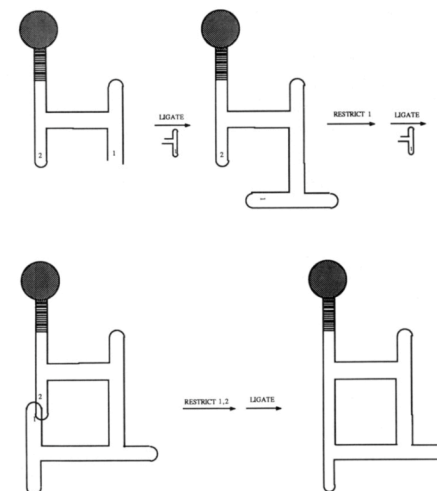
Figure 3. Stepwise restriction and ligation in the formation of a quadrilateral. This is an autoradiogram of an 8% denaturing gel, illustrating

Construction of a DNA-Truncated Octahedron

Yuwen Zhang and Nadrian C. Seeman[*]

Abstract: A covalently closed molecular complex whose double-helical edges have the connectivity of a truncated octahedron has been assembled from DNA on a solid support. This three-connected Archimedean solid contains six squares and eight hexagons, formed from 36 edges arranged about 24 vertices. The vertices are the branch points of four-arm DNA junctions, so each vertex has an extra exocyclic arm associated with it. The construct contains six single-stranded cyclic DNA molecules that form the squares and the extra arms; in addition, there are eight cyclic strands that correspond to the eight hexagons. The molecule contains 1440 nucleotides in the edges and 1110 in the extra arms; the estimated molecular weight for the 2550 nucleotides in the construct is 790 kDa. Each edge contains two turns of double-helical DNA, so that the 14 strands form a catenated structure in which each strand is linked twice to its neighbors along each edge. Synthesis is proved by demonstrating the presence of each square in the object and then by confirming that the squares are flanked by tetracatenane substructures, corresponding to the hexagons. The success of this synthesis indicates that this technology has reached the stage where the control of topology is in hand, in the sense of both helix axis connectivity and strand linkage.

LaBean COMPSCI 296.5
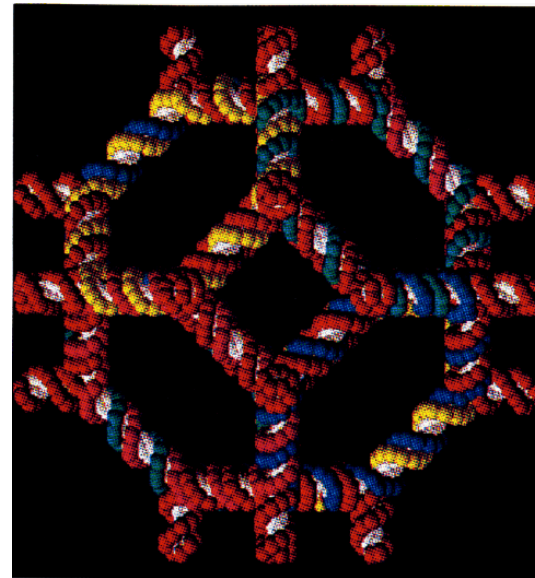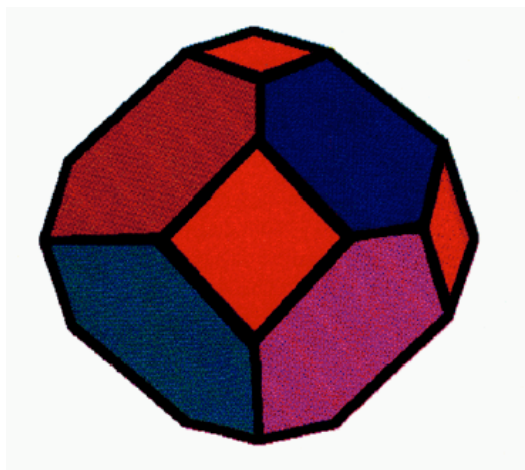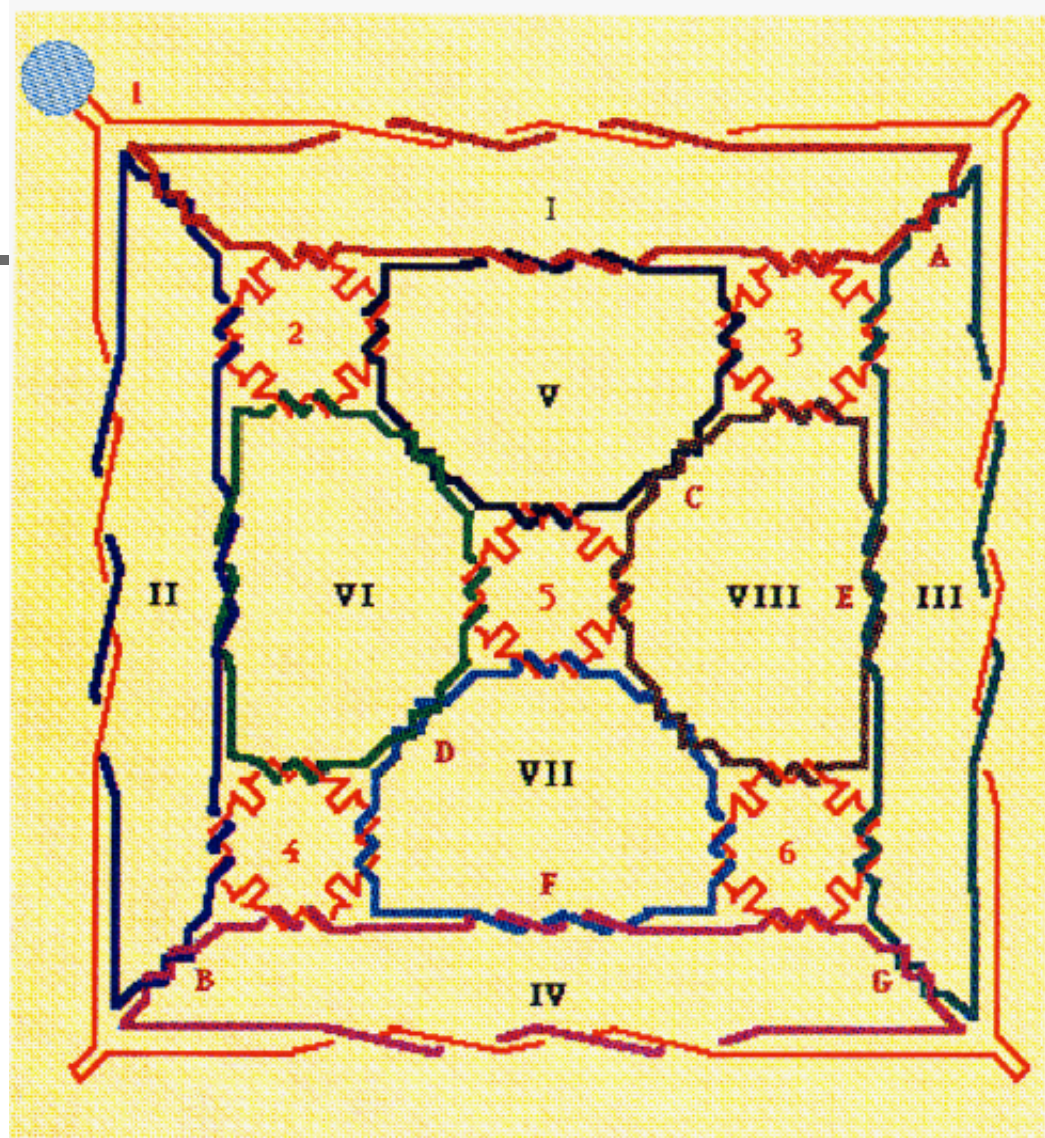
SQUARE ASSEMBLY

TETRASQUARE ASSEMBLY

LaBean COMPSCI 296.5
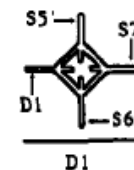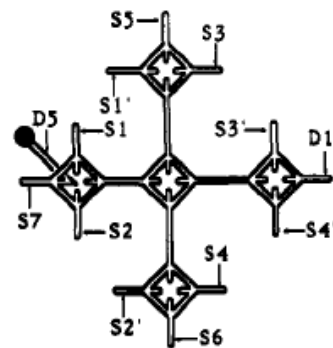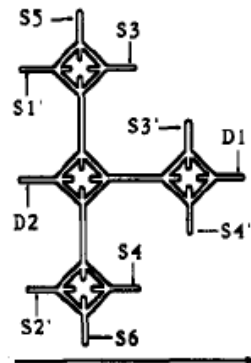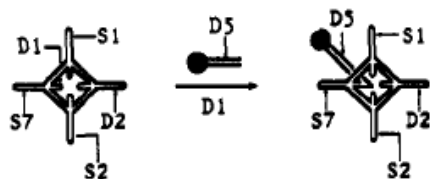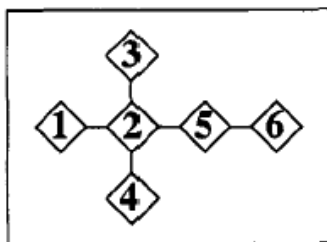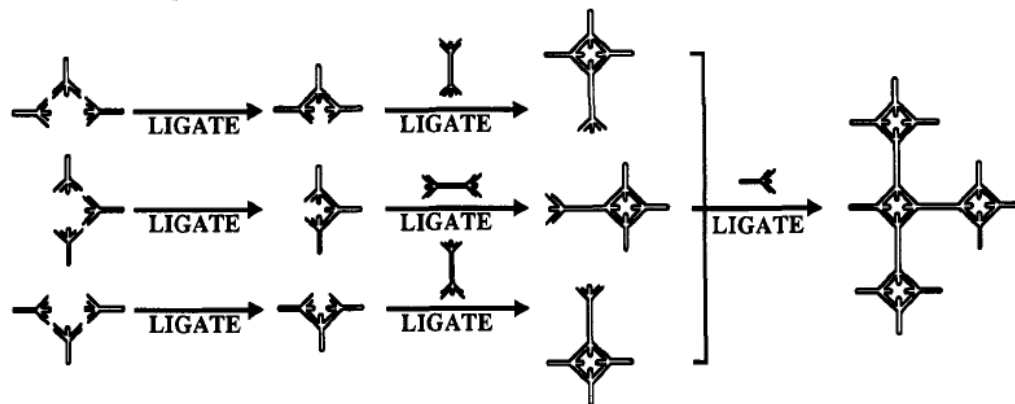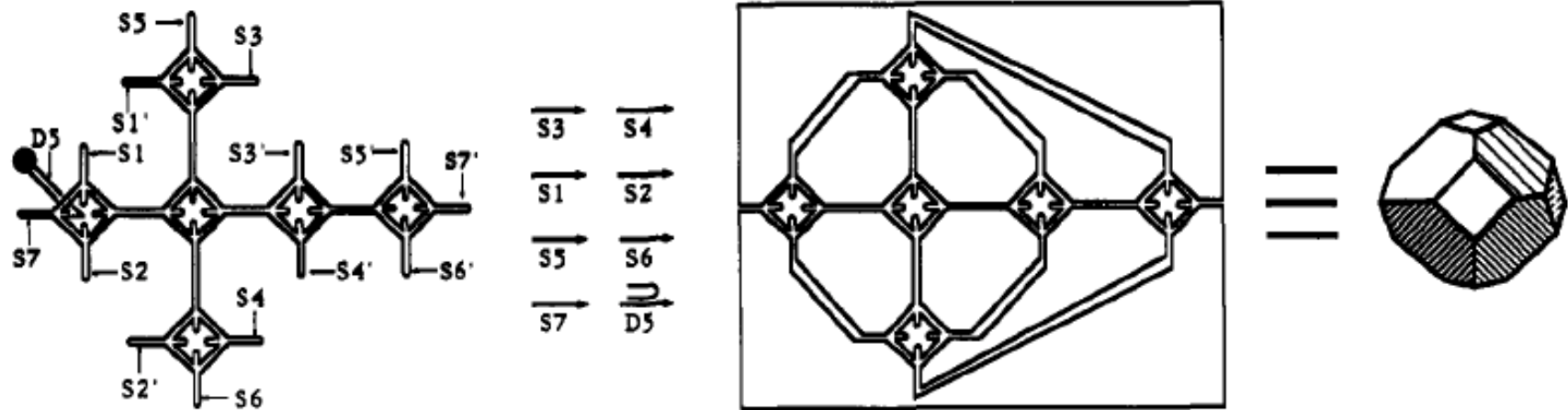
- Gel evidence of successful synthesis.
- Yield = 15 femtomoles (3X more than yield of cube using solution phase chemistry!)
- Problems noted with restriction enzymes and ligase.
- Automation desirable.

Ligation of Triangles Built from Bulged 3-Arm DNA Branched Junctions

Jing Qi, Xiaojun Li, Xiaoping Yang, and Nadrian C. Seeman*

Abstract: An important stepping stone to controlled construction on the nanometer scale is the development of rigid components, building blocks whose directions of bonding bear fixed angular relationships to each other. We are exploring nanoconstruction with branched DNA junctions. Branched junctions with three and four arms are known to be flexible, but 3-arm branched junctions containing bulges are known to have a preferred stacking direction. Here, we have tested the rigidity of equilateral triangles whose vertices are all bulged 3-arm branched junctions. There are two kinds of equilateral triangles with an integral number of turns per edge that can be made from these components: those with the bulges on the inside strand, and those with the bulges on the outside strand. Alternating the two species generates a reporter strand. Each triangle is assembled and purified as a topologically closed species. Assembly of the triangle with the bulges on the inner strand results in two topoisomers that can be separated. Sticky ends are generated on the triangles by restricting their external arms. Incompletely restricted triangles and completely restricted hairpins are removed by binding magnetic streptavidin beads to biotin groups incorporated in the hairpins. Assembly of rigid triangles would result in a closed hexamer of triangles. Ligation experiments have been performed, in which twisting was varied about the expected values. In all cases, the primary intact product is seen to be the cyclic tetramer. Thus, triangles with bulged 3-arm branched junctions at the vertices do not constitute a rigid component :
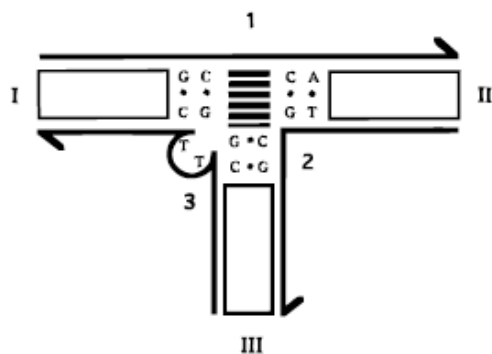
Leontis and colleagues have shown that these molecules are more stable than conventional 3-arm branched junctions. The structural basis of this finding has been confirmed by NMR to be a stacking arrangement between two of the arms of the junction.

3/20/06 LaBean COMPSCI 296.5

APPLY DIRECTLY   **EXONUCLEASE FIRST**

DENATURING GEL AUTORADIOGRAM

LINEAR AND CYCLIC MOLECULES

CYCLIC MOLECULES
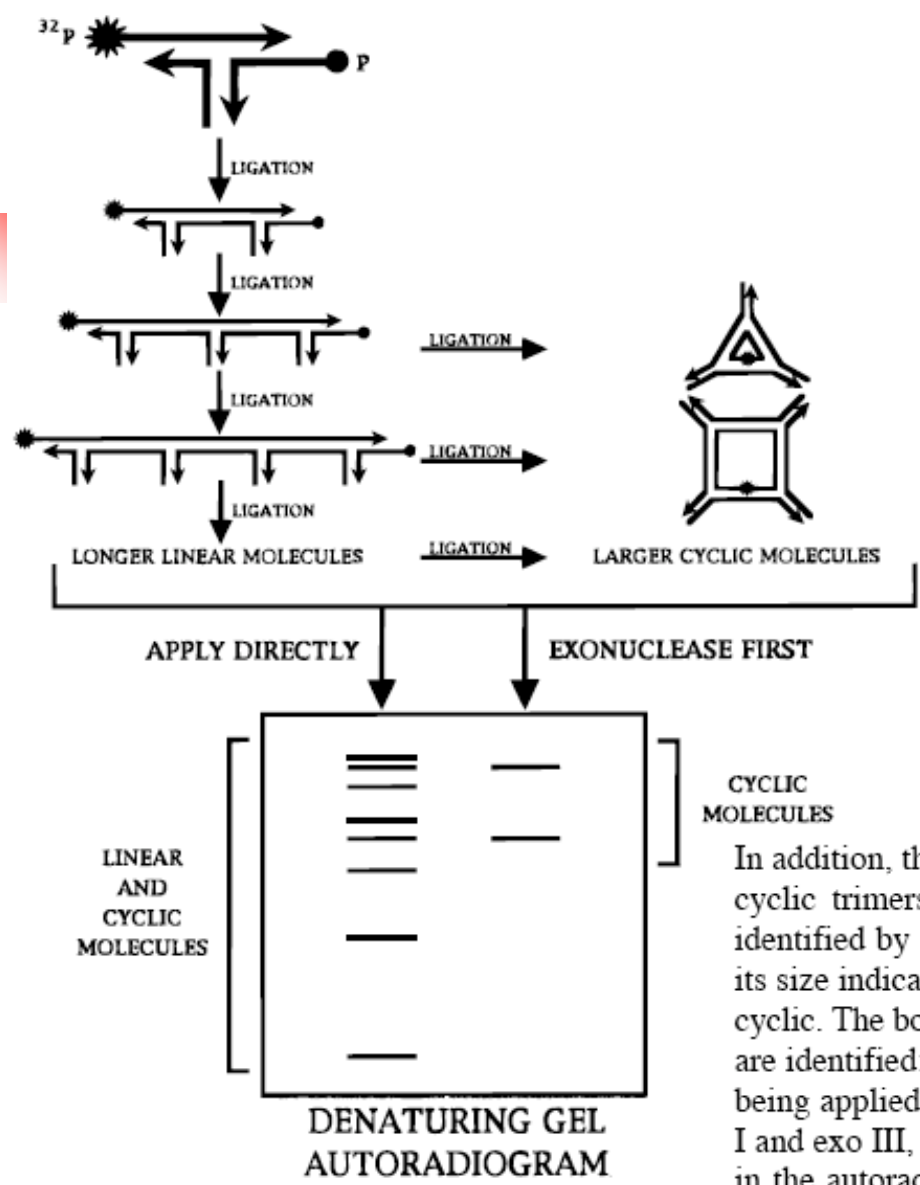
In addition, the linear trimer and the linear tetramer are shown to form cyclic trimers and cyclic tetramers. Note that each product can be identified by the identification of the radioactive strand. If it is linear, its size indicates the extent of oligomerization. The same is true if it is cyclic. The bottom portion of the drawing shows how the cyclic strands are identified: The products of ligation are run on a denaturing gel by being applied directly, or after treatment by exonucleases, such as exo I and exo III, which are used here; only the reporter strands are visible in the autoradiogram. The cyclic molecules are resistant to treatment by exonucleases, whereas the linear strands are digested.
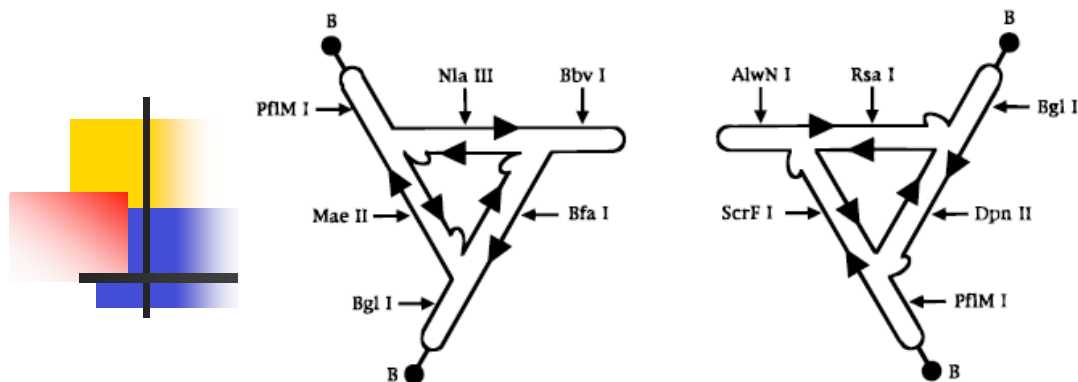
Figure 2. Equilateral triangles built from three bulged 3-arm DNA branched junctions. Two triangles are illustrated. Each contains a bulged 3-arm branched junction at each vertex. The arrowheads indicate the strand polarities, and the bulges are indicated schematically as rounded segments of the chain. The two triangles shown are 3-fold symmetric equilateral triangles, with the same number of double helical turns in each edge. The strand structure has been simplified so that it is drawn as parallel lines. This is valid, so long as each edge contains an integral number of double helical turns. These are not the only triangles possible;
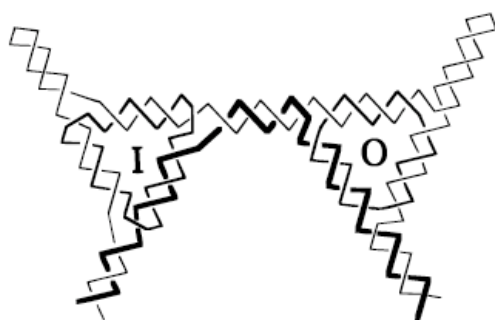
Figure 3. A helical diagram representing the reporter strand formed
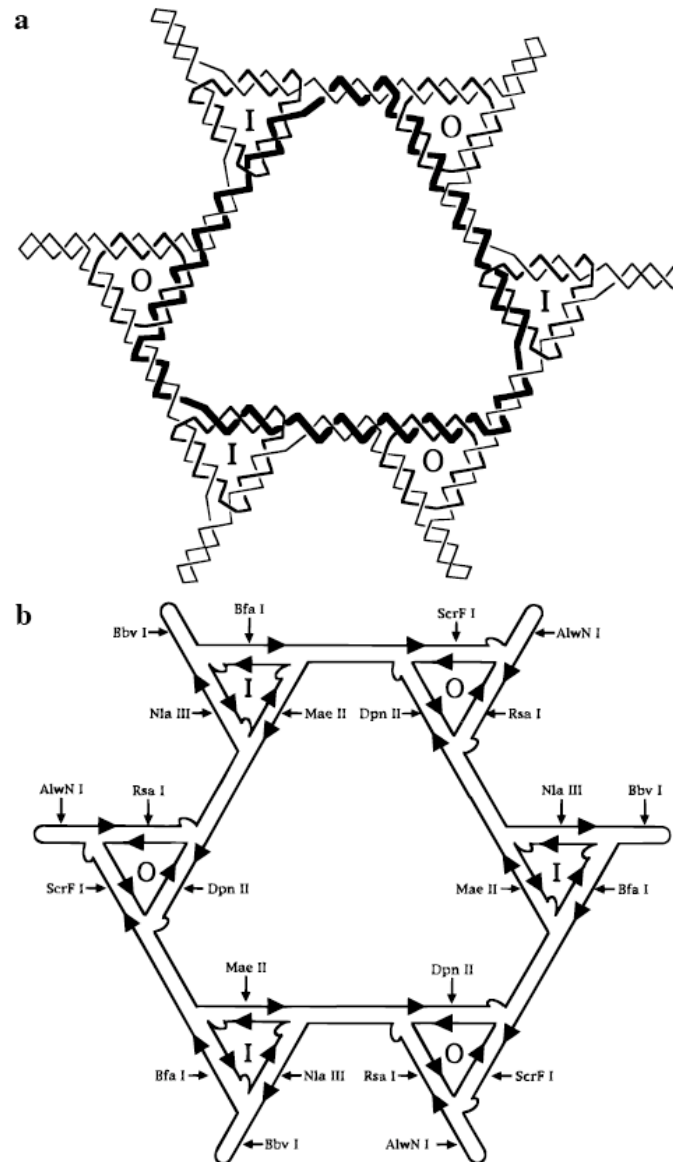
Figure 4. The target molecule to be formed if the bulged triangles are rigid components. (a) A helical diagram of the target molecule.
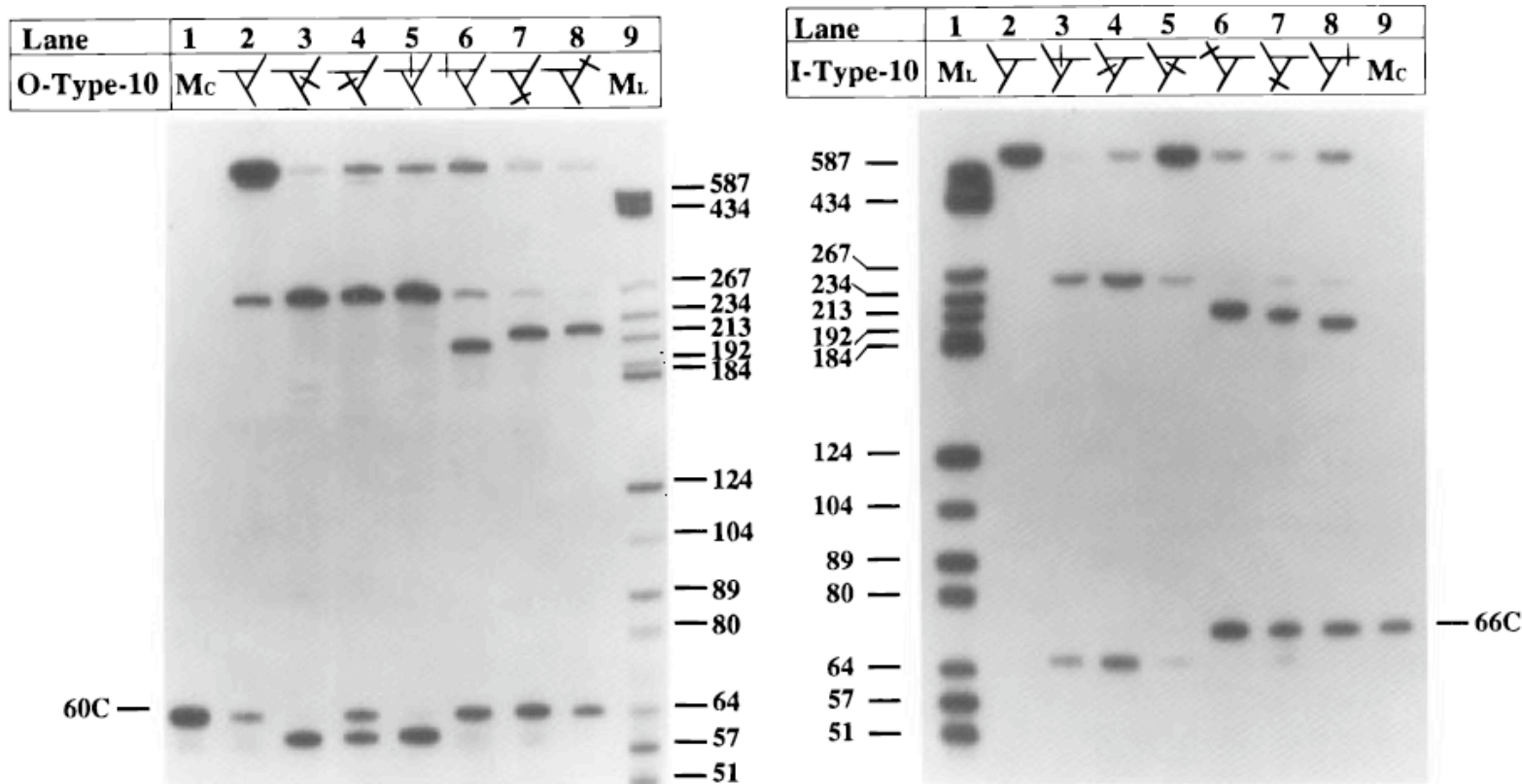
Figure 6. Characterization of the Triangles. These are both autoradiograms of 20% formamide denaturing gels. Circular markers are in a lane labeled "Mc" and linear markers are in a lane labeled "ML". Above each lane a triangle, including its external arms is drawn schematically (e.g., lane 2). The site of scission by a restriction endonuclease is indicated by a line perpendicular to the triangle, either through an edge (lanes 3−5), or through an external arm (lanes 6−8). (a, left) The O-type triangle. Lane 1 contains a 60-mer circular marker, and lane 9 contains a pBR322-Hae III digest that generates linear markers. The material in lane 2 is undigested O-type triangle. Some breakdown of the triangle is seen in this lane. Lanes 3−5 respectively contain the digestion of this triangle by the edge-cleaving restriction enzymes Dpn I, ScrF I, and Rsa I. Lanes 6−8 respectively contain the digestion of this triangle by external-arm digestion enzymes Bbv I, Bbs I, and BsmA I. These sites were later modified to those shown in Figure 2, when the enzymes were found to be ineffective for purposes of ligation. Note that the products of edge-cleavage are all the same, a

Assembly of Borromean rings from DNA

Chengde Mao
Weiqiong Sun
Nadrian C. Seeman*
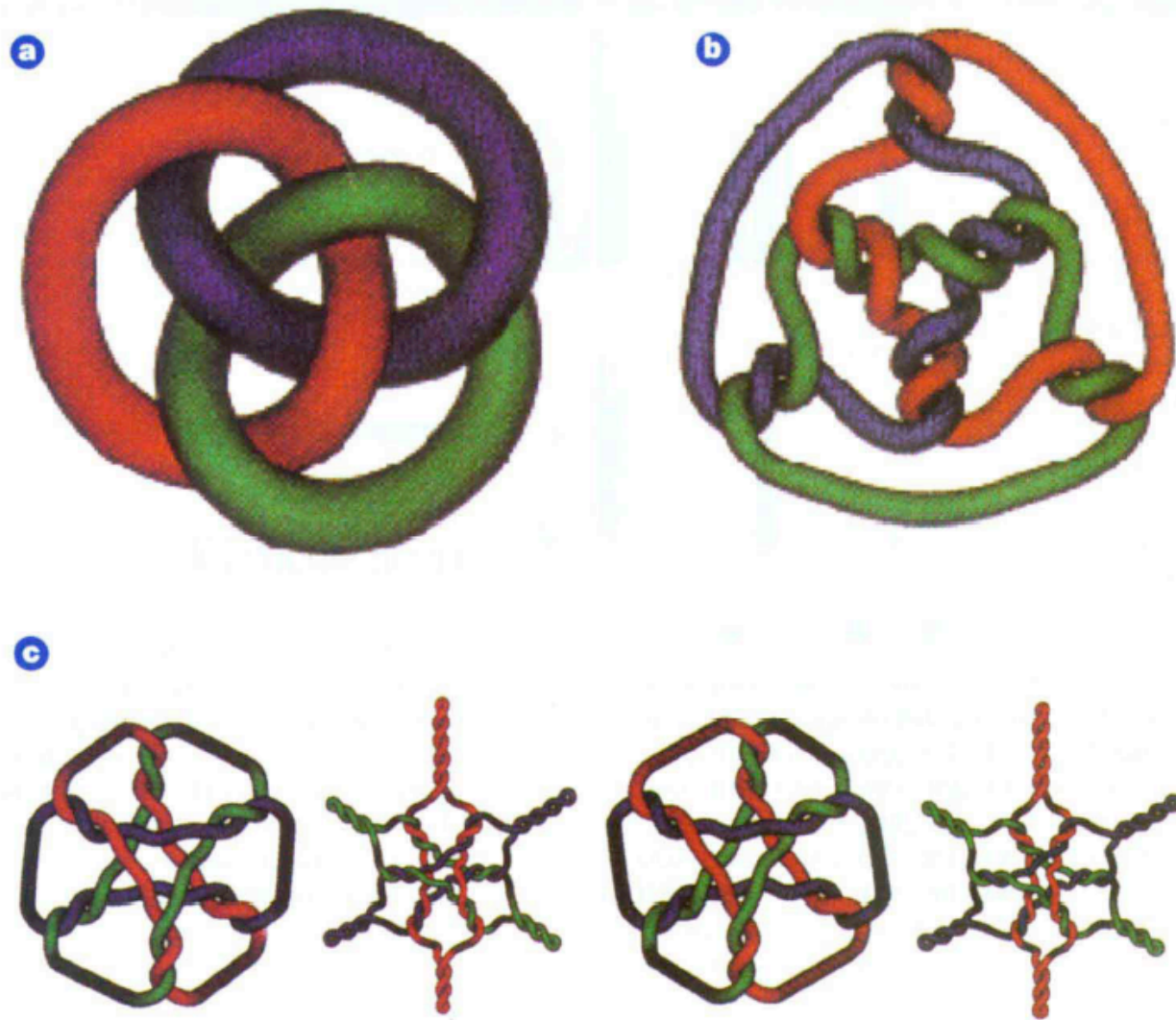
Figure 1 a, **Traditional Borromean rings.** b, Borromean rings with each node replaced by three nodes, derived from 1.5 turns of double helix. The inner double helices are right-handed and the outer double helices are left-handed. c, Left, stereoscopic representation of (b), where a B-DNA junction flanks the 'north pole' and a Z-DNA junction flanks the 'south pole'. Right, stereoscopic views of the molecules synthesized. Two hairpins have been added to the 'equatorial' sections of each strand. Drawings made using the KnotPlot program, written by R. Scharein; http://www.cs.ubc.ca/nest/imager/contributions/scharein/KnotPlot.html

Assembly of Borromean rings from DNA

Chengde Mao
Weiqiong Sun
Nadrian C. Seeman*
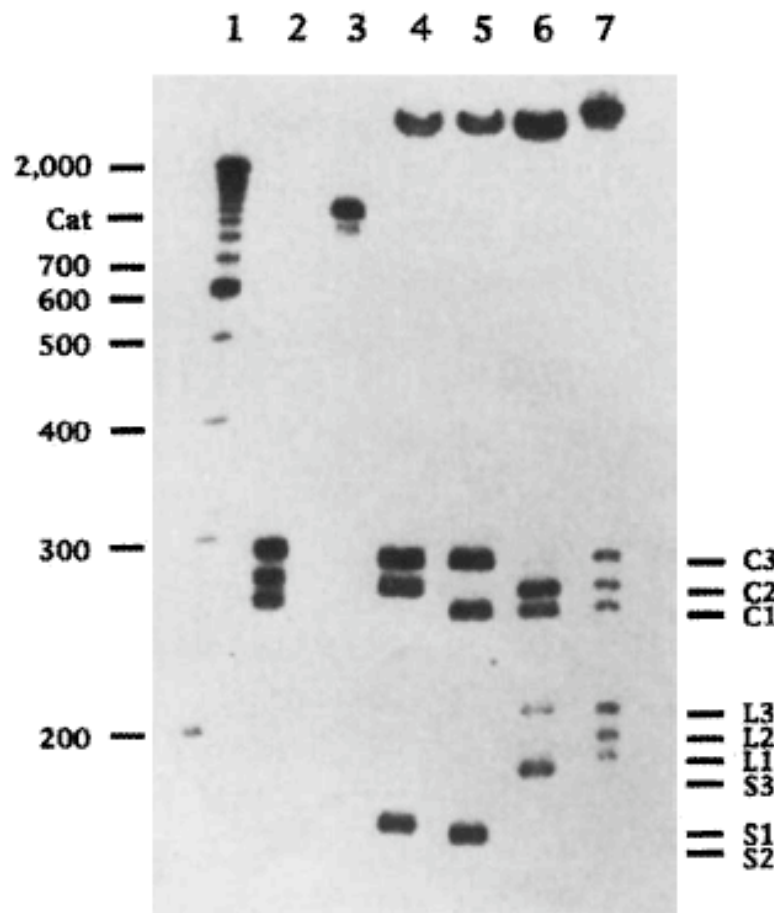
Figure 2 **Analysis of the Borromean DNA.**
A 6% polyacrylamide denaturing gel containing 40% formamide is shown. Lane 1, 100-base oligonucleotide DNA ladder (GibcoBRL). Lane 2, three individual circles of 196, 206 and 216 nucleotides (C1, C2 and C3). Lane 3, a catenane of circles 2 and 3. Lanes 4–6, the target Borromean rings and the products of their digestion by *Pvu*II (strand 1), *Eco*RV (strand 2), and *Xba*I (strand 3), respectively. Lane 7, a mixture of the Borromean rings (top), the three individual circles, and their three linear counterparts (L1, L2 and L3). The scission products of the three rings (shorter than linear molecules) are labelled S1, S2 and S3. Traces of linear strand 3 (most heavily labelled) are visible owing to its spontaneous breakdown. Strand sequences and details of the synthesis methods are available at http://seemanlab4.chem.nyu.edu.

Antiparallel DNA Double Crossover Molecules As Components for Nanoconstruction

Xiaojun Li, Xiaoping Yang, Jing Qi, and Nadrian C. Seeman*

Abstract: Double crossover molecules are DNA structures containing two Holliday junctions connected by two double helical arms. There are several types of double crossover molecules, differentiated by the relative orientations of their helix axes, parallel or antiparallel, and by the number of double helical half-turns (even or odd) between the two crossovers. We have examined these molecules from the viewpoint of their potential utility in nanoconstruction. Whereas the parallel double helical molecules are usually not well behaved, we have focused on the antiparallel molecules; antiparallel molecules with an even number of half turns between crossovers (termed DAE molecules) produce a reporter strand when ligated, so these have been characterized in a ligation cyclization assay. In contrast to other molecules that contain branched junctions, we find that these molecules cyclize rarely or not at all. The double crossover molecules cyclize no more readily than the linear molecule containing the same sequence as the ligation domain. We have tested both a conventional DAE molecule and one containing a bulged three-arm branched junction between the crossovers. The conventional DAE molecule appears to be slightly stiffer, but so few cyclic products are obtained in either case that quantitative comparisons are not possible. Thus, it appears that these molecules may be able to serve as the rigid components that are needed to assemble symmetric molecular structures, such as periodic lattices. We suggest that they be combined with DNA triangles and deltahedra in order to accomplish this goal.
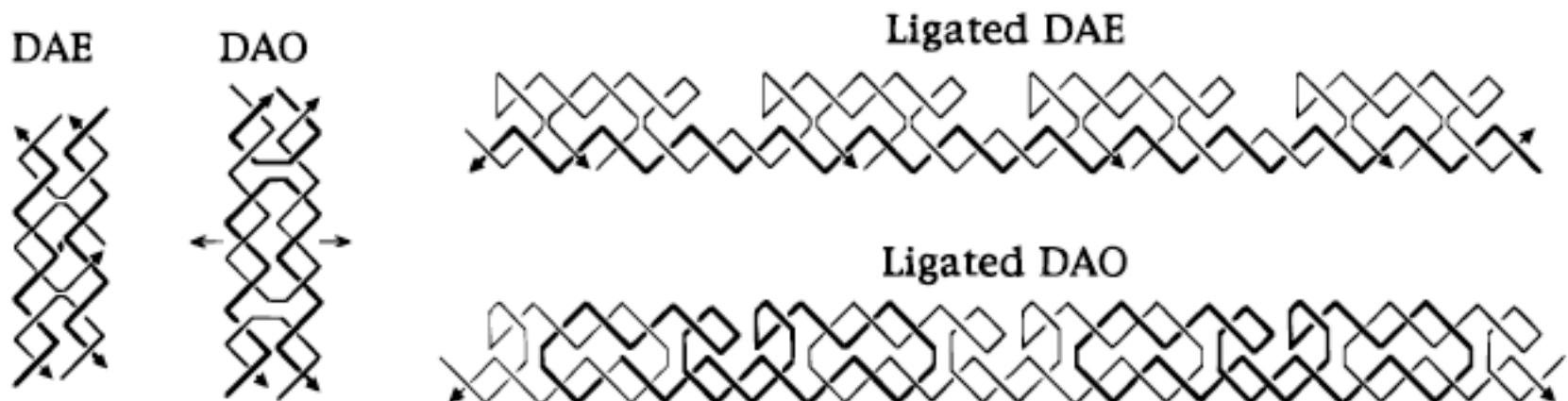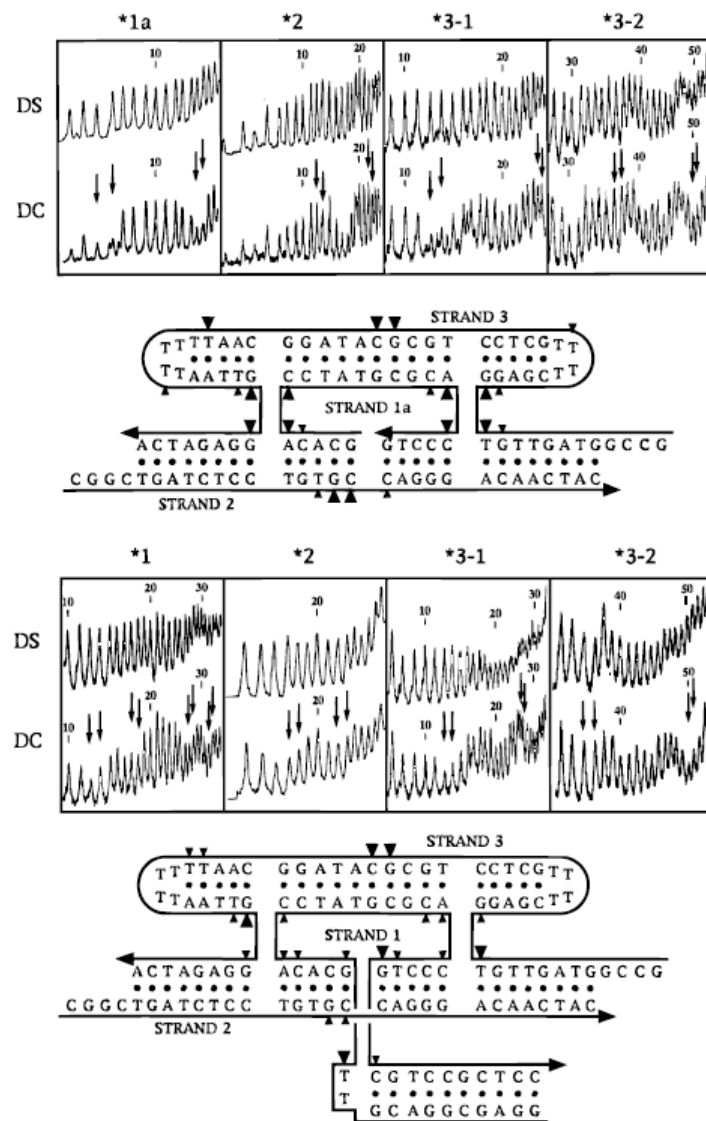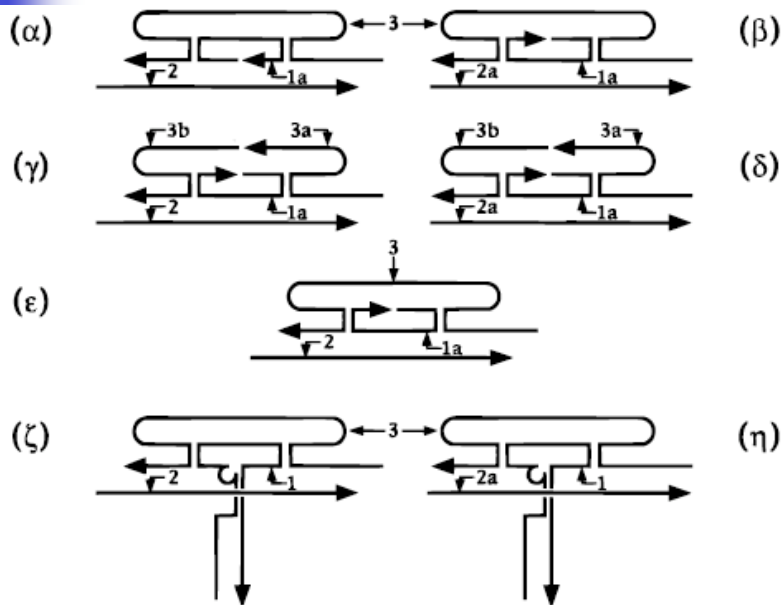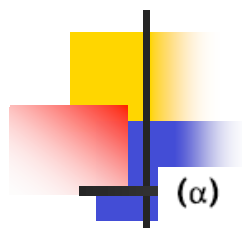
Figure 3. Hydroxyl radical cleavage patterns of the DAE molecules. (a) The conventional DAE molecule. The densitometer traces for each strand are shown above a summary drawn on the sequence of the molecule. Each panel shows the strand that has been labeled at the top. The double strand (DS) is compared with the double crossover (DC). The arrows indicate the sites of the crossovers. Residues are
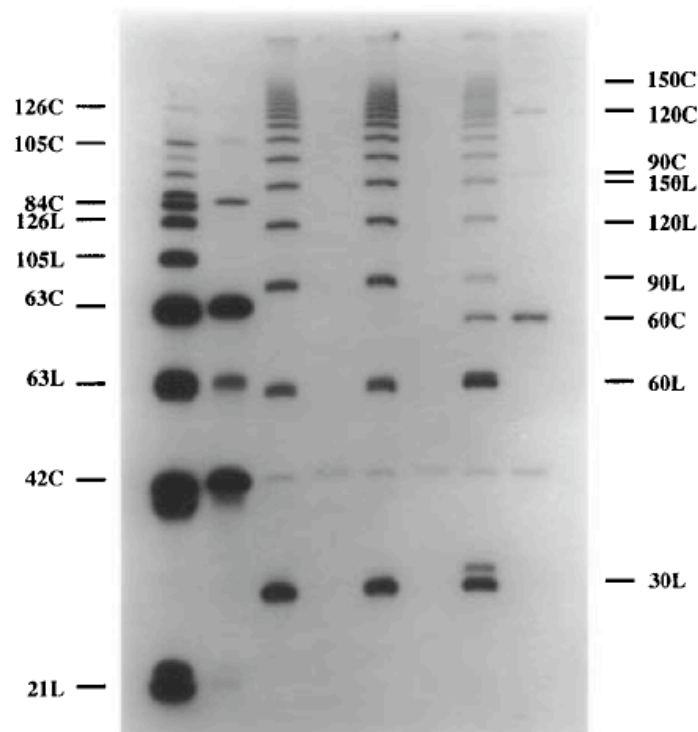
Figure 4. Ligation of DAE Molecules. (a) The Conventional DAE Molecule. This is an autoradiogram of a denaturing gel. Lanes 1 and 2 contain a standard three-arm branched junction,[41] "JY21", that generates linear and circular markers at a separation of 21 nucleotides; lane 2 has been treated with exonucleases, to yield only a 21-mer single-stranded circular DNA ladder. Linear markers are indicated by the suffix "L", and single-stranded cyclic markers are indicated by the suffix "C". Lanes 3–8 contain the DAE molecule (3–6) or its doubly nicked version. The column heading "DX" refers to double crossover molecules. A fixed amount of a cyclic 42-mer has been added to each of lanes 3–8, so that the intensity of each lane can be compared directly, regardless of the total radioactivity of the lane. Lanes 3 and 5 contain ligation ladders of labeled strand 2 of the DAE molecule (molecule α, Figure 1b), lanes 4 and 6 have been treated with exonucleases I and III, and lane 6 has also been treated with Hha I restriction endonuclease. No cyclic material is visible in these lanes. Any that appeared in lane 4 would correspond to single strand ligations,

DX tiles

- Longer ligation products (increase from 7 units to 17 units).
- No circular products.
- Nanocomponent at least as rigid as dsDNA.

In what way can the stiffness of DAE or DAO molecules be used in the construction of complex DNA materials? One could imagine the construction of a lattice of DAE or DAO molecules that would contain parallel and antiparallel helix axis vectors; its direct physical applications are not obvious, although it has been suggested for use in DNA computing.[47]

(47) Winfree, E. In: *DNA Computing*; Baum, E., Lipton, R., Eds.; American Mathematical Society: In press.
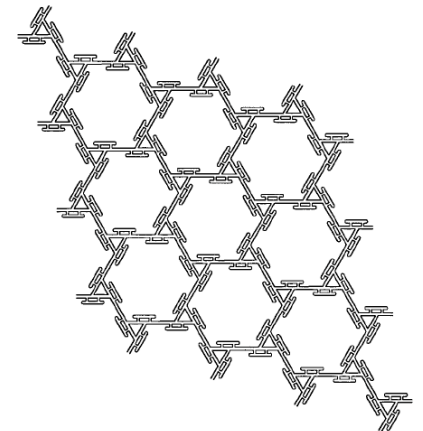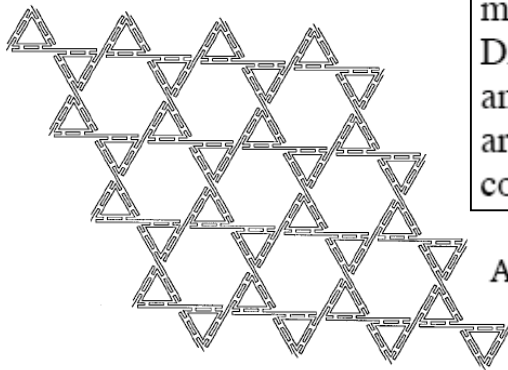
DNA NANOTECHNOLOGY:
Novel DNA Constructions

Nadrian C. Seeman
Department of Chemistry, New York University, New York, NY
e-mail: ned.seeman@nyu.edu
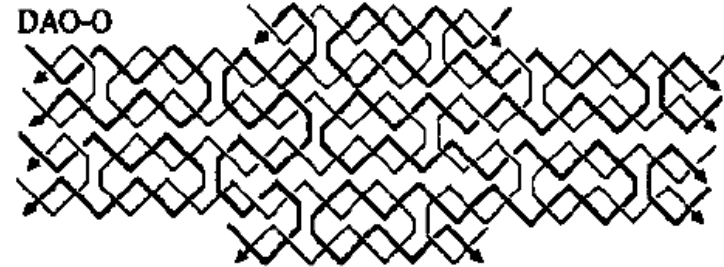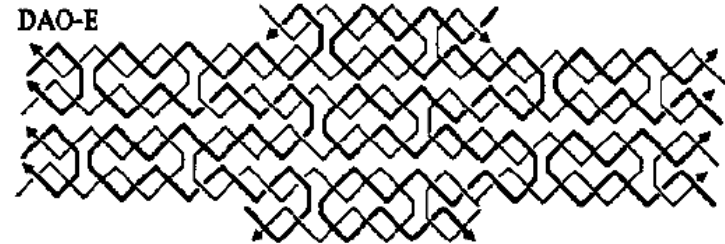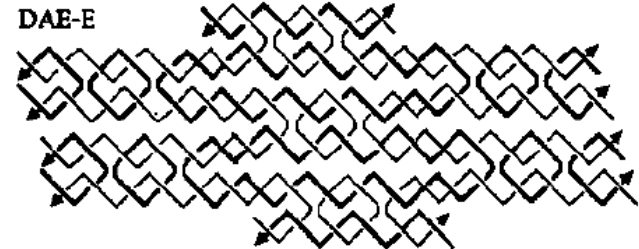
DNA Nicks and Nodes and Nanotechnology

Nadrian C. Seeman*

Department of Chemistry, New York University, New York, New York 10012

Figure 4. *Reciprocal exchange between a hairpin and a 4-arm junction produces a 5-arm junction.* A 4-arm junction is shown on the left, with each strand colored individually. The dark green hairpin fuses with the purple strand to produce a 5-arm junction. The green and purple strand colors are conserved to show the origin of the strands constituting the fifth arm. A symmetrized version of the molecule is shown at the far right.

Reciprocal Exchange in a Double Helical Context
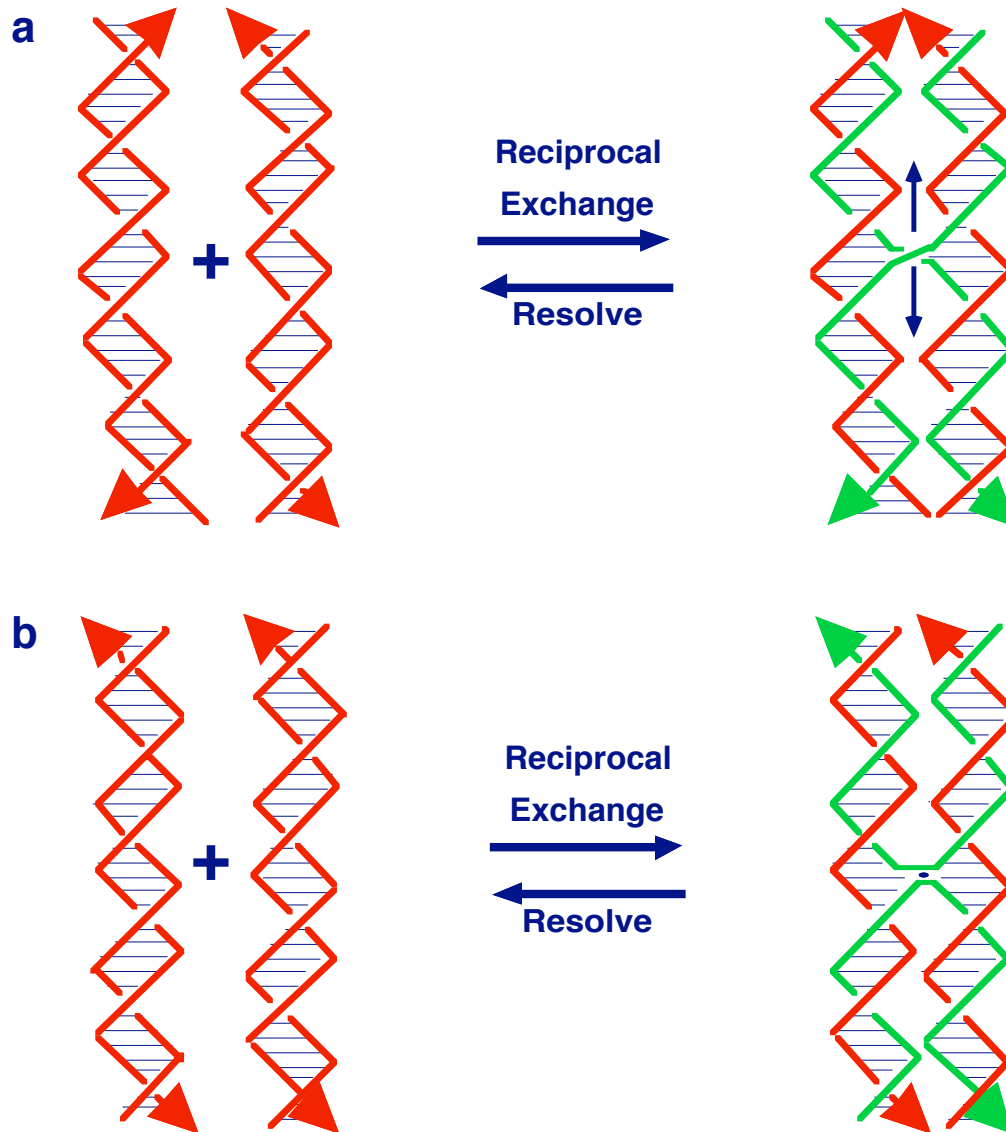
Derivation of DX+J Molecules

DX

HP

DX+J

+

Reciprocal Exchange

Resolve

Seeman, N.C. (2001) *NanoLetters* **1**, 22-26.
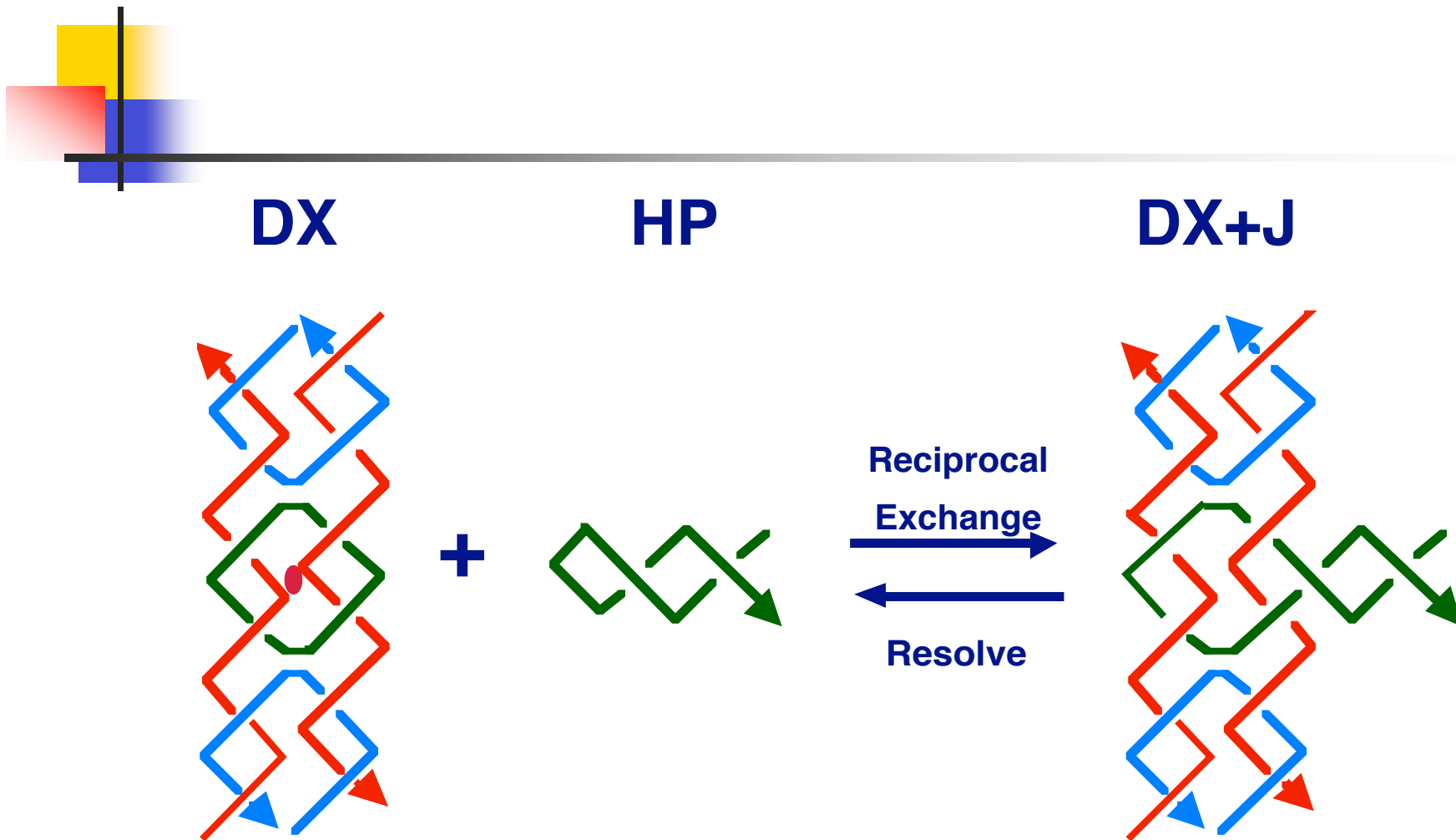
Design and self-assembly of two-dimensional DNA crystals

Erik Winfree*, Furong Liu†, Lisa A. Wenzler† & Nadrian C. Seeman†

* Computation and Neural Systems, California Institute of Technology, Pasadena, California 91125, USA
† Department of Chemistry, New York University, New York, New York 10003, USA
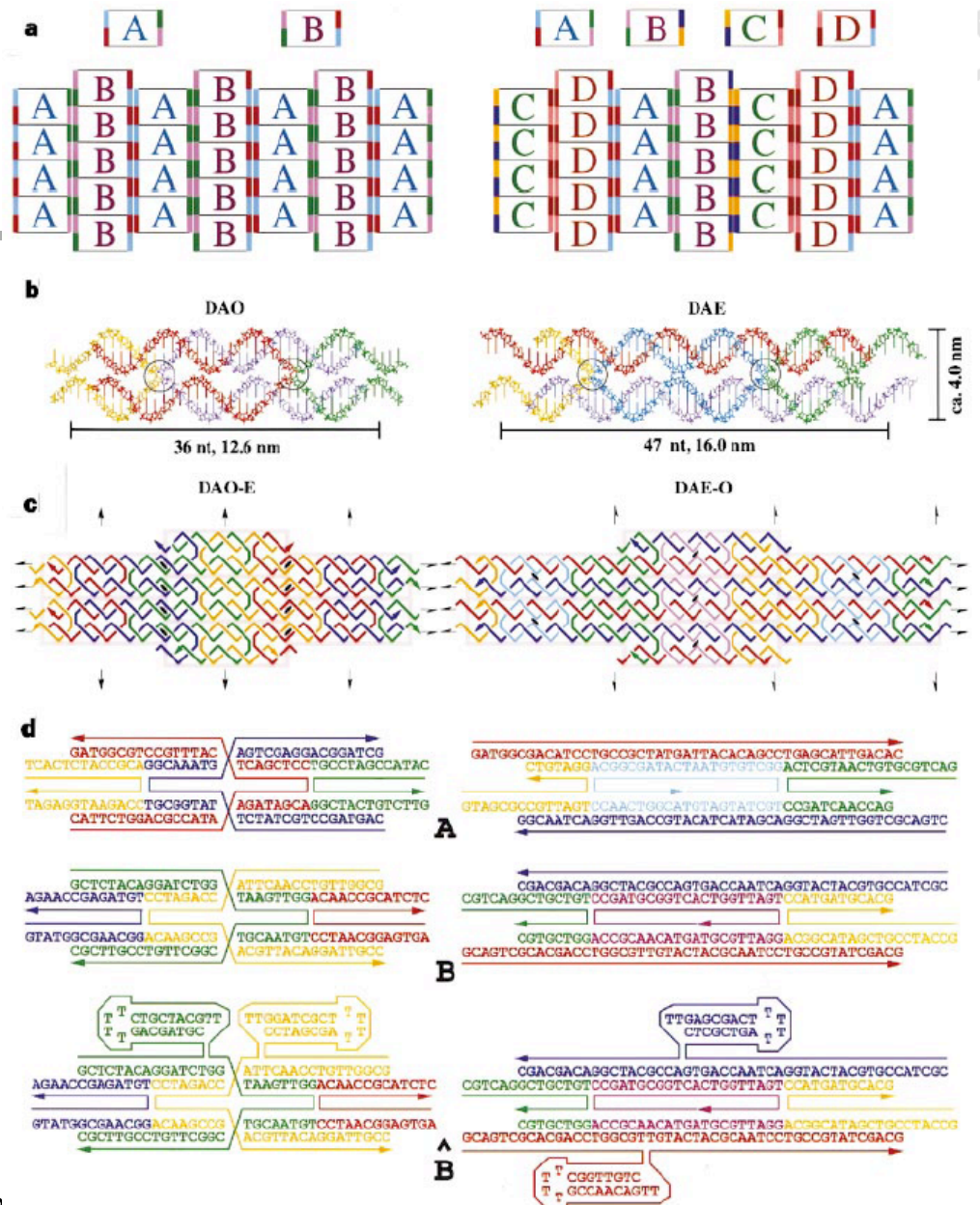
3/20/06   LaBe
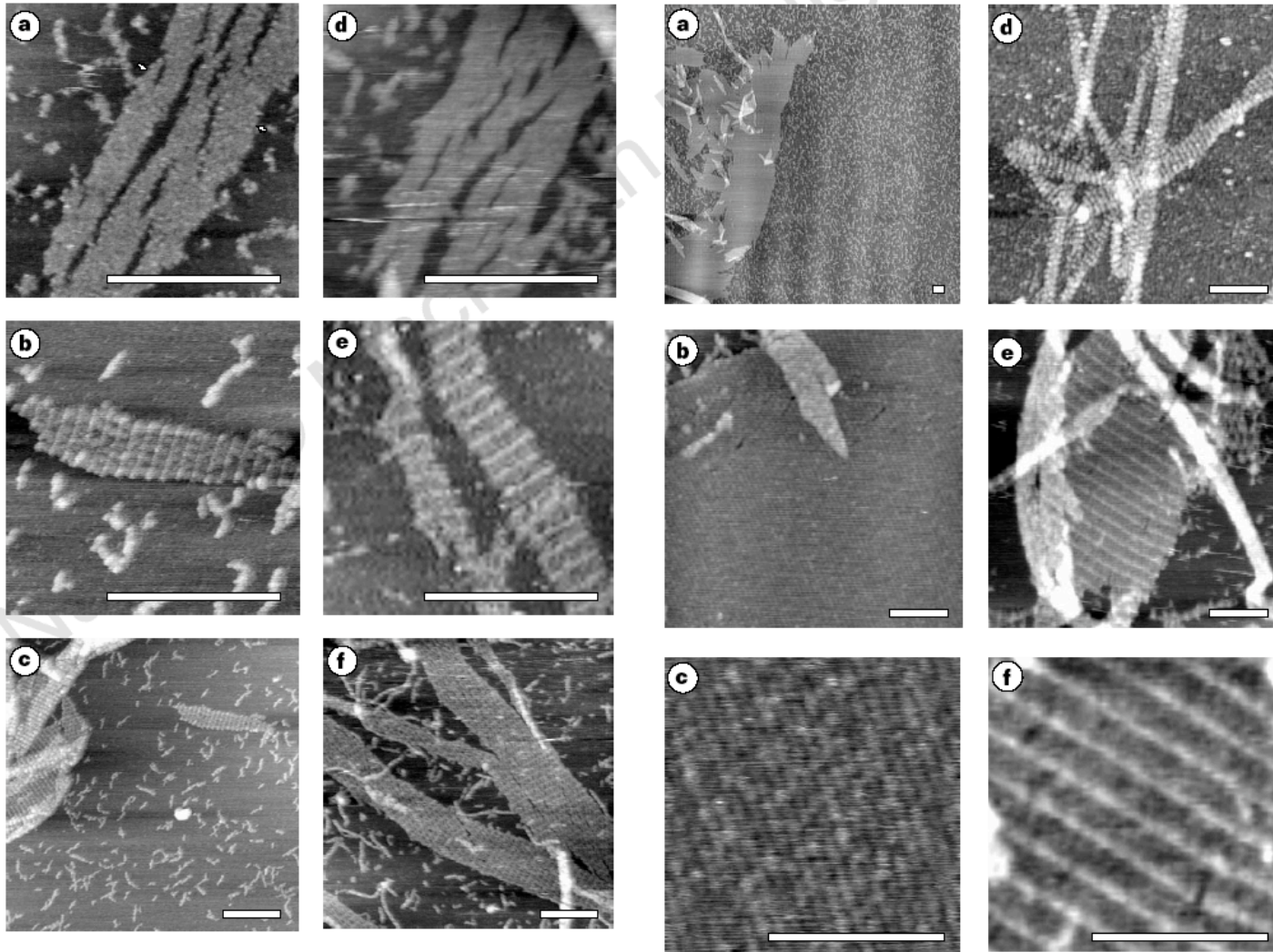
Figure 3 AFM images of two-unit lattices. **a**, DAO-E **AB** lattice. A possible vertical column is indicated by the arrows. Fourier analysis shows 13 ± 1 nm periodicity; each DAO is 12.6 nm wide. **b** and **c**, DAO-E **AB̂** lattice (two views of the same sample). Stripes have 25 ± 2 nm periodicity; the expected value is 25.2 nm. **d**, DAE-O **AB** lattice. **e** and **f**, DAE-O **AB̂** lattice (for different samples, see Methods). Stripes have 33 ± 3 nm periodicity; the expected value is 32 nm. All scale bars are 300 nm; images show 500 × 500 nm or 1.5 × 1.5 μm. The grey scale indicates the height above the mica surface; the apparent lattice height is between 1 and 2 nm.

Figure 4 AFM images showing large crystals and modifications of lattice periodicity and surface features. **a–c**, DAO-E **AB̂** lattice at three levels of detail (all the same sample). The largest domain is ~2 × 8 μm, and contains ~500,000 DX units. **d**, DAE-O **AB** lattice in which **B** has been labelled with biotin–streptavidin–nanogold. **e** and **f**, DAE-O **ABCD̂** lattice at two levels of detail (the same sample). Stripes have 66 ± 5 nm periodicity; the expected value is 64 nm. All scale bars are 300 nm; images show 500 × 500 nm, 1.5 × 1.5 μm, or 10 × 10 μm. The grey scale indicates the height above the mica surface; the apparent lattice height is between 1 and 2 nm.

2D DX lattice

Schematic of a Lattice Containing
1 DX Tile and 1 DX+J Tile

AFM of a Lattice Containing
1 DX Tile and 1 DX+J Tile

~33 nm

0   492 nm

A$\hat{B}$

2 x 15.98 nm
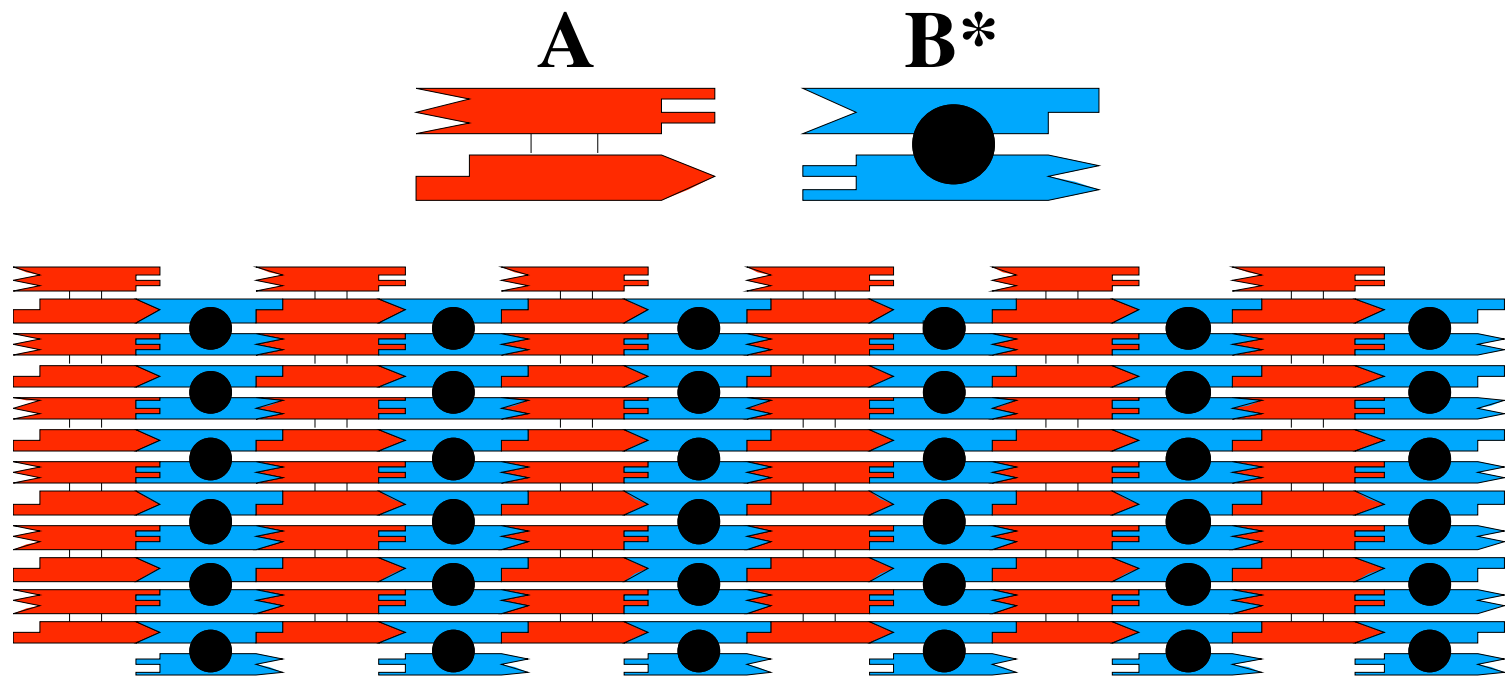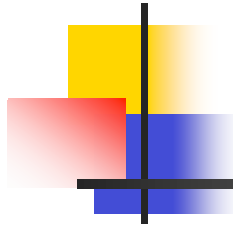
Winfree, E., Liu, F., Wenzler, L.A. & Seeman, N.C. (1998), *Nature* **394**, 539-544.
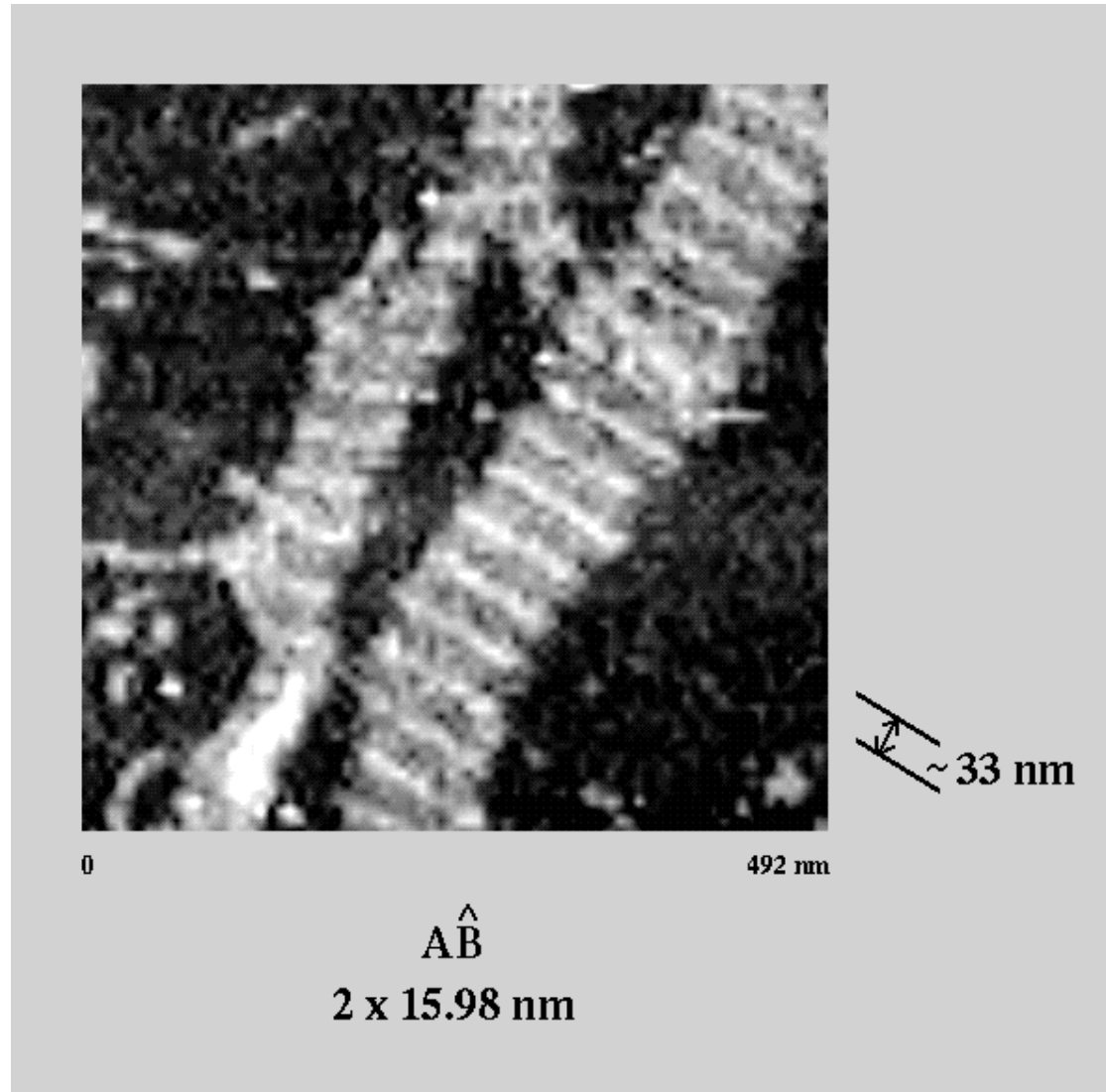
Schematic of a Lattice Containing 3 DX Tiles and 1 DX+J Tile

AFM of a Lattice Containing
3 DX Tiles and 1 DX+J Tile

~65 nm

0   500 nm

ABCD̂

4 x 15.98 nm
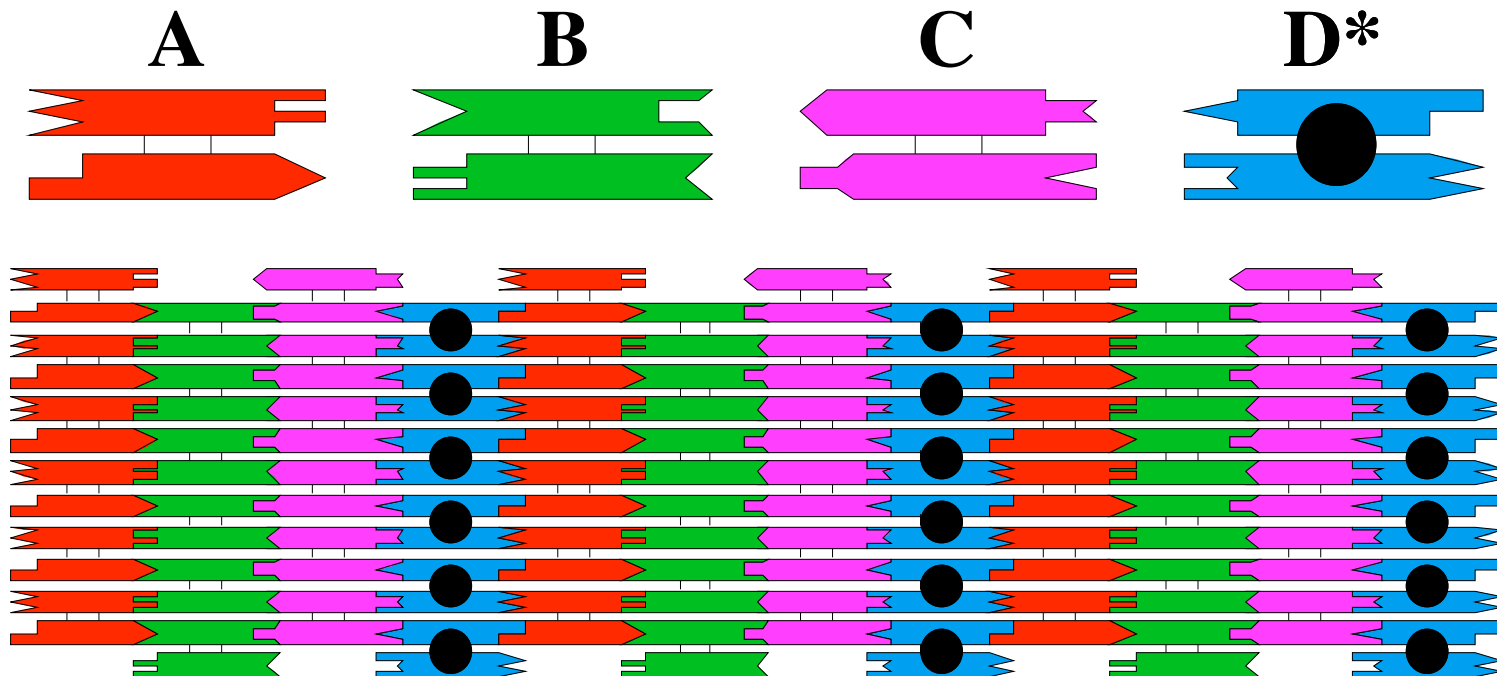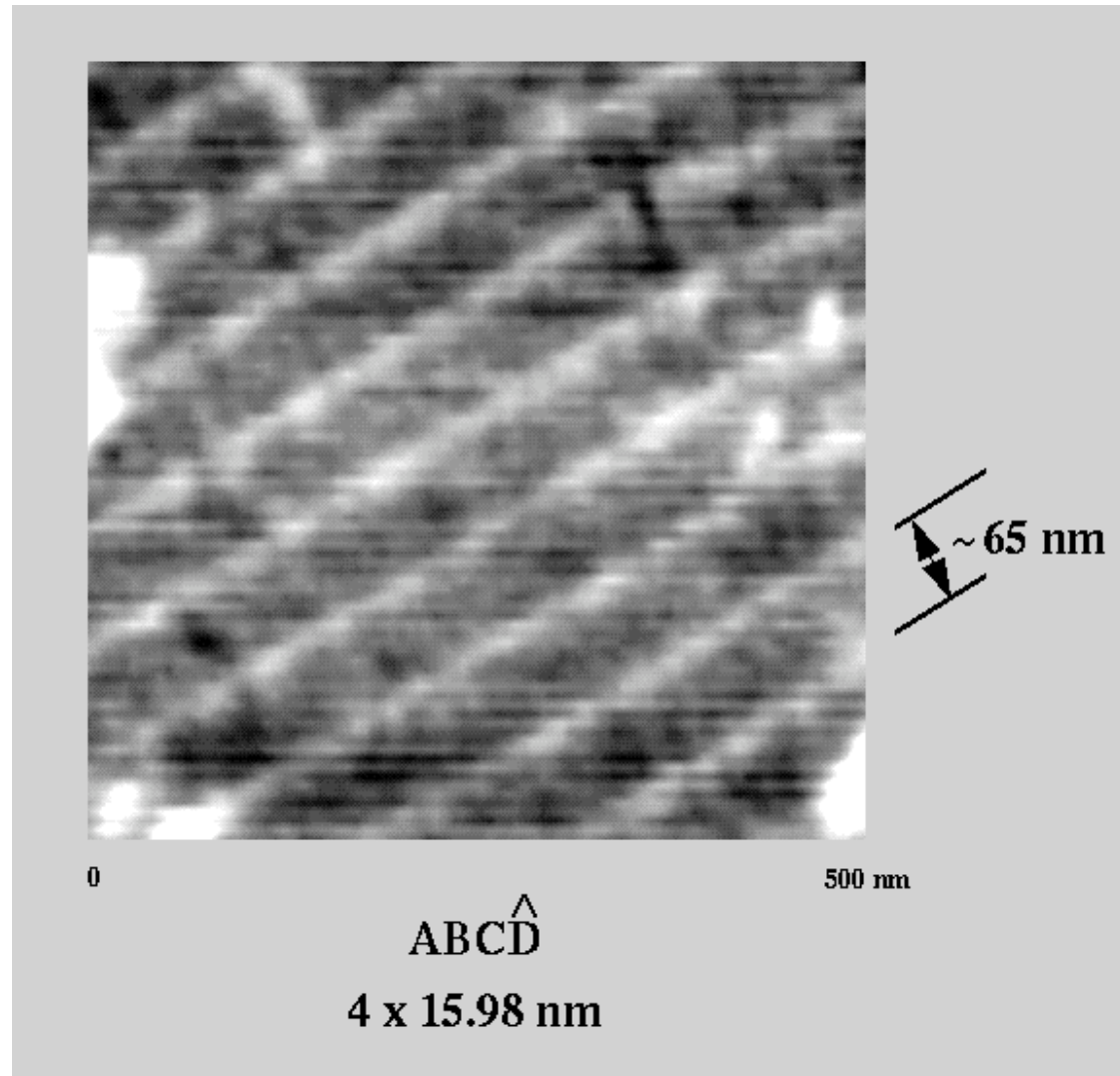
Winfree, E., Liu, F., Wenzler, L.A. & Seeman, N.C. (1998), *Nature* **394**, 539-544.

Modifying the Surface Features of Two-Dimensional DNA Crystals

Furong Liu, Ruojie Sha, and Nadrian C. Seeman*
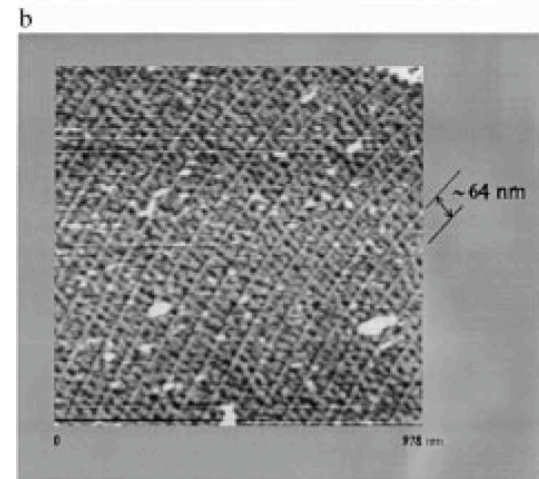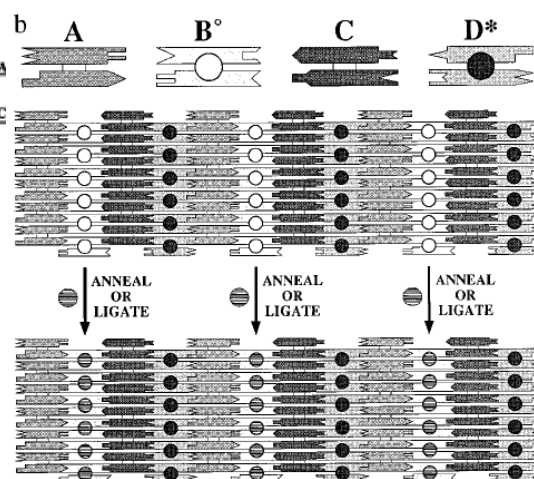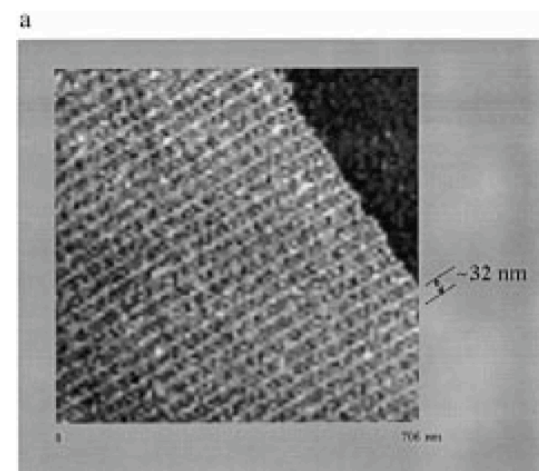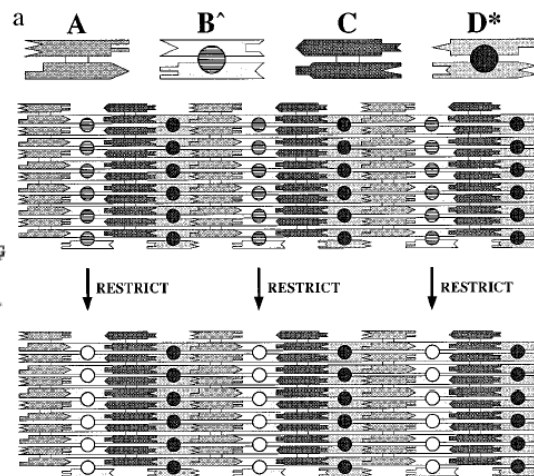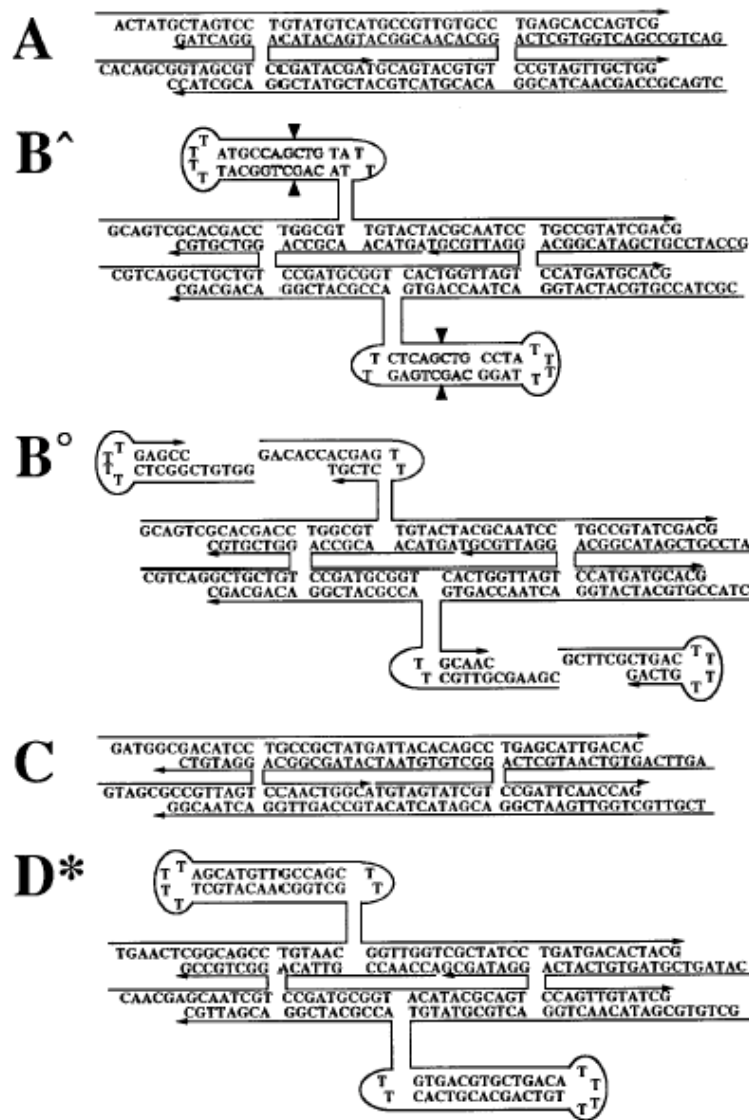
Parallel Helical Domains in DNA Branched Junctions Containing 5′,5′ and 3′,3′ Linkages[†]

Ruojie Sha,[‡] Furong Liu,[‡] Michael F. Bruist,[§] and Nadrian C. Seeman*,[‡]

ABSTRACT: The Holliday junction is a central intermediate in genetic recombination. It contains four strands of DNA that are paired into four double helical arms that flank a branch point. In the presence of Mg^{2+}, the four arms are known to stack in pairs forming two helical domains whose orientations are antiparallel but twisted by about 60°. The basis for the antiparallel orientation of the domains could be either junction structure or the effect of electrostatic repulsion between domains. To discriminate between these two possibilities, we have constructed and characterized an analogue, called a bowtie junction, in which one strand contains a 3′,3′ linkage at the branch point, the strand opposite it contains a 5′,5′ linkage, and the other two strands contain conventional 3′,5′ linkages. Electrostatic effects are expected to lead to an antiparallel structure in this system. We have characterized the molecule in comparison with a conventional immobile branched junction by Ferguson analysis and by observing its thermal transition profile; the two molecules behave virtually identically in these assays. Hydroxyl radical autofootprinting has been used to establish that the unusual linkages occur at the branch point and that the arms stack to form the same domains as the conventional junction. Cooper−Hagerman gel mobility analyses have been used to determine the relative orientations of the helical domains. Remarkably, we find them to be closer to parallel than to antiparallel, suggesting that the preferred structure of the branch point dominates over electrostatic repulsion. We have controlled for the number of available bonds in the branch point, for gel concentration, and for the role of divalent cations. This finding suggests that control of branch point structure alone can lead to parallel domains, which are generally consistent with recombination models derived from genetic data.

> Note: Cooper-Hagerman analysis involves attaching pairs of long helical segments to each possible pair of arms flanking a junction. Gel mobility increases with increasing junction angle.

a
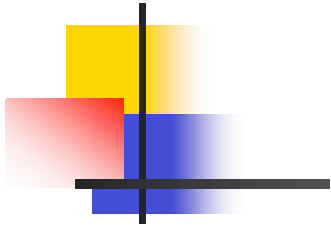
Normal Junctions
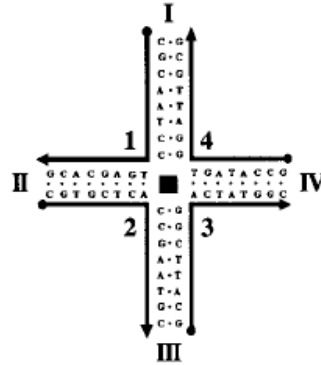
Bowtie Junctions
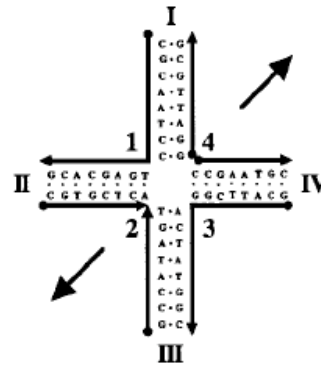
b

Antiparallel   **Parallel**
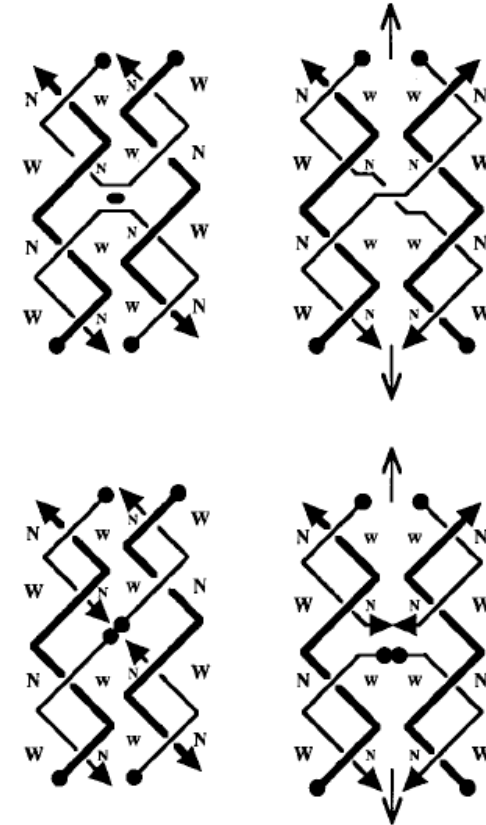
a
Ferguson Analysis of Normal & Bowtie Junctions

□ Bowtie Junction
○ Normal Junction

Log (Mobility)

Percent Polyacrylamide
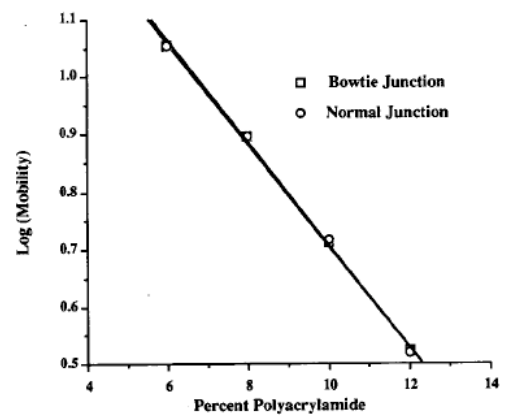
Stability = OK
Axes = Parallel

b
Thermal Transition Profiles of Normal & Bowtie Junctions

← Normal Junction
← Bowtie Junction

Relative Hyperchromicity (268 nm)

Temperature (°C)

LaBean COMPSCI 296.5
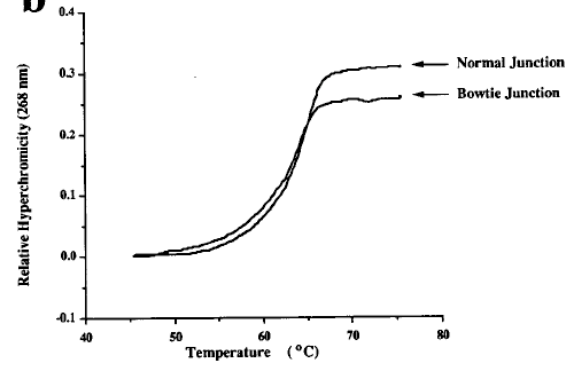
Ligation of DNA Triangles Containing Double Crossover Molecules

Xiaoping Yang, Lisa A. Wenzler, Jing Qi, Xiaojun Li, and Nadrian C. Seeman*

Contribution from the Department of Chemistry, New York University, New York, New York 10003

Three strands: 280, 90, 20 bases

3/20/06 LaBean COMPSCI 296.5
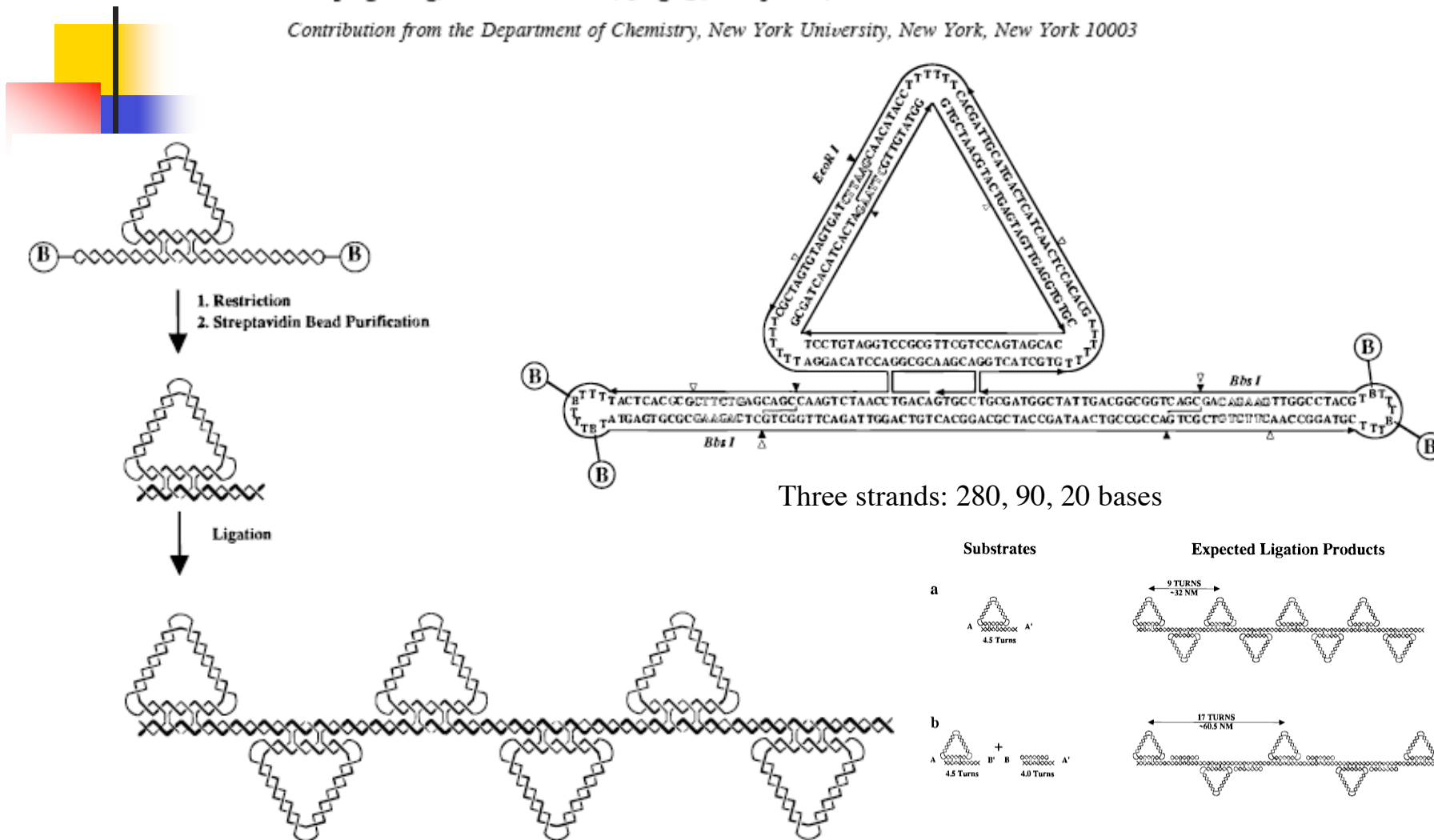
DNA Triangles
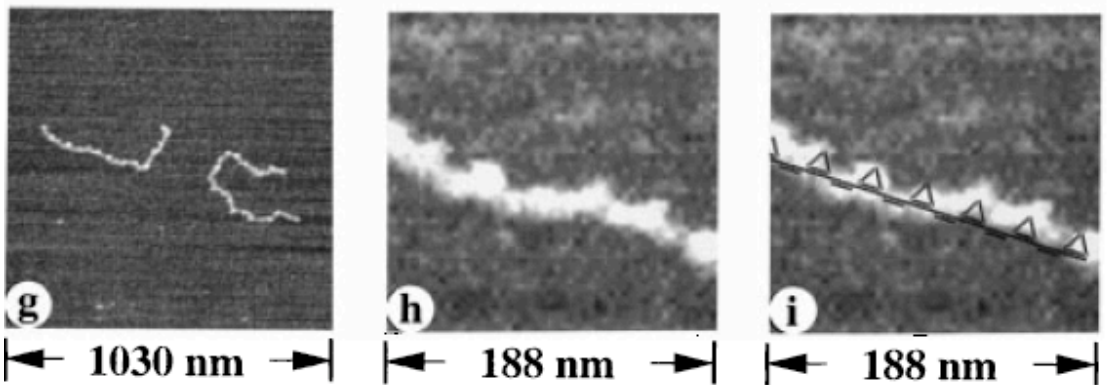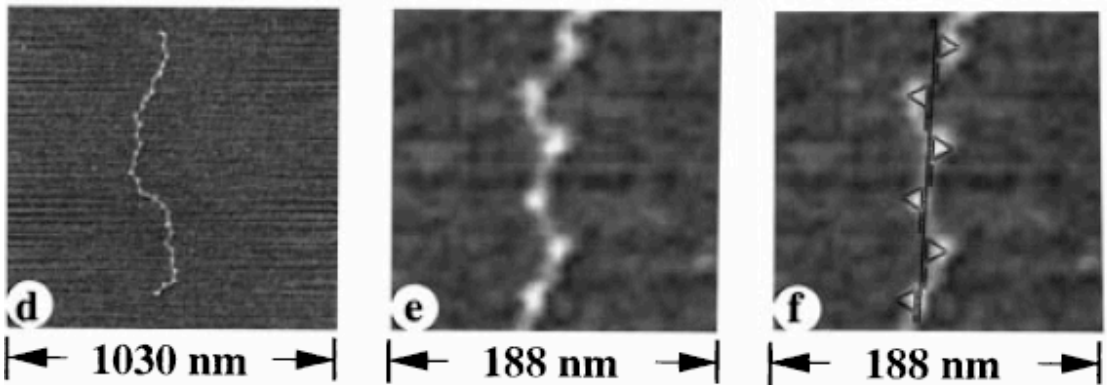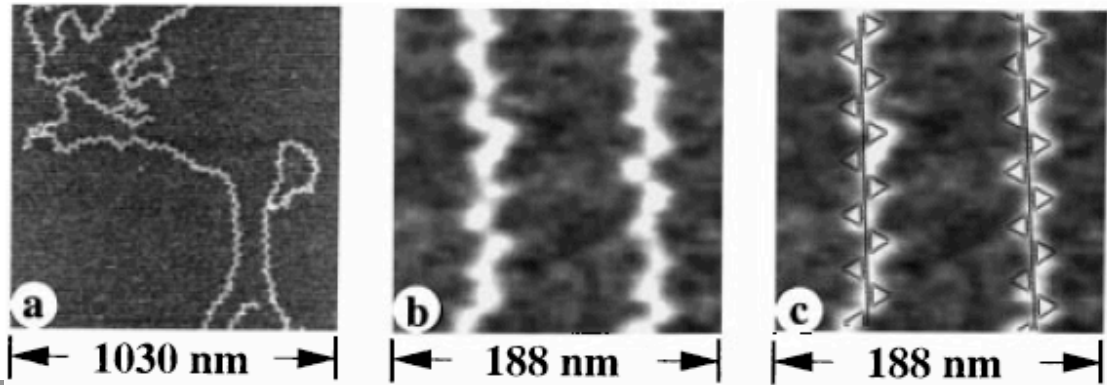
J. Am. Chem. Soc. 1998, 120, 9779−9786

Parallelogram tiles

Designed Two-Dimensional DNA Holliday Junction Arrays
Visualized by Atomic Force Microscopy

Chengde Mao, Weiqiong Sun, and Nadrian C. Seeman*

Contribution from the Department of Chemistry, New York University, New York, New Y

(a) (b) (c) (d) (e) (f)
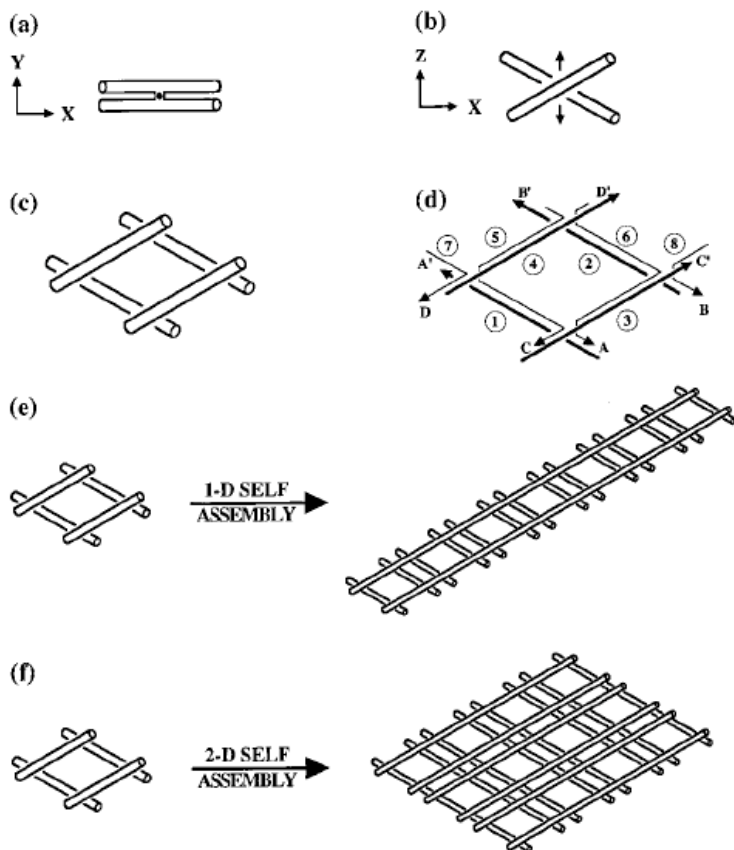
Figure 1. Schematic representations of the molecular components and their assembly. (a) A view down the dyad axis of the Holliday junction. The dyad axis is indicated by the small lens-shaped figure. The upper helical domain is rotated 30° about the vertical so that its right end penetrates the page, and the lower helical domain is rotated 30° about the vertical so that its left end penetrates the page. The X and Y axes of a right-handed coordinate system are shown to help orient the reader. (b) A view with the dyad axis vertical. The molecule has been rotated 90° about the X axis, as indicated. The dyad axis is indicated by the double arrows. (c) The combination of four junctions into a rhombus-like motif. Four molecules, in the orientation of (b) are combined. There are six turns of DNA in each helix, and four turns between crossover points, leading to one-turn overhangs on the ends. (d) The strand structure of the rhombus-like motif. The strand structure of the molecule in (c) is shown. Strands that are continuous helices (numbered 1−4) are drawn with a dark line, and those involved in crossovers (numbered 5−8) are drawn with a thin line. Arrowheads indicate the 3′ ends of the strands. Sticky ends are shown by the letters A, B, C, and D, and A′, B′, C′, and D′, respectively, represent their complements. The molecule is constructed from the strands synthesized as shown, rather than from the ligation of four junctions. (e) One-dimensional self-assembly of the motif into an array. One-dimensional self-assembly is shown to produce a railroad-track-like arrangement, with helices representing two "rails", extending for the length of the assembly, and "ties" separated by alternating distances of four turns and two turns. (f) Two-dimensional self-assembly produces a latticework of DNA. The array shows the two-dimensional self-assembly product of the motif; the long separations between helices contain four helical turns, and the short separations contain two helical turns. Note that the latticework array contains two separate layers, an upper layer oriented from lower left to upper right, and a lower layer oriented from lower right to upper left.

3/20/06 LaBean COMPSCI 296.5
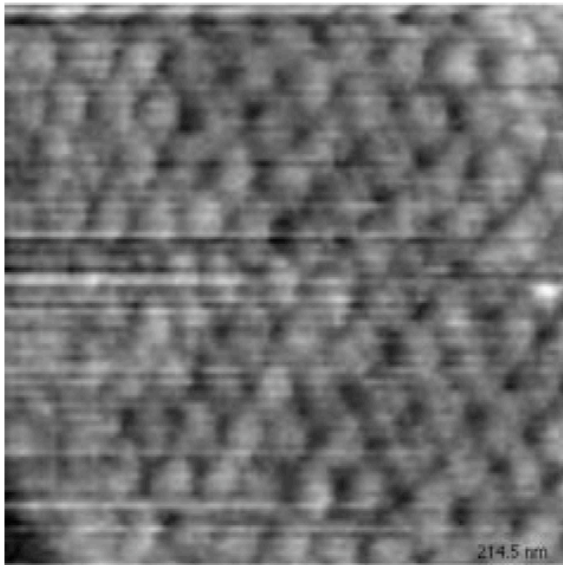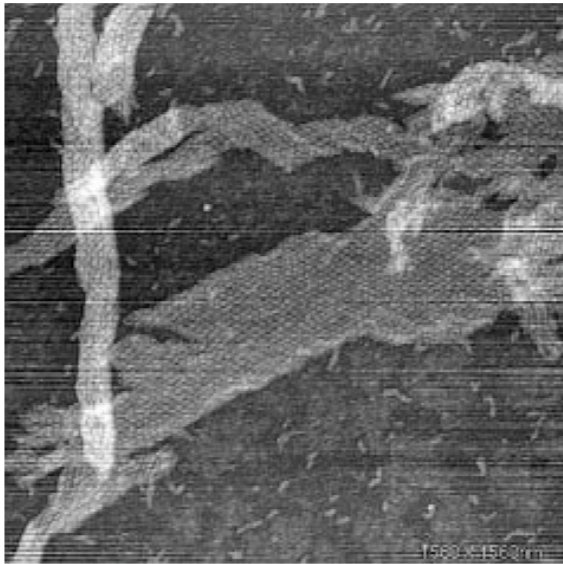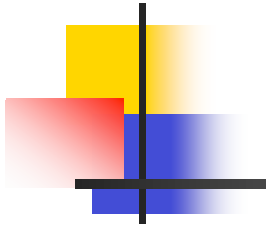
Figure 3. AFM images of the assembled rhombus-shaped component (4 + 2 helices per repeat in each direction). (a, top) An image of dimensions 1568 × 1568 nm. The unit cell is 20.5 ± 0.2 and 21.1 ± 0.5 nm, in good agreement with the expected dimensions. The features seen are fused helices, separated by two turns of double helix. (b, bottom) A zoomed view of a better-resolved but less extensive rhombus-shaped array. The narrow (two-turn) spacing between helices is evident in this view.
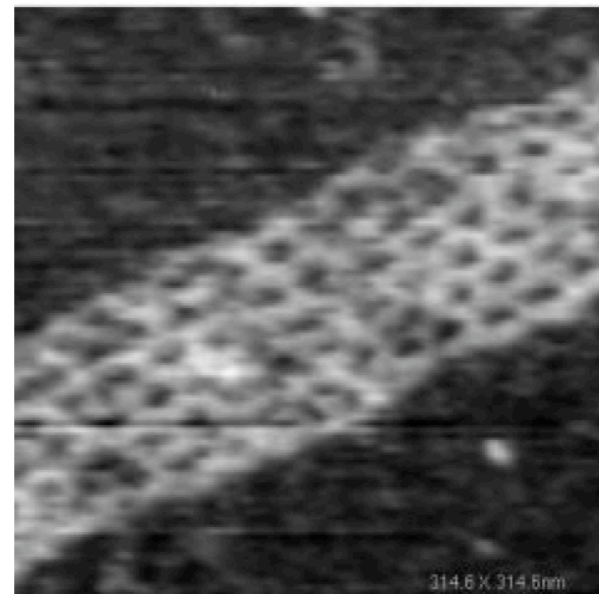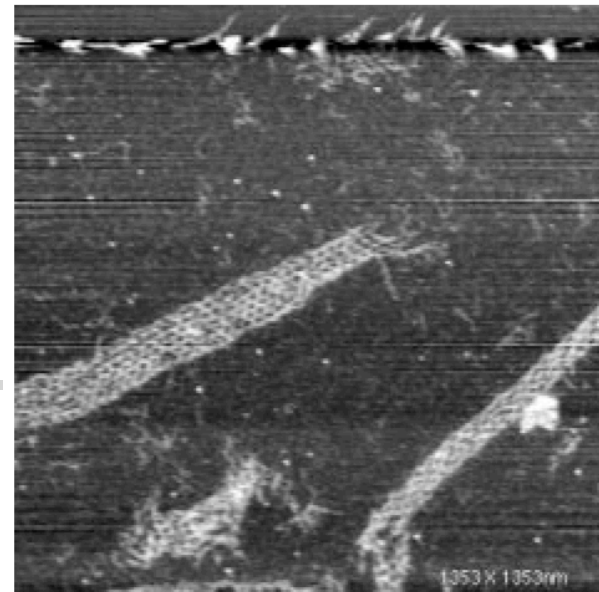
Figure 4. AFM images of the assembled parallelogram-shaped component (4 + 2 helices per repeat by 6 + 2 helices per repeat) (a, top) An image of dimensions 1353 × 1353 nm. (b, bottom) A zoom to 315 × 315 nm. The observed unit cell is 27.7 ± 0.8 and 20.9 ± 0.8 nm, in good agreement with the model.

J. Am. Chem. Soc. **1999,** *121,* 5437−5443

Paranemic Cohesion of Topologically-Closed DNA Molecules

Xiaoping Zhang, Hao Yan, Zhiyong Shen, and Nadrian C. Seeman*
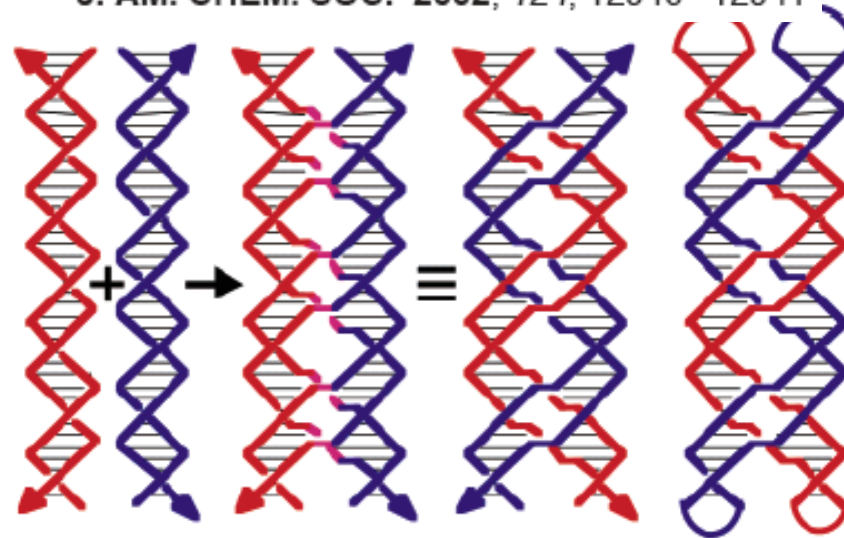
Figure 1. PX motif. The origin of the motif is shown at the left, where a red and a blue double helix exchange strands at every point, where they come into contact, to produce purple crossovers. The covalent strand structure is shown to the right of the identity sign, where a red and a blue double helix are seen to interwrap. The paranemic relationship of the interwrapped helices is emphasized on the right where the blue and red helices are capped in hairpin loops.

- **Paranemic** is a topological term for the joint that is made by wrapping one circle around another without cutting either circle. The two circles can always be pulled apart. Paranemic is distinguished from plectonemic.

- **Plectonemic joints** are joints in which one molecule is topologically wound around the other molecule.

Here, we present a solution to the problem of large-object noncovalent DNA assembly that circumvents sticky ends. The essence of this method is the paranemic cohesion of two topologically closed molecules by use of a motif known as paranemic crossover (PX) DNA

Lanes	1	2	3	4
	M	T1	T1+T2	T2
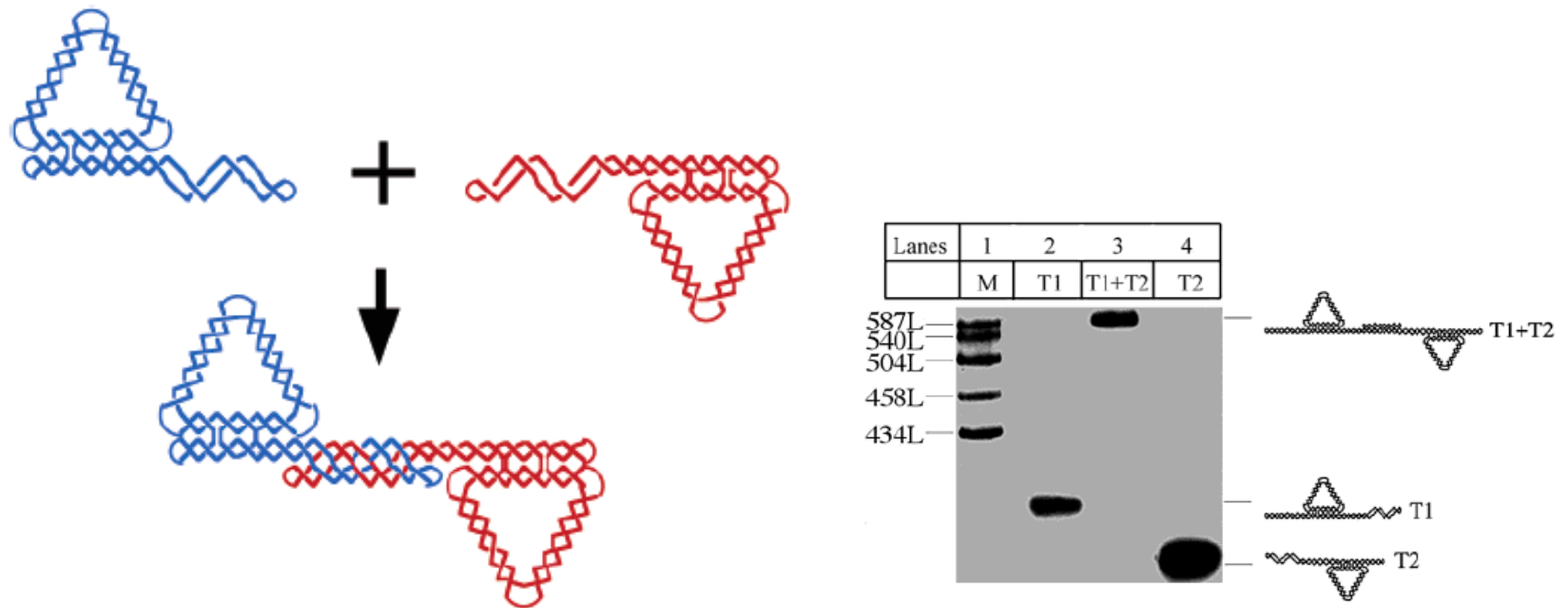
Figure 2. Paranemic cohesion. The blue triangle on the left and the red triangle on the right have one edge consisting of a DX motif. The small circle at the center of the DX is not sealed. Each nontriangular DX domain is tailed in a segment that can pair with the opposite segment on the other triangle by PX complementarity.

Derivation of DX and TX Molecules

Seeman, N.C. (2001) *NanoLetters* **1**, 22-26.
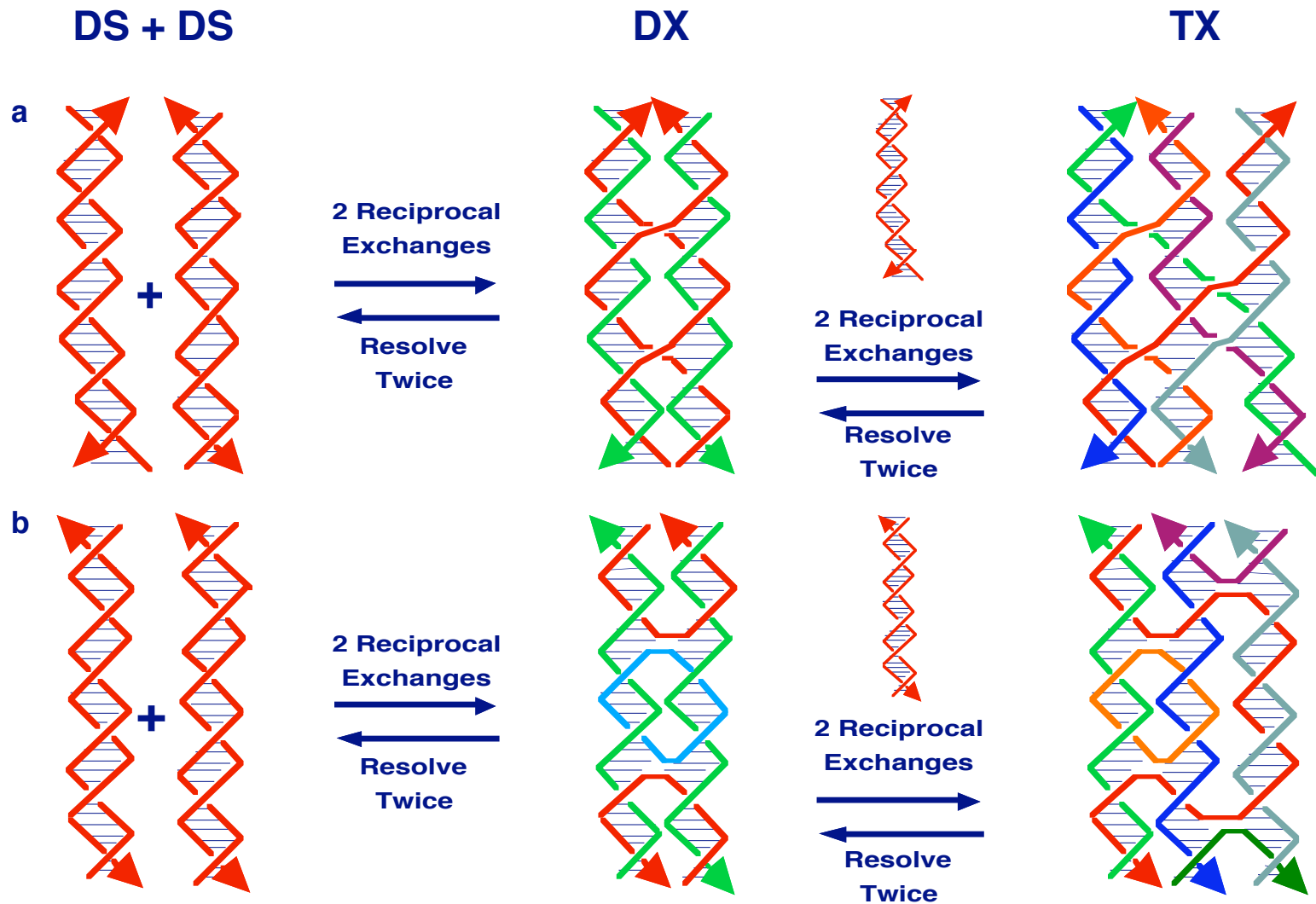
Articles

Construction, Analysis, Ligation, and Self-Assembly of DNA Triple Crossover Complexes

Thomas H. LaBean,[†] Hao Yan,[‡] Jens Kopatsch,[‡] Furong Liu,[‡] Erik Winfree,[§] John H. Reif,*,[†] and Nadrian C. Seeman*,[‡]

Contribution from the Department of Computer Science, Duke University, Durham, North Carolina 27707, Department of Chemistry, New York University, New York, New York 10003, and Computer Science and Computation and Neural Systems, California Institute of Technology, Pasadena, California 91125

DNA Triple Crossover Complexes

J. Am. Chem. Soc., Vol. 122, No. 9, 2000   1853
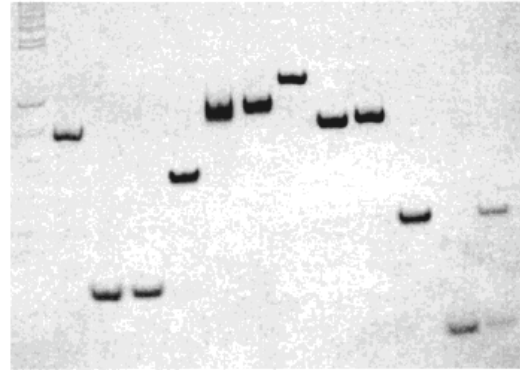
Figure 3. Nondenaturing gels of the TX complex. The top panel shows an 8% stained polyacrylamide gel indicating association complexes between various equimolar combinations of TX component strands. Equimolar mixtures at 3 nM concentration per included strand were annealed and electrophoresed at room temperature. Strands included in the annealing are indicated with a "1" above the lane. Formation of dimer, trimer, and tetramer are shown in the expected lanes. In the bottom panel, the trimeric complex of strands 1, 2, and 3 is titrated with varying amounts of strand 4. The stoichiometric mixture is shown in the lane labeled 1:1:1:1, and strand ratios in other lanes are as indicated. Each strand is present at 3 nM concentration in the equimolar mixture.
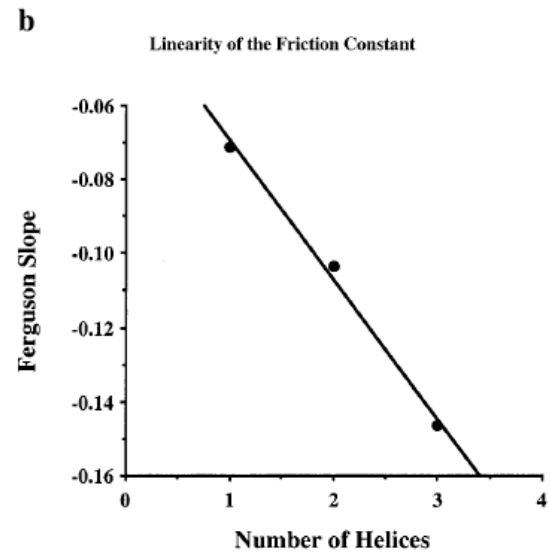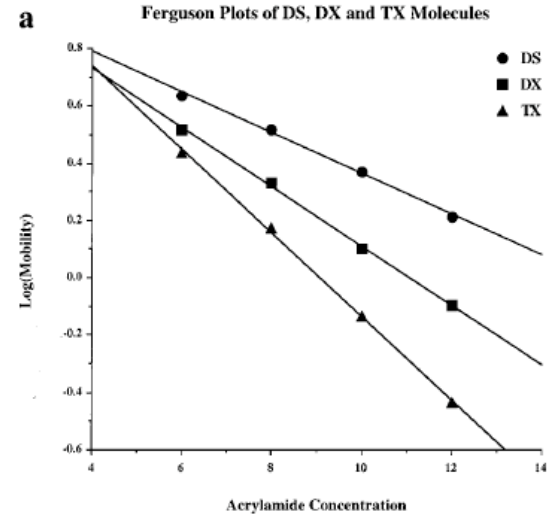
Figure 4. Ferguson analysis. (a) Ferguson plots. Log(mobility) as a function of polyacrylamide concentration is shown for double-stranded DNA (DS, circles), for a double crossover complex (DX, squares) and a triple crossover (TX, triangles). The overall length of each complex is 42 base pairs. The graph shows the log of absolute mobility in cm/h for each of the structures. (b) Analysis of the Ferguson slopes. The increase in relative friction constant with increasing numbers of helical domains in the complex is roughly linear.

3/20/06

*1 (5')   *1 (3')   *2 (5')   *2 (3')

*3 (5')   *3 (3')   *4 (5')   *4 (3')

2
GTTCAGCCTTAGT CCACAGTCACGGATGG ACTCGATAGCCAA
CAAGTCGGAATCA GGTGTCAGTGCCTACC TGAGCTATCGGTT
                                                    1

TCTGG ACTCC TGGCATCTCATTCGCA GGACA GGTAG
AGACC TGAGG ACCGTAGAGTAAGCGT CCTGT CCATC

4
GTAGAGCA GGAACGCAAAGCGGTTAGGTC TTCGG ACGCTCGT
CATCTCGT CCTTGCGTTTCGCCAATCCAG AAGCC TGCGAGCA
                                                    3
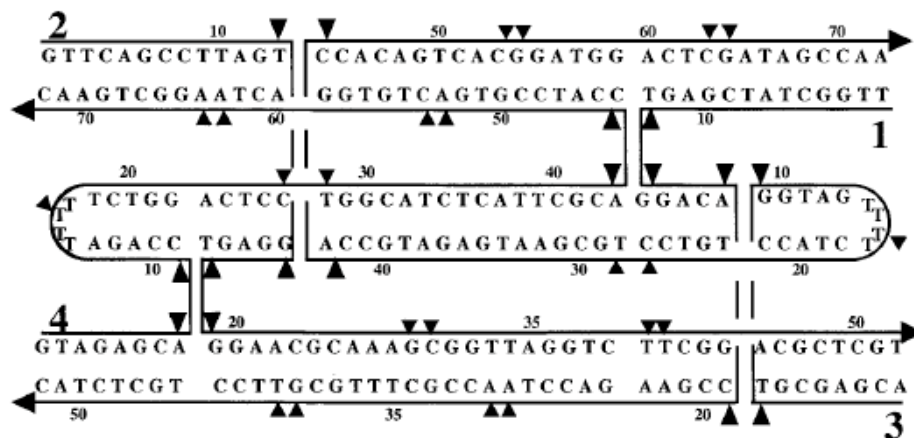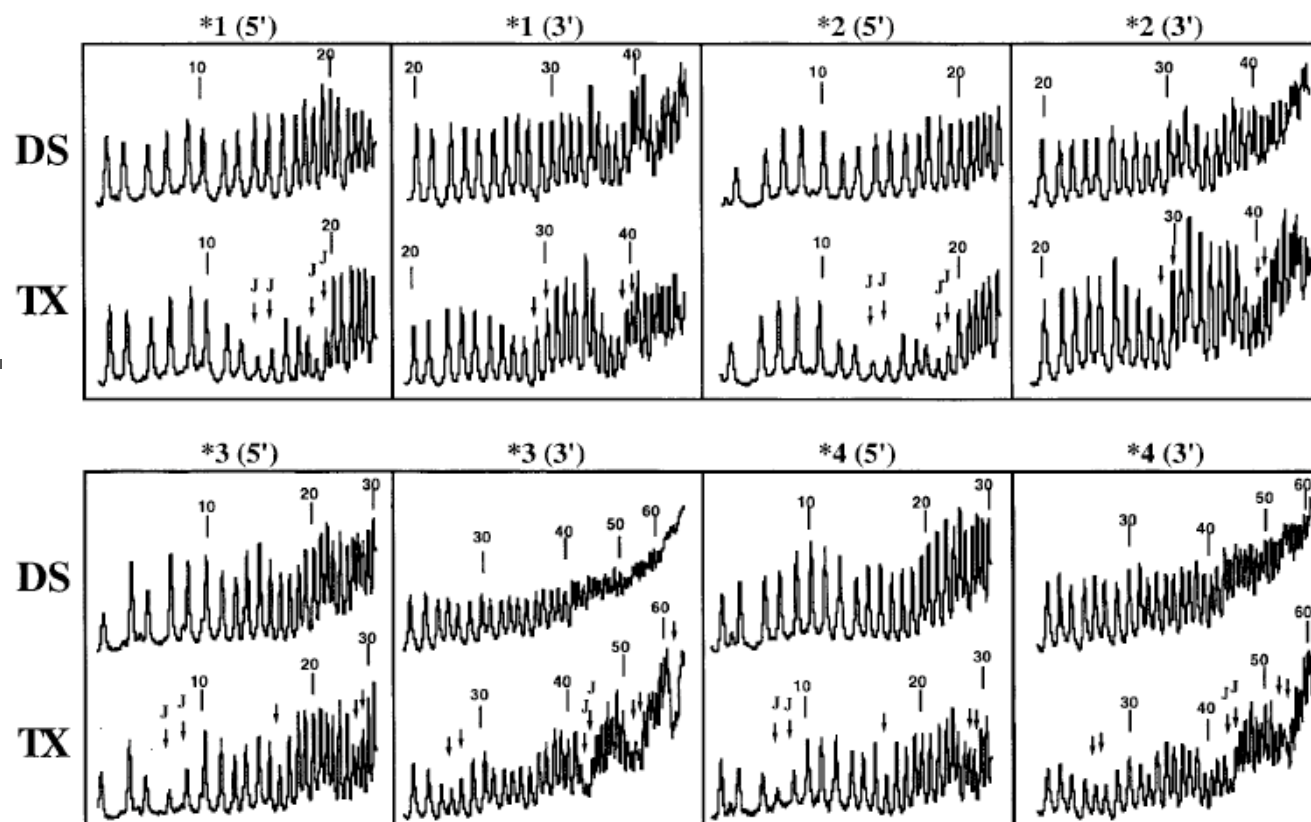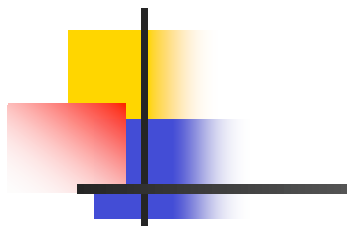
J. Am. Chem. Soc. 2000, 122, 1848−1860

3/20/06

a

A   B   C   C'   D

AB Array

ABC'D Array

b

c

34.6 ± 1.6 nm

0   1317 nm

0   359 nm
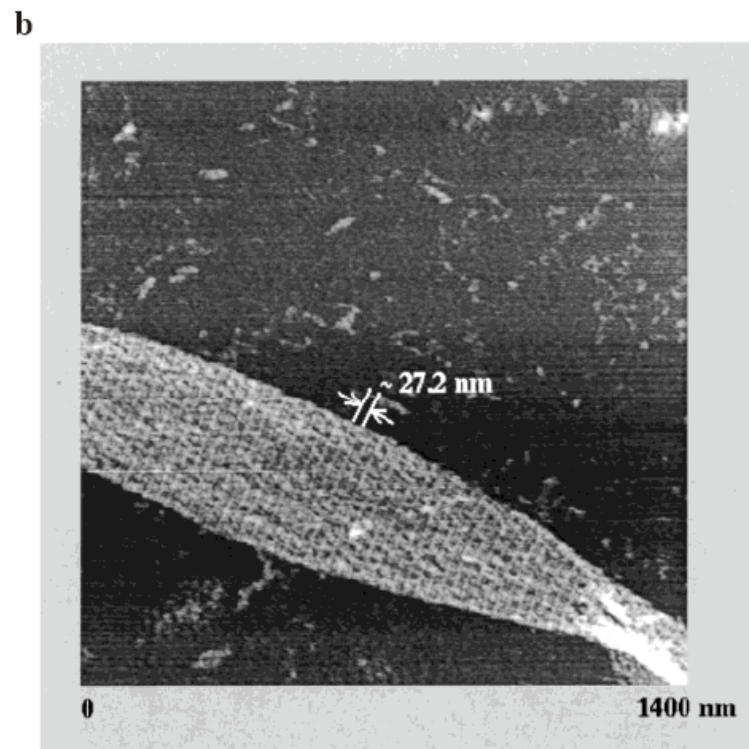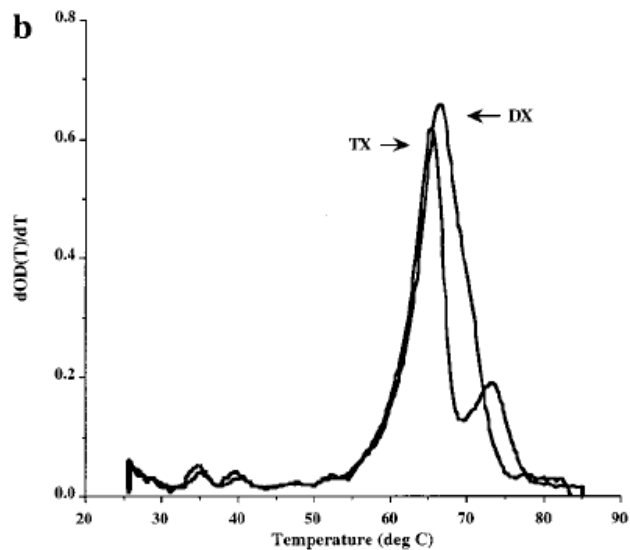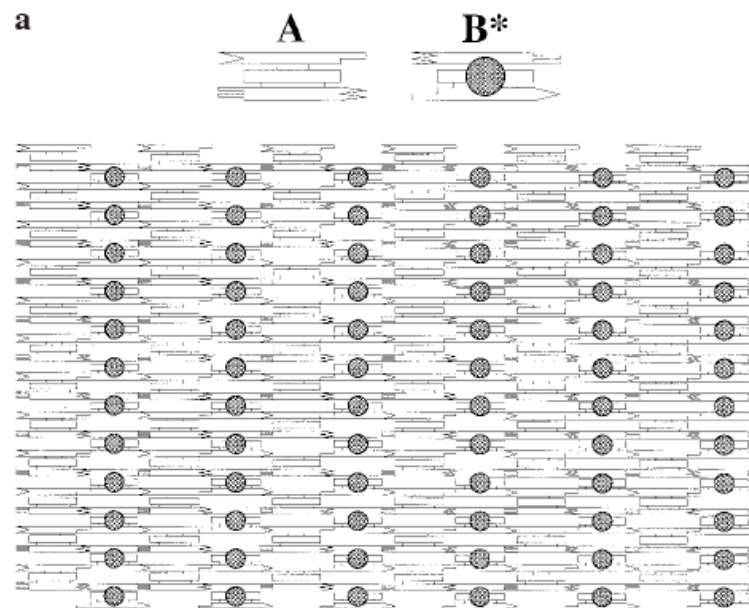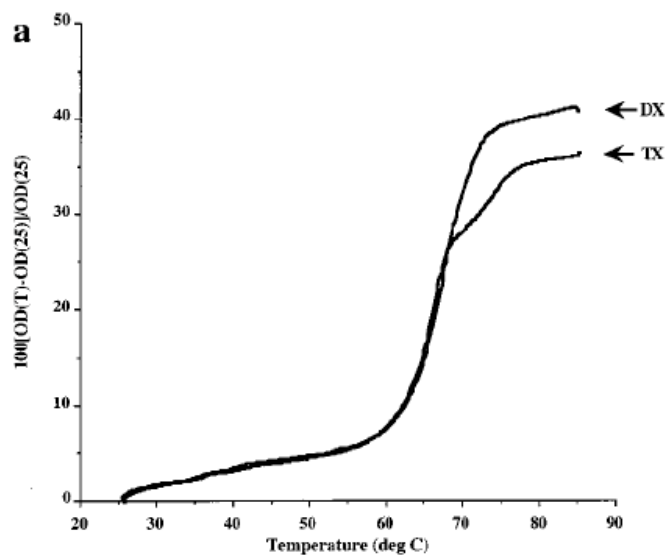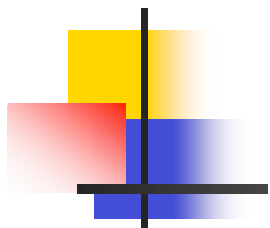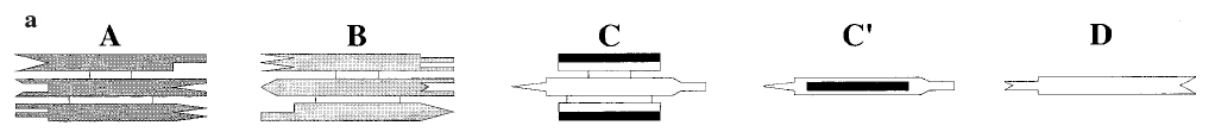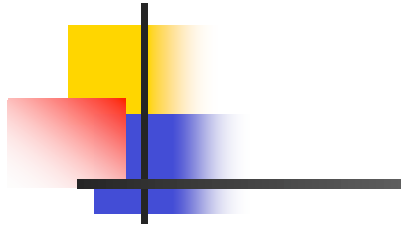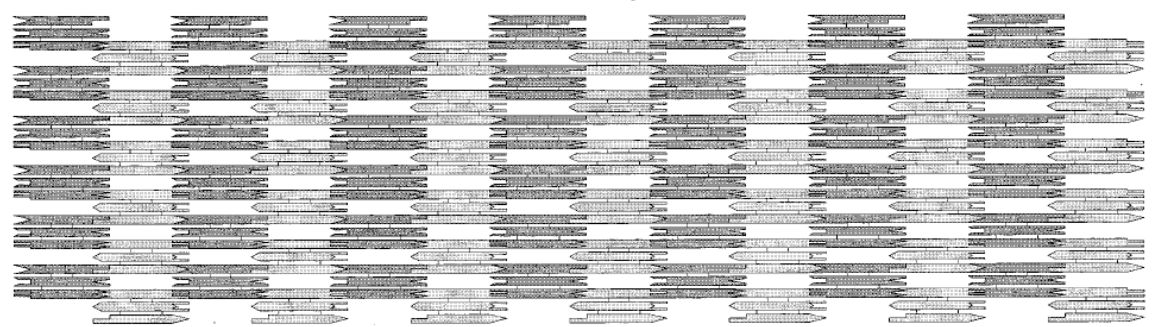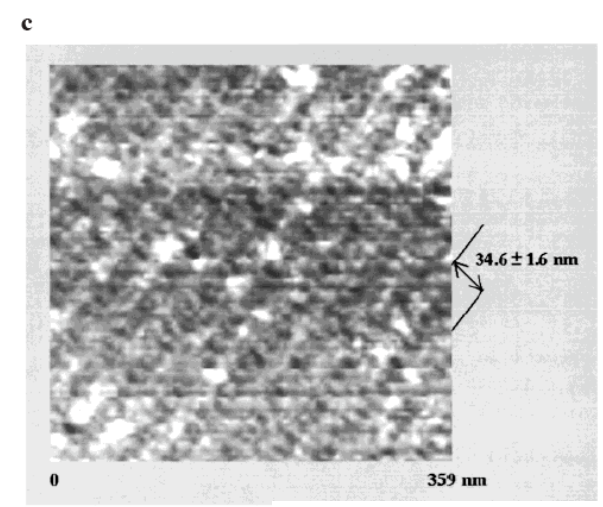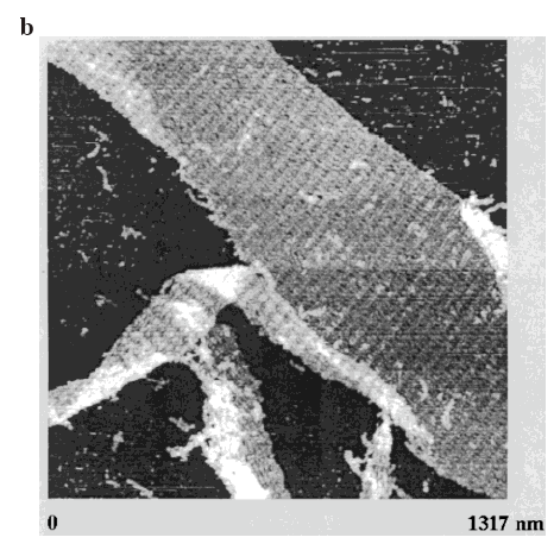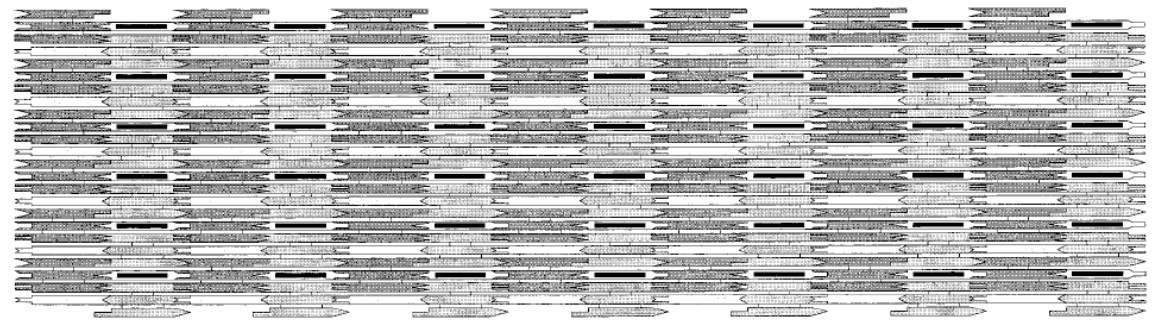
3/20/06

TX Array With Rotated Components

LaBean, T.H., Yan, H., Kopatsch, J., Liu, F., Winfree, E., Reif, J.H.
& Seeman, N.C (2000), *J. Am. Chem. Soc.* **122**, 1848-1860.

A   B   C   C'   D
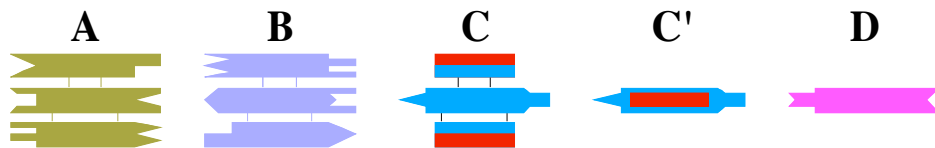
AB Array
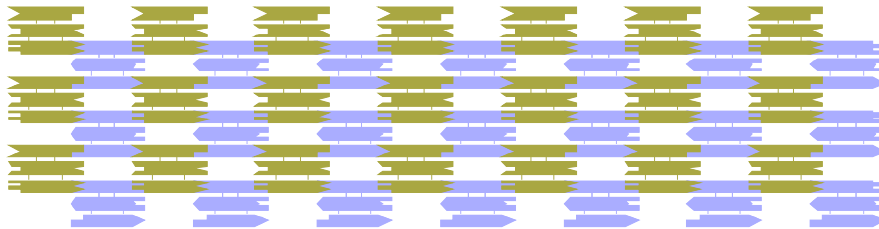
ABC'D Array
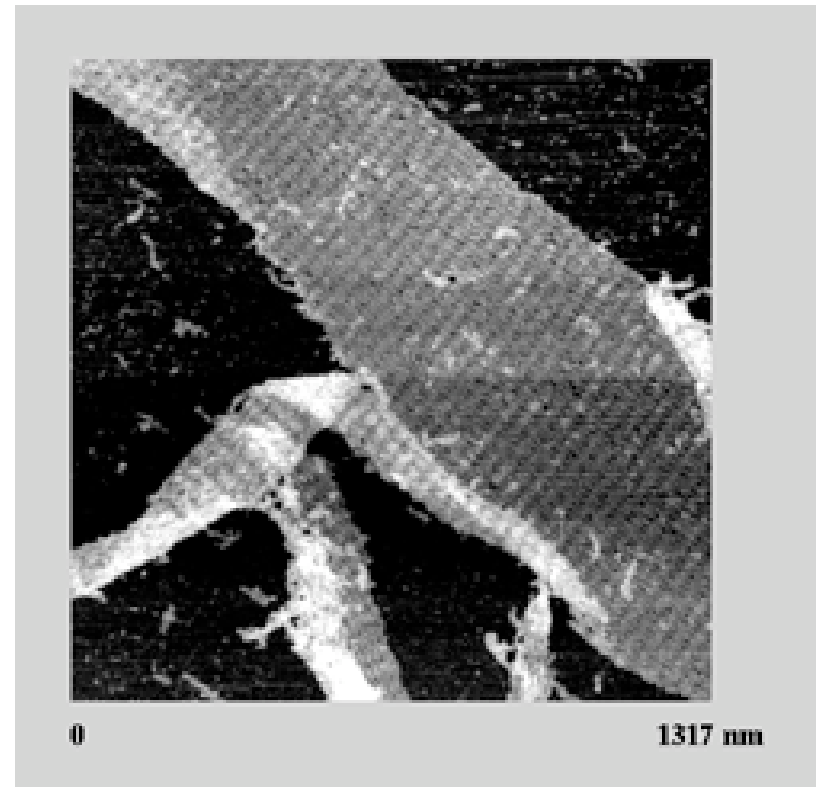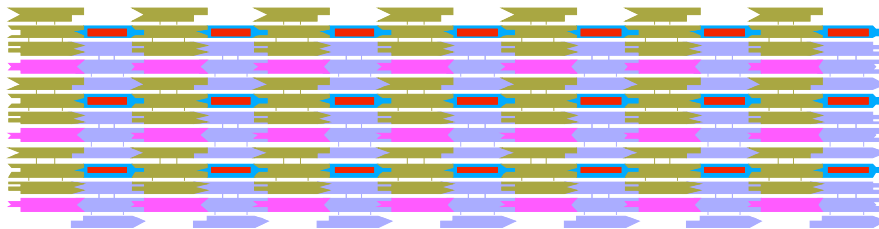
XOR Calculation by DNA Self-assembly
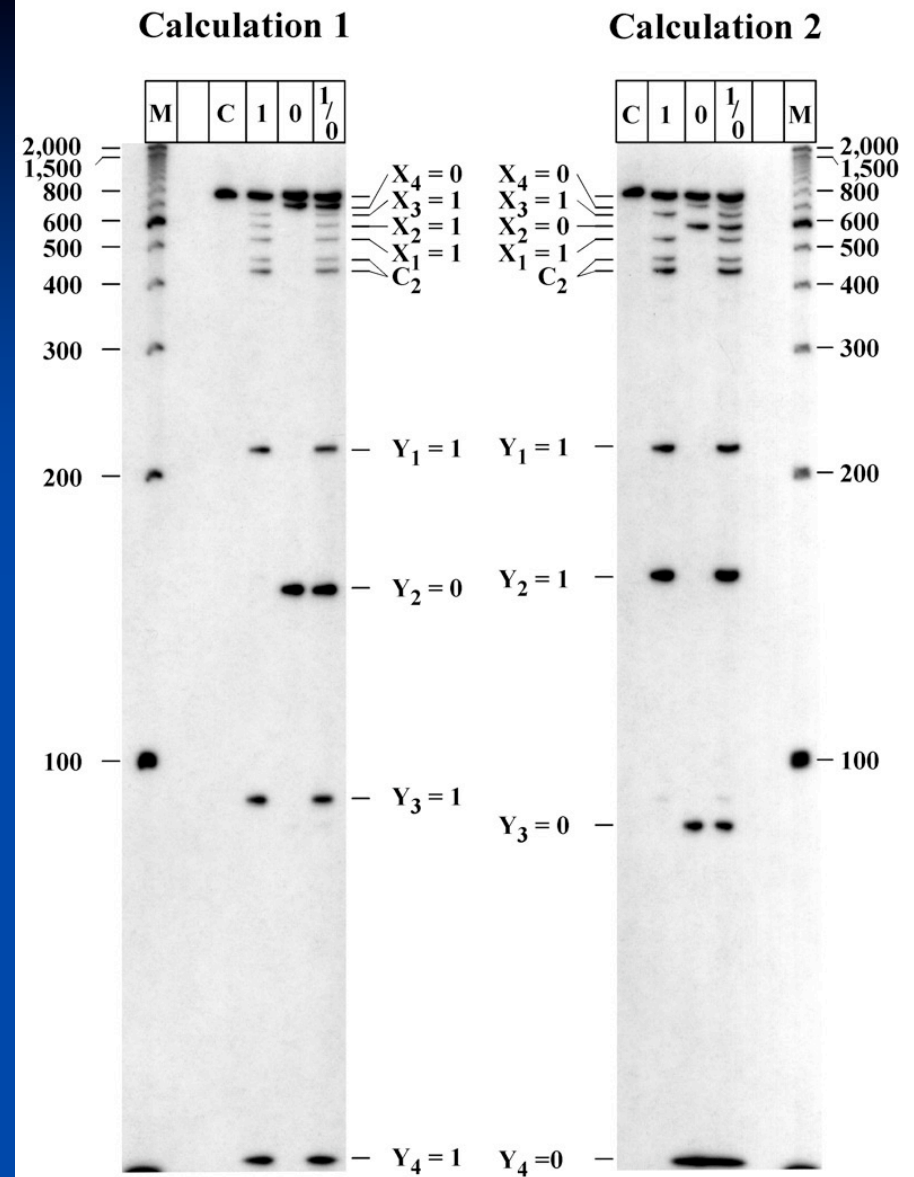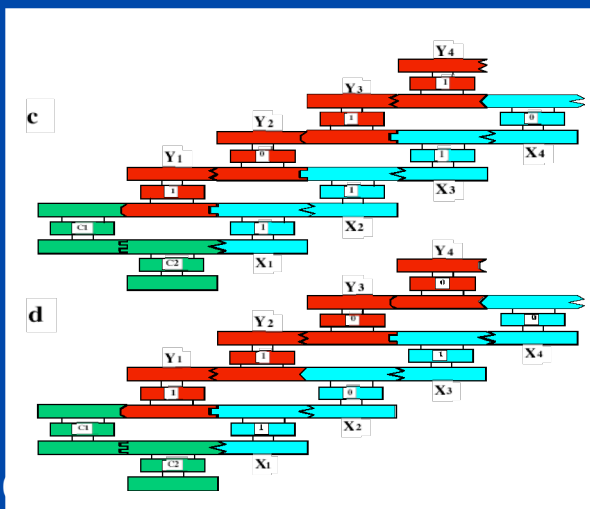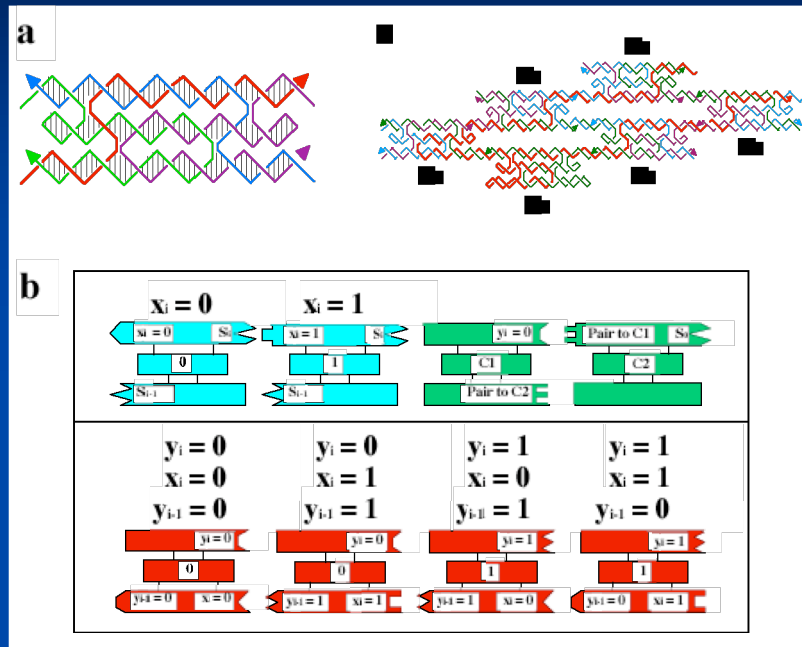
C. Mao, T.H. LaBean, J.H. Reif, N.C. Seeman, Logical Computation Using Algorithmic Self-Assembly of DNA Triple-Crossover Molecules, *Nature* 407, 493–495 (2000)
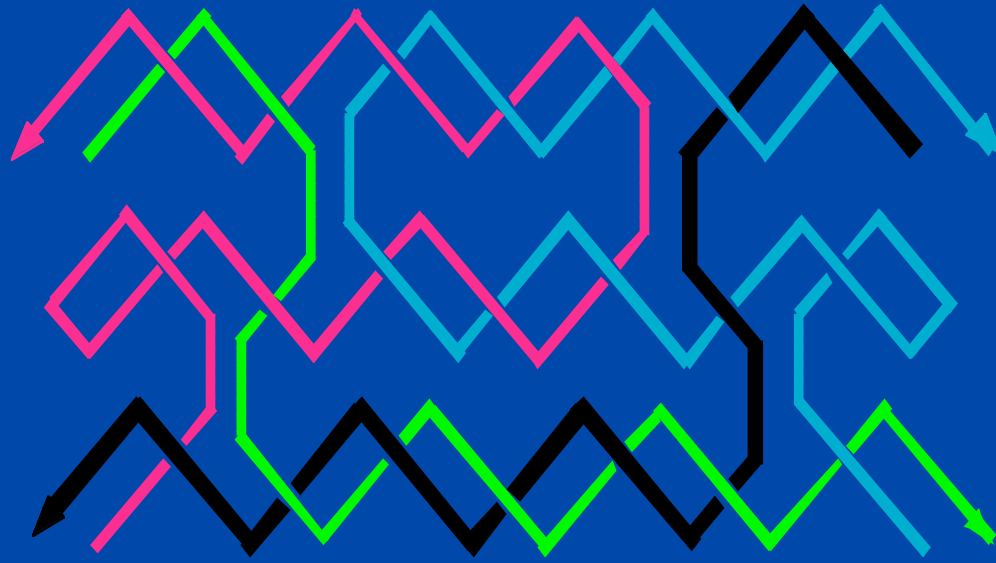
TAO35
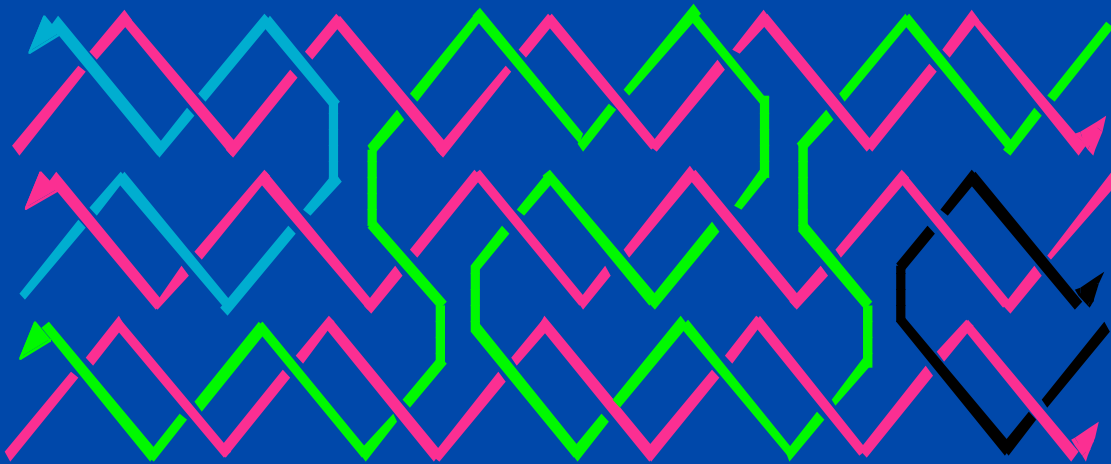
TAE 44

A Single Tile TX Lattice

A   A'
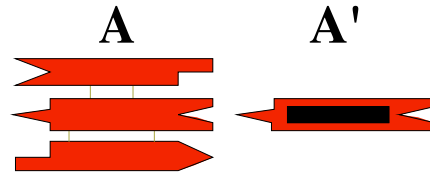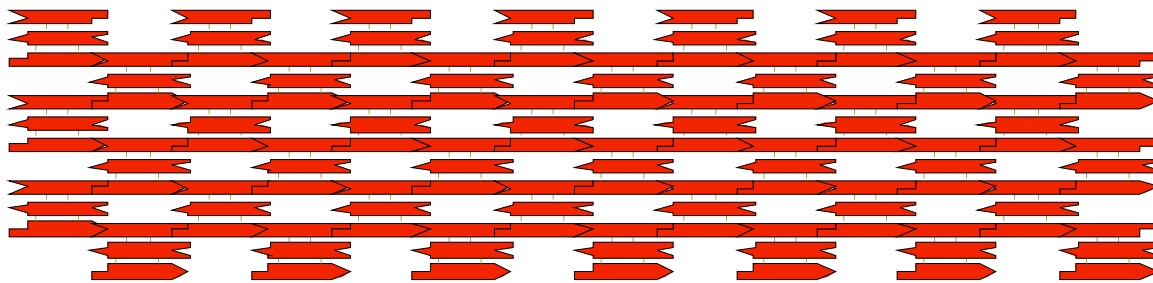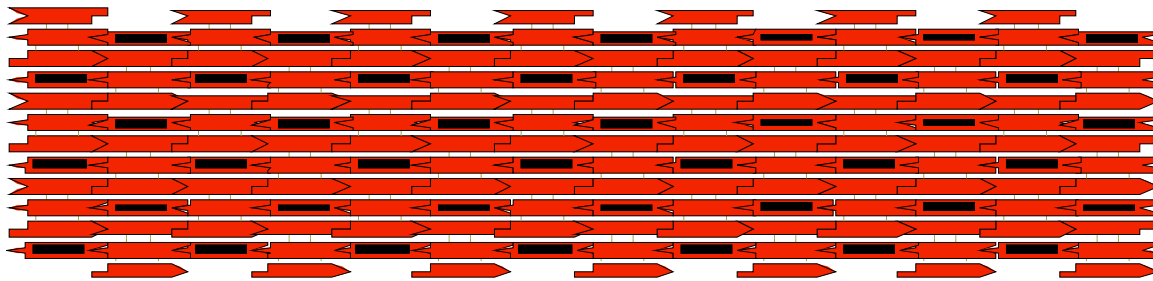
A Array -- 2D

AA' Array

A Single Fused Tile TX Lattice
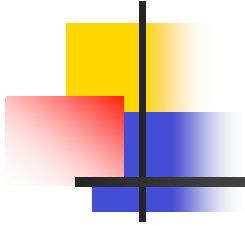
A-A'
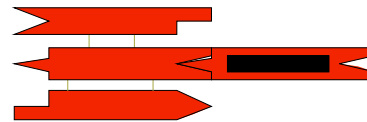
A-A' Array
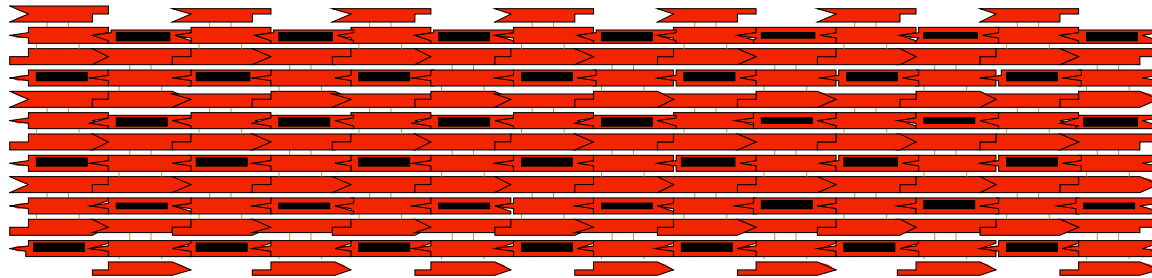
A Two Tile TX Lattice

A **B'**

A Array -- 2D
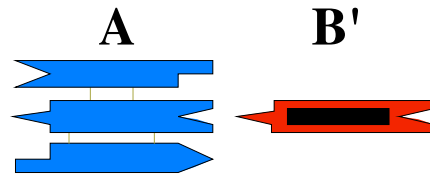
AB' Array
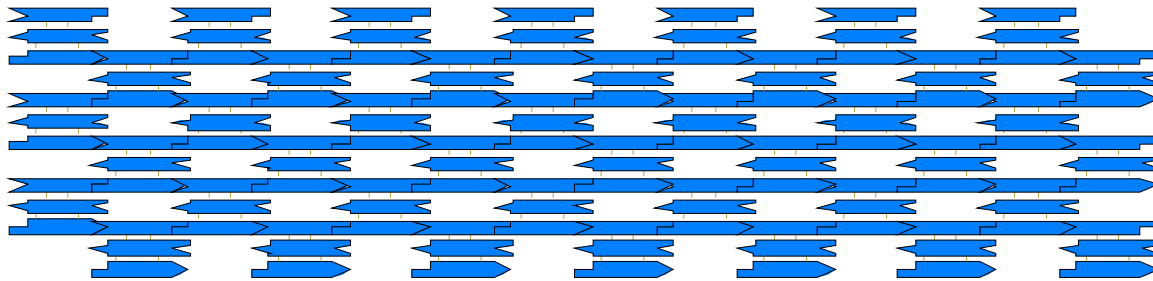
LaBean COMPSCI 296.5
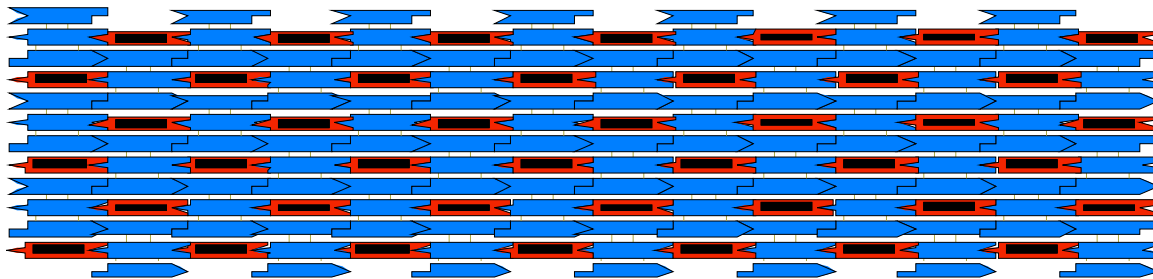
A Fused Two Tile TX Lattice

A-B'
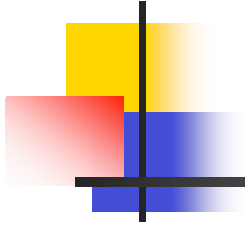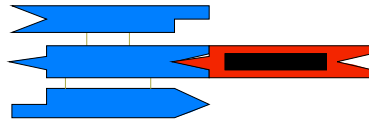
A-B' Array
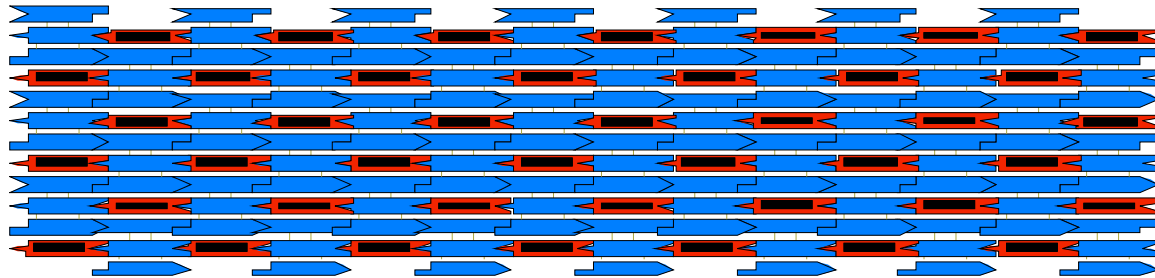
LaBean COMPSCI 296.5

A Trigonal Component...C. Mao

A Trigonal Component Lattice
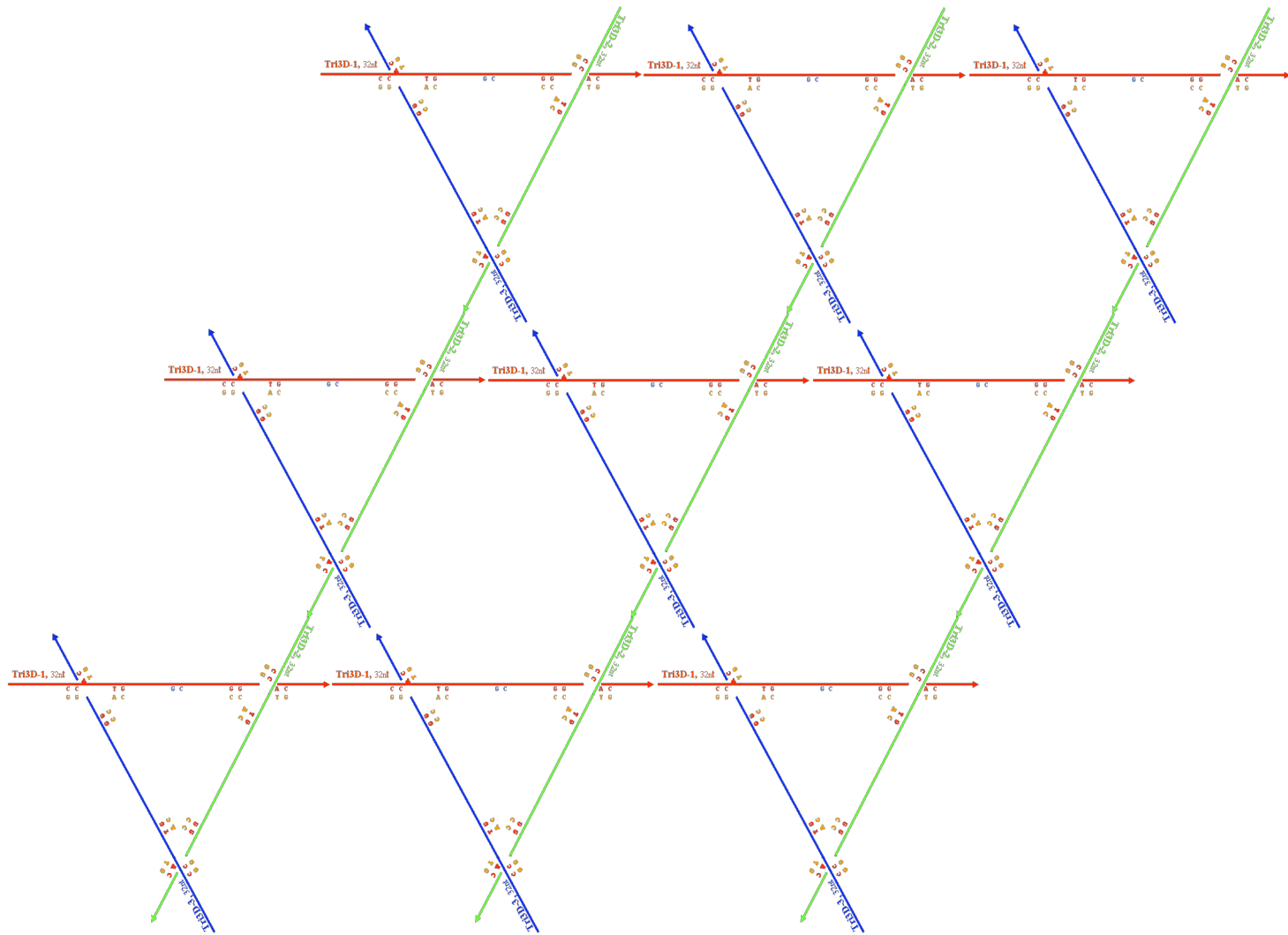
Crystals from a Trigonal Lattice
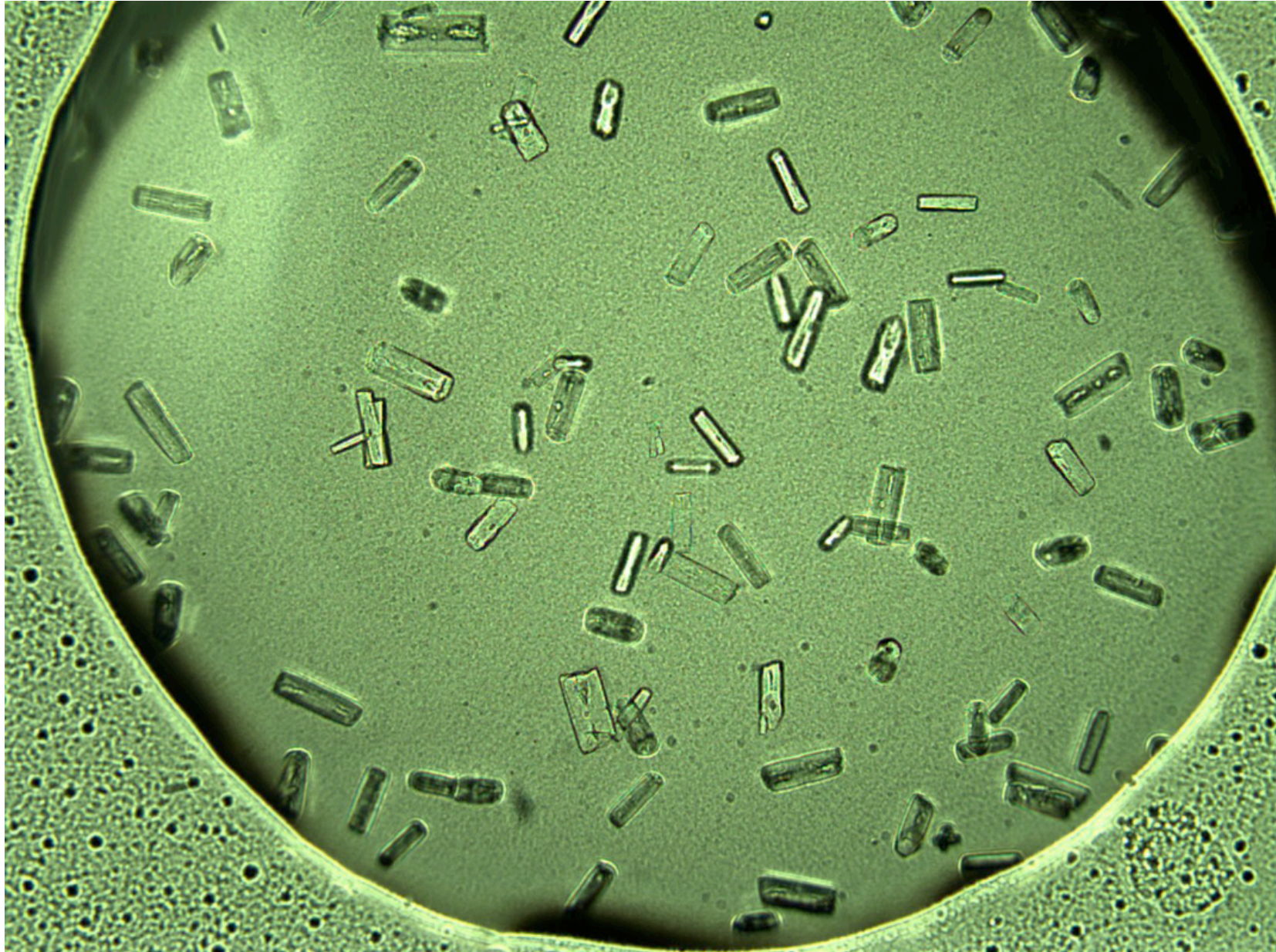
Tensegrity: Construction of Rigid DNA Triangles with Flexible Four-Arm DNA Junctions

Dage Liu, Mingsheng Wang, Zhaoxiang Deng, Richard Walulu, and Chengde Mao*

Department of Chemistry, Purdue University, West Lafayette, Indiana 47907
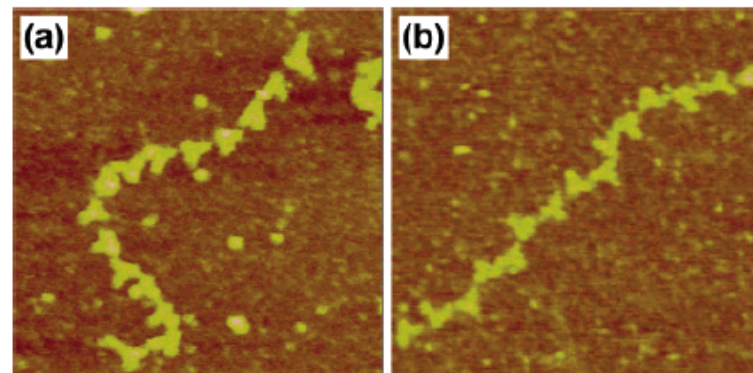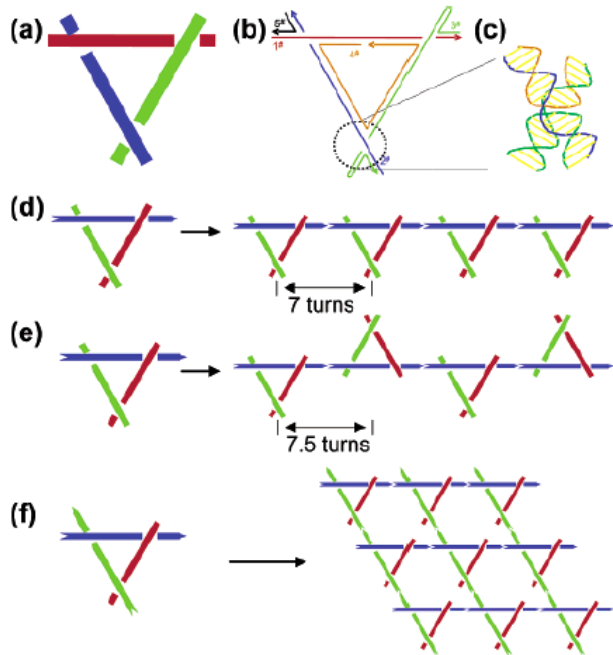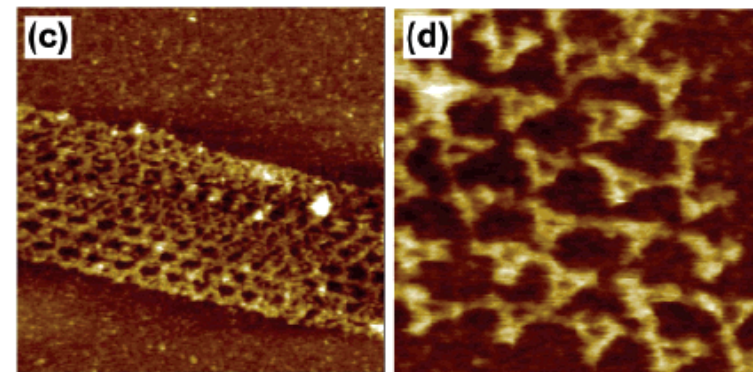
Triangular DX Design
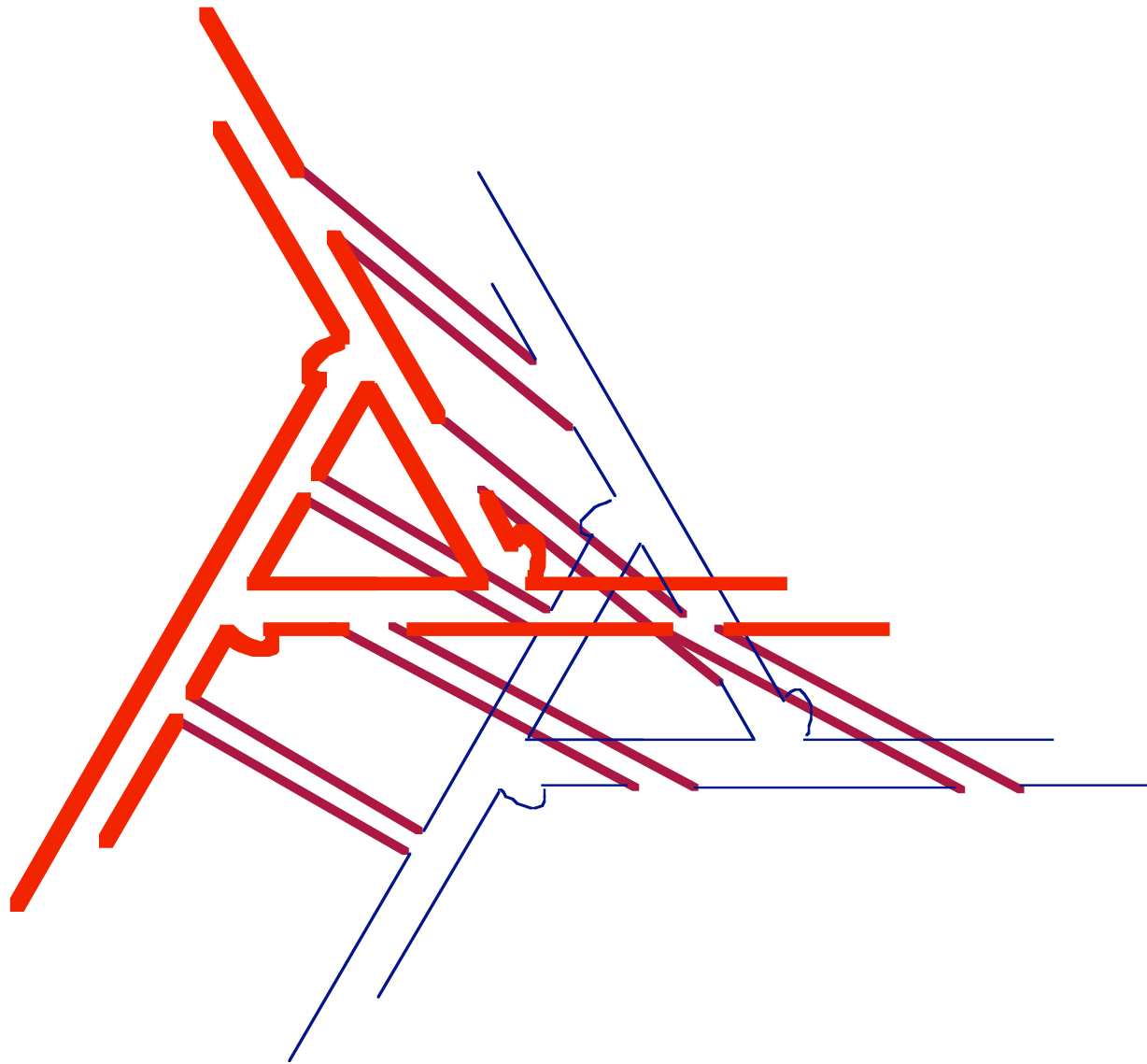
Crystal Structure of a Continuous Three-Dimensional DNA Lattice

Paul J. Paukstelis,[1,*] Jacek Nowakowski,[1]
Jens J. Birktoft,[2] and Nadrian C. Seeman[2]

- 13 base oligo
- 2.1 Å resolution
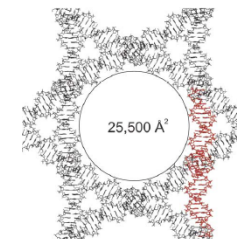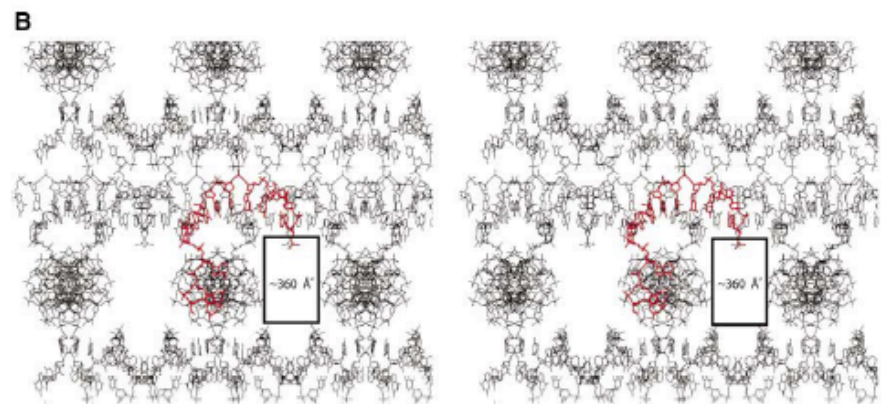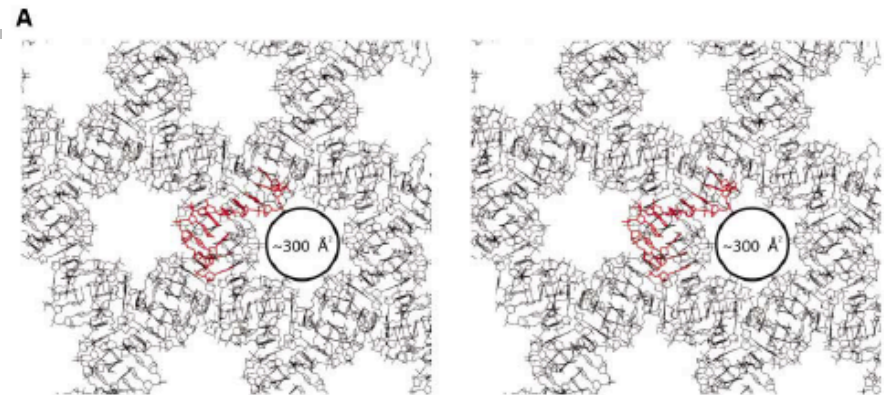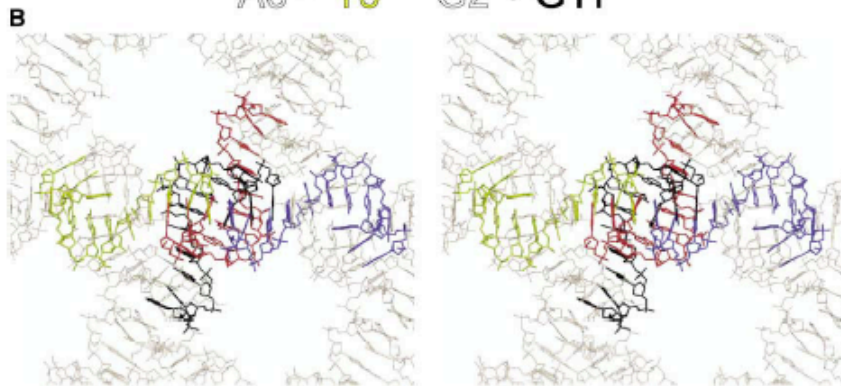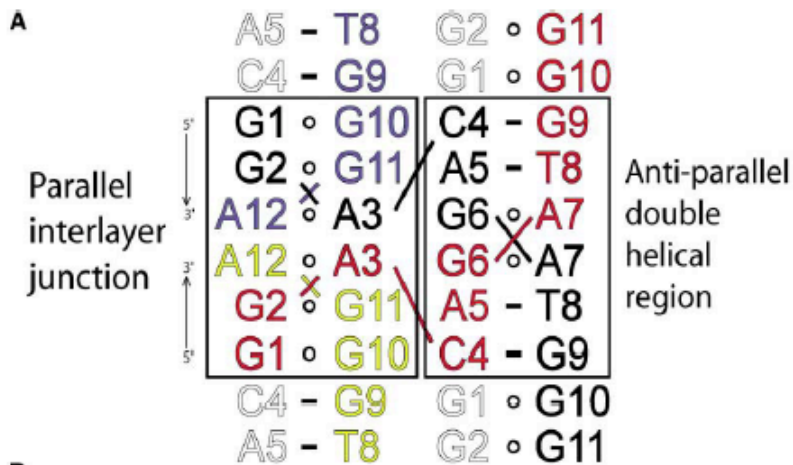
CHALLENGES FOR STRUCTURAL DNA NANOTECHNOLOGY

[1] TO EXTEND 2-D RESULTS TO 3-D WITH HIGH ORDER -- Crystallography.

[2] TO INCORPORATE DNA DEVICES IN 2-D AND 3-D ARRAYS -- Nanorobotics.

[3] TO INCORPORATE HETEROLOGOUS GUESTS IN LATTICES -- Nanoelectronics; Crystallography.

[4] TO EXTEND ALGORITHMIC ASSEMBLY TO HIGHER DIMENSIONS -- Smart Materials; Computation.

[5] TO ACHIEVE ASSEMBLIES WITH HIERARCHICAL CHARACTER -- Complex Materials.

[6] TO ACHIEVE FUNCTIONAL AS WELL AS STRUCTURAL SYSTEMS -- Active Materials; Sensor Systems.

[7] TO INTERFACE WITH TOP-DOWN METHODS AND THE MACROSCOPIC WORLD -- Nanoelectronic Reality.

[8] TO INCORPORATE COMBINATORIAL APPROACHES IN TILE DESIGN -- Diversity; Programmability.

[9] TO PRODUCE SYSTEMS CAPABLE OF SELF-REPLICATION -- Economy; Evolvability.

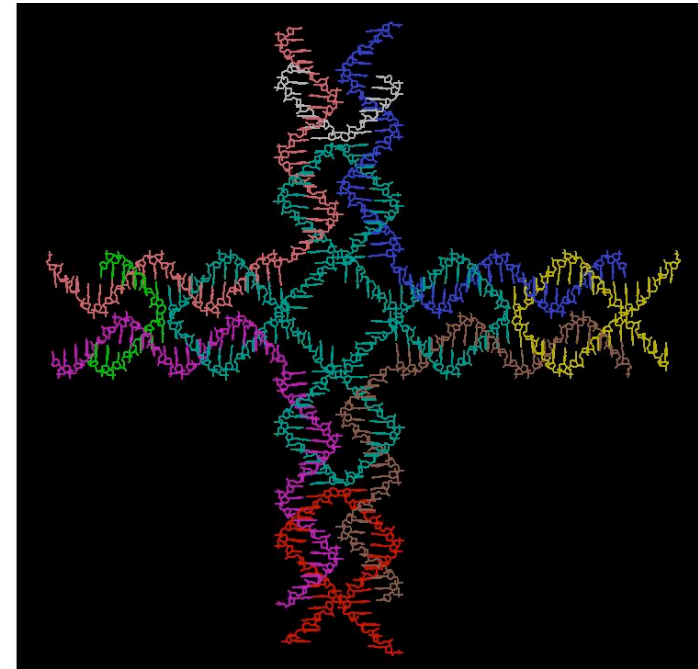[10] TO ADVANCE FROM BIOKLEPTIC SYSTEMS TO BIOMIMETIC SYSTEMS -- Chemical Control.
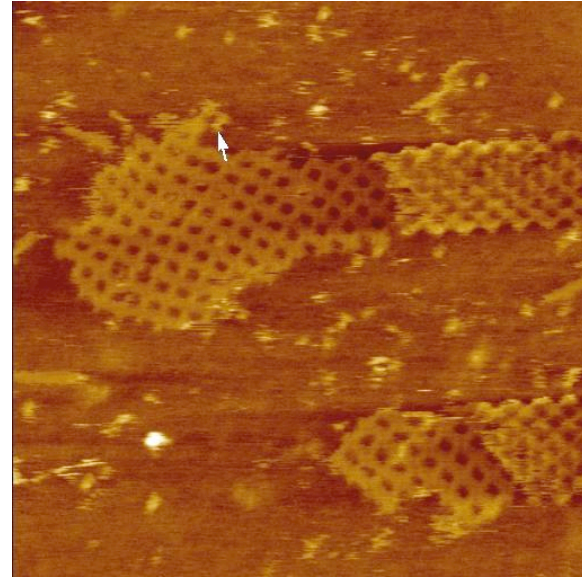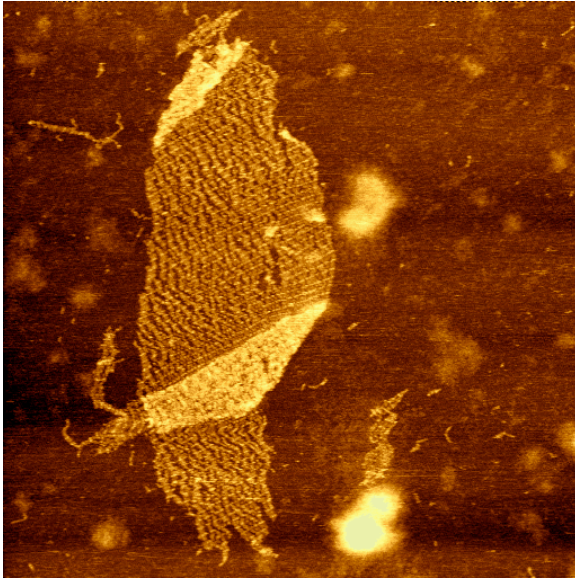
DNA tiles
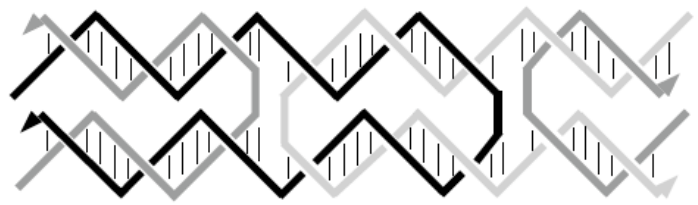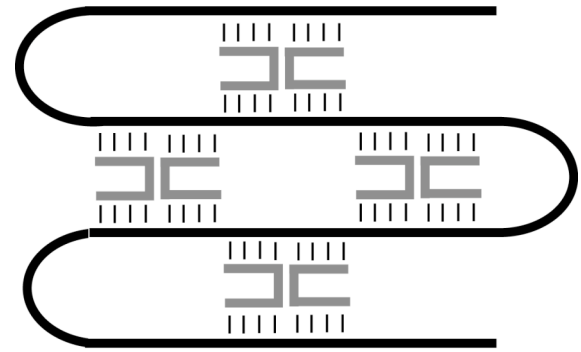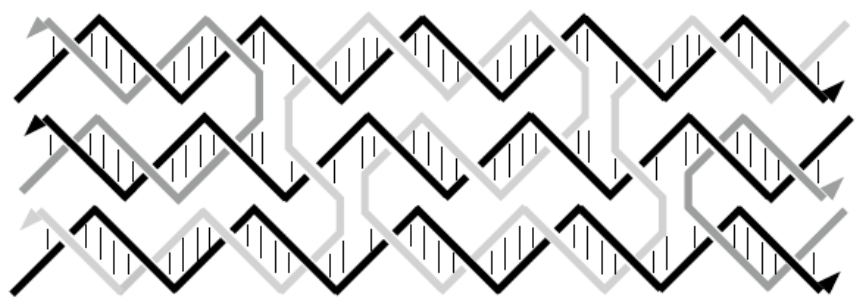
Self-Assembly Strategies

- ⊙ Unmediated (single step).
- ⊙ Nucleated (scaffold strand).
- ⊙ Serial or Sequential (multi stage).
- ⊙ Hierarchical (multi stage).
- ⊙ Algorithmic.